

Dissertation zur Erlangung des Doktorgrades
der Fakultät für Chemie und Pharmazie
der Ludwig-Maximilian-Universität München

Identification and Functional Characterization of MiRNAs in Gammaherpesvirus Infection

Jiayun Zhu

aus

Shanghai, China

2010

Erklärung

Diese Dissertation wurde im Sinne von § 13 Abs. 3 bzw. 4 der Promotionsordnung vom 29. Januar 1998 von Herrn Prof. Karl-Peter Hopfner betreut.

Ehrenwörtliche Versicherung

Diese Dissertation wurde selbständig, ohne unerlaubte Hilfe erarbeitet.

München, am

Dissertation eingereicht am 17.08.2010

1. Gutachter Prof. Dr. Karl-Peter Hopfner

2. Gutachter Prof. Dr. Gunter Meister

Mündliche Prüfung am 05.10.2010

SUMMARY

MicroRNAs (miRNAs) are a conserved class of small non-coding RNA genes with 19 to 25 nucleotides in length that are found in all higher eukaryotes as well as some DNA viruses. MiRNAs have been elucidated to exert important regulatory functions in many biological and pathological processes, by imperfect base pairing to the 3' untranslated region (UTR) of target mRNAs, leading to translational repression or mRNA degradation. In the recent years, the rapid development of next generation sequencing (NGS) technologies has tremendously enhanced the identification of novel miRNA genes as well as the profiling of miRNA expression levels. In this study, NGS method has been applied to two different gammaherpesviruses (γ -herpesviruses) associated models: Epstein-Barr virus (EBV)-infected nasopharyngeal carcinoma (NPC) in human and murine gammaherpesvirus 68 (MHV-68)-infected cell lines from mouse. As a result, two novel miRNA precursors from EBV and six novel miRNA precursors from MHV-68 have been successfully identified and characterized. In addition, the completion of MHV-68 miRNA set has revealed a unique viral tRNA (vtRNA)-miRNA-miRNA structure in MHV-68 genome. Furthermore, expression levels of the viral miRNAs suggest a distinct pattern during different stages of the viral life cycle. On the other hand, the profiling of cellular miRNAs also defined a number of miRNAs that have been dysregulated in EBV-positive NPC tissues compared to healthy control tissues, and in MHV-68-infected compared to non-infected NIH 3T3 murine fibroblasts. Among them, miR-15 and miR-16 were upregulated upon EBV or MHV-68 infection. The tumor suppressor gene BRCA1 has been revealed to be the repressed target protein of miR-15/16 in both models, implying an interesting role of miRNAs in the pathogenesis of γ -herpesviruses. Meanwhile, to facilitate the analysis of NGS data, an automated software was designed and developed. Additional information gained during the analysis processes revealed the possible mis-annotations existing in the miRNA registry database, suggesting that the definition and characterization of novel miRNA genes has to be performed with much more caution.

SUMMARY	1
1. INTRODUCTION	1
1.1 MIRNA GENES.....	1
1.1.1 <i>MiRNAs and Ago proteins</i>	1
1.1.2 <i>Identification of miRNA genes and miRNA database</i>	3
1.1.3 <i>MiRNAs and cancers</i>	4
1.2 GAMMAHERPESVIRUS AND MIRNAS	5
1.2.1 <i>Epstein-Barr Virus and Murine Herpesvirus 68</i>	5
1.2.2 <i>Identification of miRNAs in gammaherpesviruses</i>	7
1.2.3 <i>MiRNA functions in gammaherpesvirus infection</i>	8
1.3 NEXT GENERATION SEQUENCING AND MIRNA STUDY	9
1.3.1 <i>Advent of next generation sequencing</i>	9
1.3.2 <i>Working principles of 454 sequencing</i>	9
1.3.3 <i>Working principles of Solexa sequencing</i>	12
1.3.4 <i>Small RNA sequencing by NGS</i>	12
1.3.5 <i>Analysis tools for NGS data</i>	14
1.4 AIM OF THE THESIS	15
2. RESULT.....	16
2.1 NGS DATA PROCESSING SOFTWARE	16
2.2 ANALYSIS OF SMALL RNA LIBRARIES FROM EBV-INFECTED NPC SAMPLES	18
2.2.1 <i>Small RNA cloning and sequencing from NPC and control samples</i>	18
2.2.2 <i>Identification of novel EBV miRNA genes</i>	19
2.2.3 <i>Identification of novel human miRNA genes</i>	21
2.2.4 <i>Validation of novel EBV miRNAs</i>	22
2.2.5 <i>MiRNA expression analysis suggests an NPC-specific miRNA signature</i>	24
2.2.6 <i>Misregulated miRNAs hsa-mir-15a and hsa-mir-16 inhibit expression of tumor suppressor BRCA1</i>	26
2.2.7 <i>Summary of results from NGS data in NPC samples</i>	28
2.3 ANALYSIS OF SMALL RNA LIBRARIES FROM MHV-68 INFECTED CELL LINES	28
2.3.1 <i>Small RNA cloning and sequencing of MHV-68 infected cells</i>	29
2.3.2 <i>Identification of novel MHV-68 miRNA genes</i>	30
2.3.3 <i>Genomic organization of novel MHV-68 miRNAs</i>	33
2.3.4 <i>Validation of the novel MHV-68 miRNA expression</i>	35
2.3.5 <i>Cellular miRNA profiles in NIH 3T3 and S11 cells</i>	37
2.3.6 <i>Summary of results from NGS data in MHV-68 infected cells</i>	41

2.4	MIS-ANNOTATION OF MICRORNA GENES IN miRBASE.....	41
2.4.1	<i>Examination of murine miRNA genes.....</i>	42
2.4.2	<i>Examination of human miRNA genes.....</i>	47
2.4.3	<i>Summary of examination of mis-annotated miRNAs in miRBase</i>	50
3.	DISCUSSION.....	52
3.1	ADVANTAGES OF DEVELOPED SOFTWARE FOR NGS DATA ANALYSIS	52
3.2	IDENTIFICATION OF NOVEL GAMMAHERPESVIRUS miRNAs	54
3.3	GENOME ORGANIZATION AND EVOLUTIONARY CONSERVATION OF GAMMAHERPESVIRUS miRNAs	55
3.4	EBV AND TUMORIGENESIS	57
3.5	MHV-68 miRNA EXPRESSION SIGNATURES	59
3.6	FURTHER APPLICATION OF NGS IN miRNA STUDIES.....	60
4.	MATERIALS & METHODS.....	63
4.1	MATERIALS	63
4.1.1	<i>Chemicals and enzymes</i>	63
4.1.2	<i>Plasmid.....</i>	63
4.1.3	<i>Antibodies</i>	63
4.1.4	<i>Tissue samples.....</i>	64
4.1.5	<i>Bacterial strains, virus stock and cell lines.....</i>	64
4.1.6	<i>Cell culture media</i>	65
4.1.7	<i>Buffers and solutions</i>	66
4.2	METHODS	70
4.2.1	<i>Molecular biological methods</i>	70
4.2.1.1	General methods.....	70
4.2.1.2	Cloning of 3'UTRs from cDNA library into pMIR-TK-RNL.....	70
4.2.1.3	RNA Extraction from tissue samples or cultured cells.....	70
4.2.1.4	Ago complex purification	71
4.2.1.5	RNA polyacrylamide gel electrophoresis.....	72
4.2.1.6	Northern blotting	72
4.2.1.7	Reverse transcription and qRT-PCR of mRNA detection.....	73
4.2.1.8	Reverse transcription and qRT-PCR of miRNA detection.....	74
4.2.1.9	Reverse transcription and stem-loop qRT-PCR of miRNA detection.....	75
4.2.1.10	Western blotting	75
4.2.1.11	Generation of small RNA libraries for 454 sequencing.....	76
4.2.2	<i>Cellular biological methods</i>	77
4.2.2.1	Culturing of mammalian cells.....	77
4.2.2.2	Virus infection and lytic cycle induction	77
4.2.2.3	2'OMe- miRNA inhibitor transfection	77
4.2.2.4	Cotransfection of 2' OMe- inhibitors and luciferase reporter constructs	78

4.2.2.5	Luciferase assay.....	78
4.2.3	<i>Computational methods</i>	78
4.2.3.1	Sequence analysis of 454 sequencing libraries.....	78
4.2.3.2	Programming method.....	79
ABBREVIATIONS		80
FIGURE INDEX		82
TABLE INDEX		83
REFERENCES		84
APPENDIX		92
APPENDIX TABLE I	92
APPENDIX TABLE II	100
APPENDIX TABLE III	112
APPENDIX TABLE IV	125
PUBLICATIONS		136
ACKNOWLEDGEMENTS		137
CURRICULUM VITAE		139

1. INTRODUCTION

1.1 MiRNA Genes

1.1.1 MiRNAs and Ago proteins

MicroRNAs (miRNAs) are a conserved class of small non-coding RNAs of approximately 19 to 25 nucleotides in length, identified from various organisms during the recent two decades. MiRNA genes are normally transcribed by RNA polymerase II or III as primary transcripts (Borchert et al., 2006; Lee et al., 2004), which are further processed into stem-loop structured precursors (pre-miRNA), mainly by the nuclear microprocessor complex containing the RNase III Drosha (Lee et al., 2003) and its cofactor DGCR8 (Gregory et al., 2004). Pre-miRNAs are then transported by the export receptor exportin-5 into the cytoplasm (Lund et al., 2004; Yi et al., 2003), where the RNase III Dicer cleaves off the loop of the hairpin, thus creating a short double-stranded RNA (Bernstein et al., 2001; Hammond et al., 2000) (Figure 1.1). Such intermediates are subsequently unwound, and one strand, referred to as the mature miRNA, is loaded into the RNA-induced-silencing-complexes (RISCs) (Hutvagner and Zamore, 2002; Mourelatos et al., 2002), while the other strand, referred to as miRNA*, is degraded (Khvorova et al., 2003; Schwarz et al., 2003).

The key players of RISCs in miRNA pathway are members of the Argonaute (Ago) protein family (Meister and Tuschl, 2004). Ago genes vary in their numbers among species, and can be sub-grouped according to the sequence similarities into Ago and Piwi subfamilies (Peters and Meister, 2007). In human, Ago subfamily consists of hAgo1-4, which are approximately 100kDa, ubiquitously expressed, and mainly function in miRNA pathway. Further studies revealed that, hAgo2, distinct from the other three members, possesses endogenous cleavage activity in its catalytic domain, thus is able to cleave the fully complementary sequences guided by artificial short interfere RNAs (siRNAs) or miRNAs (Liu et al., 2004; Meister et al., 2004b). All four hAgo proteins are capable of loading miRNAs and guiding them to the mRNA of target proteins. In common cases, miRNAs interact with the target sites in the 3' untranslated region (UTR) of the mRNAs by partial complementarity. It is believed that nucleotides 2-8 of the miRNA, referred to as the seed sequence, is important for the miRNA-mRNA interaction (Lewis et al., 2005; Rajewsky, 2006). The complementarity of seed sequences is the basic idea behind most of the target prediction algorithms that are widely used for miRNA target identification. Whether there is any

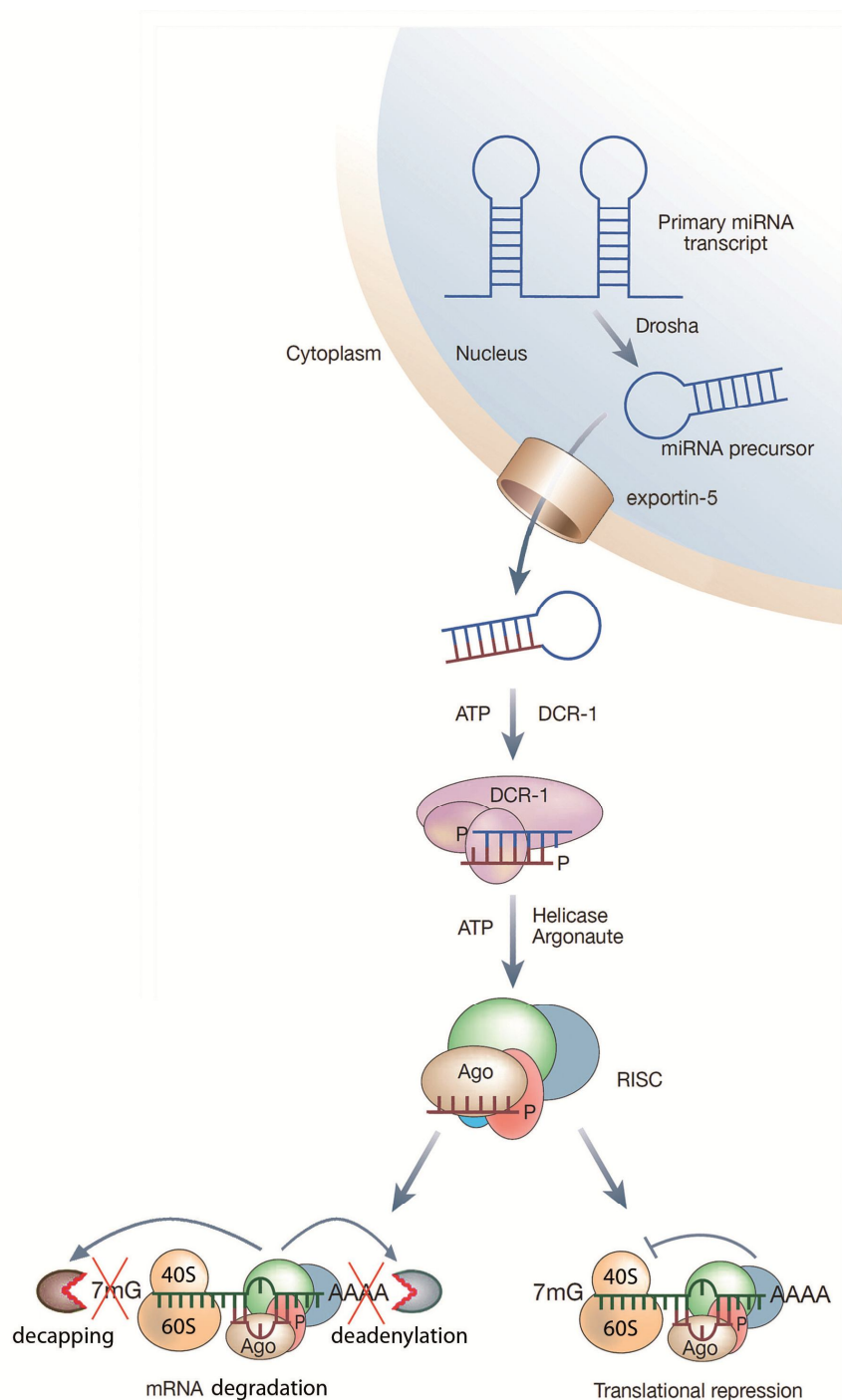


Figure 1.1 Model of miRNA-guided post-transcriptional regulation of gene expression. Primary miRNA transcripts are processed to miRNA precursors by Drosha in the nucleus. The miRNA precursors are then transported into cytoplasm by exportin-5, and further processed by Dicer (DCR-1) to the double-stranded RNAs. The strand of mature miRNA is loaded in to RNA-induced-silencing-complexes (RISCs). Argonaute (Ago) proteins, the key players of RISCs, guide the miRNA to the 3' UTR of its target mRNA by partial complementarity. The expression of target mRNA will be downregulated by different mechanisms. Translation of target mRNA is repressed either at initiation or post-initiation stages. The stability of target mRNAs can be also affected, by activating the decapping and deadenylation complexes, leading to mRNA degradation. (modified from (Meister and Tuschl, 2004))

preference of the four hAgo for distinct miRNA or mRNA species association remains unclear.

The expression of target proteins will subsequently be downregulated through different mechanisms (Figure 1.1). In animals, miRNAs were reported to repress the translational initiation step by interfering with the recognition of the 7-methyl guanosine (m⁷GpppG) cap structure on the mRNAs (Mathonnet et al., 2007; Pillai et al., 2005; Thermann and Hentze, 2007). The suppression effect was also observed at the post-initiation stage of translation, because miRNAs were found to repress the translation-initiated mRNAs by causing ribosomes to exit prematurely from the associated mRNAs (Olsen and Ambros, 1999; Petersen et al., 2006). MiRNAs were demonstrated to affect the stability of their mRNA targets as well. Deadenylation of the poly(A) tail followed by decapping of the m⁷GpppG cap leads to the degradation of target mRNAs (Behm-Ansmant et al., 2006; Wu et al., 2006). The mRNAs targeted by miRNAs were illustrated to be localized in processing bodies (P-bodies) in the cytoplasm (Liu et al., 2005; Sen and Blau, 2005). The decapping complex (consisting of DCP1 and DCP2), required for the mRNA decay inside P-bodies, was revealed to be crucial for miRNA-mediated gene silencing (Rehwinkel et al., 2005). GW182 proteins are the major proteins found in P-bodies, stabilizing the integrity of P-bodies. The physical interaction between GW182 and Ago proteins suggested the functional link between the cytoplasmic P-bodies and the ability of miRNAs to suppress the target mRNAs (Liu et al., 2005; Rehwinkel et al., 2005). The identification and characterization of the other RISC components promote the clarification of the whole picture of miRNA silencing pathway (Hock et al., 2007; Meister et al., 2005; Weinmann et al., 2009).

1.1.2 Identification of miRNA genes and miRNA database

The small regulatory RNA genes was first identified in *Caenorhabditis elegans*, and described as small temporal RNA (stRNA) by the labs of Ambros and Ruvkun (Lee et al., 1993; Wightman et al., 1993). StRNA lin-4 was found important in developmental timing by regulating lin-14 mRNA by imperfect base pairing in the 3' UTR. It was not until seven years later that the second stRNA let-7 was discovered in *C. elegans* (Pasquinelli et al., 2000; Reinhart et al., 2000; Slack et al., 2000). Shortly thereafter, the small regulatory RNAs were identified to be an abundantly expressed gene class (Lagos-Quintana et al., 2001; Lau et al., 2001; Lee and Ambros, 2001; Reinhart et al., 2000), and termed as microRNAs (miRNAs). The explosive development of miRNA studies soon expanded into the fields of animals, plants, as well as viruses

(Lagos-Quintana et al., 2003; Lagos-Quintana et al., 2002; Llave et al., 2002; Pfeffer et al., 2004; Reinhart et al., 2002). The identification and characterization of miRNA genes from various organisms revealed their feature of evolutionary conservation, and their regulatory functions involved in different biological pathways.

The identification work of novel miRNAs was first carried out by genetic screening method, classical small RNA cloning, and sometimes with the assistance of miRNA prediction programs (Zhang et al., 2006). This resulted in the discovery of hundreds of miRNA genes in the genomes of many model organisms. During the recent few years, however, the advent of Next Generation Sequencing (NGS) technologies, which is capable of producing large numbers of short sequences at low cost (Metzker, 2010) turned out to be an advanced methodology for miRNA identification. Highly improved sensitivity of NGS technologies has led to the characterization of formerly undetectable, low abundant miRNA genes (Landgraf et al., 2007).

The rapid identification of new miRNA genes led to the basic need of a public database as a reliable storage pool for the up-to-date miRNA sequences, with rational rules for nomenclature and useful annotations of sequence characteristics. Although several databases emerged at similar time, one of them, the miRBase (Griffiths-Jones, 2004; Griffiths-Jones et al., 2006; Griffiths-Jones et al., 2008), has gradually become the most popularly referred database in the literature and in miRNA field. Launched by The Wellcome Trust Sanger Institute in 2003, miRBase contained only 506 miRNA entries from six organisms when accessible for the first time. Keeping with the accelerating pace in miRNA studies, miRBase was also expanding rapidly by accepting the registration of novel miRNA genes from publications. The newest 15th version of miRBase was just released in April of 2010, with 14197 entries from more than 100 organisms, and it's still growing.

1.1.3 MiRNAs and cancers

The identification and characterization of miRNA genes has revealed a so far unrecognized complexity of gene networks which are important for development, as well as other physiological and pathological processes. MiRNAs-guided gene regulation was found to be involved in diverse diseases, ranging from the nervous system and the cardiovascular system, to the immune system (Latronico and Condorelli, 2009; Lodish et al., 2008; Schratt, 2009). Cancers, being one of the biggest challenges to the world, are also demonstrated to be associated with miRNA dysregulation (Croce, 2009).

During the studies of miRNA functions in tumorigenesis, miRNA profiling has become a new focus to systemically explore differentially expressed miRNAs (Barbarotto et al., 2008; Cummins and Velculescu, 2006). The distinct patterns of cellular miRNA expression levels are not only useful for disease diagnosis, staging, progression, prognosis and response to treatment, but also suggest a list of dysregulated miRNA genes that may contribute to the epigenetic regulation of oncogenetic pathway (Lee and Dutta, 2009). The alterations in the expression of miRNA genes can be caused by various mechanisms, including genomic deletions, amplifications or mutations of miRNA loci, epigenetic silencing such as DNA methylation or the dysregulation of transcription factors that target specific miRNAs and posttranscriptional modification of the miRNA sequences (Croce, 2009). Much effort has been devoted to figure out the significant targets of the miRNAs that are responsible for the tumorigenesis as well. The overexpressed miRNA genes, often referred to as oncomirs (Cho, 2007; He et al., 2005), are frequently found to downregulate tumour suppressor genes, while the underexpressed miRNAs lead to the reduced suppression of oncogenes (Croce, 2009; Kent and Mendell, 2006; Lee and Dutta, 2009).

Progress in the clarification of miRNA functions also shed light on the research of novel cancer therapies. The overexpressed miRNA genes become a new group of candidates to be targeted, probably by using antisense miRNA inhibitors, known as antagomirs (Kasinski and Slack, 2010; Trang et al., 2008). Furthermore, the application of the artificial siRNAs have been discussed and studied for a long time, seeking an optimized way to target the upregulated oncogenes (Ashihara et al., 2010). However, huge obstacles remain in both methodologies of developing the efficient and non-toxic administration approaches (Whitehead et al., 2009), and restraining the off-target side-effects (Jackson and Linsley, 2010).

1.2 Gammaherpesvirus and MiRNAs

1.2.1 Epstein-Barr Virus and Murine Herpesvirus 68

The herpesvirus family (*Herpesviridae*) constitutes the large enveloped double-stranded DNA viruses, which are divided into three subfamilies: *Alphaherpesvirinae*, *Betaherpesvirinae* and *Gammaherpesvirinae*, according to their host and tissue specificities, together with their replication characteristics (McGeoch, 1989). A hallmark of herpesviruses is their ability to establish and maintain the latent stages during the infection, wherein the virus genome circularizes and persists as an episome, and only very limited viral gene expression takes place (Garcia-Blanco and

Cullen, 1991). Epstein-Barr Virus (EBV) and Murine Gammaherpesvirus 68 (MHV-68), two model gammaherpesviruses (γ -herpesviruses) respectively infecting human and mouse, will be further discussed in the following paragraphs.

Epstein-Barr Virus was named after its two discoverers when identified from the Burkitt's lymphoma cells more than 40 years ago (Epstein and Barr, 1965; Epstein et al., 1965). It is also called Human Herpesvirus 4 (HHV-4). B cells are the main site of EBV infection where the latency is maintained (Young and Rickinson, 2004). However, EBV is also able to infect some other cell types, such as epithelial cells, mesenchymal cells and T cells, mostly evidenced by its association with various diseases (Kutok and Wang, 2006). Despite the fact that more than ninety percent of human population is infected with EBV since childhood, mostly in a benign and uneventful status, a spectrum of diseases varying from tumors (Young and Murray, 2003) to autoimmune diseases (Niller et al., 2008), were found to be significantly related with EBV, though most of the mechanisms remain to be elucidated. Nasopharyngeal Carcinoma (NPC), which occurs in the epithelial lining of the nasopharynx, was constantly detected to be infected by EBV (Wei and Sham, 2005). This malignancy has specifically high incidence in the area of South East Asia (Busson et al., 2004). The involvement of EBV in the transformation and development of NPC has been actively studied to seek for novel therapeutic strategies.

MHV-68 is another popular topic in the γ -herpesvirus studies. Isolated from the murine host in 1980 (Blaskovic et al., 1980; Svobodova et al., 1982), it soon attracted much interest. Due to the species-specificity of the γ -herpesviruses, pathogenetic studies of human infections are restricted. The discovery of the mouse γ -herpesvirus MHV-68 allows to investigate γ -herpesvirus infection in a small animal model (Simas and Efsthathiou, 1998). B cells are also the main site wherein MHV-68 resides in its latent stage (Sunil-Chandra et al., 1992). In addition, MHV-68 readily establishes, unlike EBV, productive infections in a variety of cell lines and thus facilitates the examination of *de novo* lytic infections. Further studies in MHV-68 genome revealed a unique region, where eight so-called virus tRNAs (vtRNAs) are located. These vtRNA sequences were identified more than ten years ago with their characteristics of the homology to the classical A/B box tRNAs (Bowden et al., 1997). These sequences were observed to be posttranscriptionally modified as normal tRNAs, however, they were never detected to be actually amino-acetylated, and their functions still remain unknown.

1.2.2 Identification of miRNAs in gammaherpesviruses

After the miRNA genes had been identified from a number of animals and plants, the biologists began to wonder, whether the small-sized, compact viral genome is able to encode miRNA genes as well. The first viral miRNA genes were characterized in EBV infected B cell lymphomas, though a mutant strain with genomic deletion was utilized and the number of EBV miRNA genes was underestimated (Pfeffer et al., 2004). Later on, miRNA studies were expanded to different herpesviruses and other dsDNA viruses. So far, more than 200 viral miRNA genes have been identified, and they are believed to employ the cellular machineries during miRNA processing and functioning pathways (Skalsky and Cullen, 2010) (Table 1.1).

Before the study of this thesis, 23 miRNA genes had been found in EBV, clustering in two regions in the genome, BHRF1 and BART regions (Cai et al., 2006; Grundhoff et al., 2006; Pfeffer et al., 2004). The BHRF1 miRNAs were detected exclusively during the latency III-infected lymphoblasts and induced lytic replication (Cai et al., 2006; Xing and Kieff, 2007), while the BART miRNAs were expressed at high levels in latently infected epithelial cells and at lower, albeit detectable, levels in B cells (Cai et al., 2006; Kim do et al., 2007). In MHV-68, nine miRNA genes had been identified in

Table 1.1 Numbers of miRNA precursors in herpesviruses.

Virus Family	Virus	Host	Number of pre-miRNAs ^a
α -herpesviruses	HSV-1 (Herpes simplex virus 1)	human	16
	HSV-2 (Herpes simplex virus 2)	human	18
	MDV-1 (Marek's disease virus type 1)	avian	14
	MDV-2 (Marek's disease virus type 2)	avian	18
	HVT (Herpes virus of turkeys)	avian	17
	ILTV (Infectious laryngotracheitis virus)	avian	7
β -herpesviruses	hCMV (Human cytomegalovirus)	human	11
	mCMV (Mouse cytomegalovirus)	mouse	18
γ -herpesviruses	EBV (Epstein Barr virus)	human	23
	rLCV (Rhesus lymphocryptovirus)	primate	36
	KSHV (Kaposi sarcoma-associated herpesvirus)	human	13
	RRV (Rhesus monkey rhadinovirus)	primate	7
	MHV-68 (Mouse Gammaherpesvirus 68)	mouse	9

a. Numbers of viral miRNA precursors are according to the newest release v15.0 from miRBase.

b. The table is modified from (Skalsky and Cullen, 2010)

the first 6 kilo base-pair (kbp) of the genome, where the eight vtRNA genes are also located (Pfeffer et al., 2005). MiRNA studies has been carried out in more than ten species of herpesviruses infecting human, mouse, primate and avian, while many of them were characterized as miRNA clusters (Boss et al., 2009). Interestingly, distinct from the observation in the open reading frames (ORFs) of γ -herpesvirus genomes, there is not much conservation found among the identified miRNA genes within the γ -herpesvirus family. Only a couple of EBV miRNA genes from both BHRF1 and BART clusters show homology to the miRNA genes from Rhesus lymphocryptovirus in the primates (Cai et al., 2006; Walz et al., 2010; Yao et al., 2007).

1.2.3 MiRNA functions in gammaherpesvirus infection

Upon the identification of the significant number of miRNA genes from γ -herpesviruses, people have also been making the effort to clarify the roles of viral miRNAs during virus infection, replication, and possible pathogenetic processes.

Some studies revealed that several viral miRNAs were able to target their own mRNA transcripts. Ebv-mir-BART2 was shown to downregulate the viral DNA polymerase BALF5 (Barth et al., 2008). Other three EBV miRNAs were illustrated to synergistically fine-tune the level of the transforming viral latent membrane protein LMP1, so as to promote cancer development in NPC (Lo et al., 2007).

On the other hand, viral miRNAs also suppress the cellular proteins involved in various pathways. PUMA, the p53 up-regulated modulator of apoptosis, was demonstrated to be targeted by ebv-mir-BART5 in NPC tissues, suggesting a novel therapeutic strategy by depleting ebv-mir-BART5 to further sensitize cancer cells in response to the proapoptotic reagents (Choy et al., 2008). The miRNAs of BHRF1 cluster, expressed during latency III, were found to be inversely correlated with levels of a cellular target, the IFN-inducible T-cell attracting chemokine CXCL-11/I-TAC (Xia et al., 2008). However, compared to the numbers of identified viral miRNAs, the validated targets are few (Cullen, 2009).

Moreover, the changes of cellular miRNAs were examined during the viral infection, too. The above mentioned EBV protein LMP1 was shown to induce the level of mir-146a through NF-kappa B pathway, thus forms a negative feedback loop to modulate the intensity and/or duration of the interferon response (Cameron et al., 2008b). The oncomir mir-155 was also revealed to be transactivated by LMP1 (Gatto et al., 2008; Rahadiani et al., 2008). A few studies have attempted to systematically study the cellular miRNA levels in the EBV-infected B lymphomas by microarrays, and

suggested a list of cellular miRNAs that have been dysregulated (Cameron et al., 2008a; Godshalk et al., 2008)

Nevertheless, miRNA functions in γ -herpesvirus infection have just emerged as an important piece in the puzzle of pathogenesis of γ -herpesviruses-related diseases. Further studies on viral miRNAs and their targets, as well as the cellular miRNA response will promote the development of novel and efficient therapies.

1.3 Next Generation Sequencing and MiRNA Study

1.3.1 Advent of next generation sequencing

Automated Sanger Sequencing had been established and applied as the fundamental technology to determine DNA sequences in biological studies during the past few decades including the break-through accomplishment of the finished-grade human genome sequences (2004). However, the dominant position of this classical sequencing technology has been challenged over the past five years, whereas several revolutionary technologies became broadly available, and elevated genome sequencing to next generation.

Next Generation Sequencing (NGS) technologies, named after the reference of Automated Sanger Sequencing as the 'first-generation' (Metzker, 2005), constitute various advanced strategies in template preparation, sequencing, imaging and data analysis, and produce enormous volumes of data in a rapid and inexpensive way. Several platforms are currently available on the market, with different features in strategic design and data production, leading to the diversities in applications (Metzker, 2010). The 454 Sequencing from Roche and the Solexa Sequencing from Illumina are the two most popularly applied technologies in the literature, and were also utilized in the studies of this thesis, so the basic principles behind the two technologies will be explained in further detail.

1.3.2 Working principles of 454 sequencing

454 Life Sciences, initially founded by Jonathan Rothberg, latterly acquired by Roche Diagnostics, released the first next-generation DNA sequencer on the market in 2005 (Margulies et al., 2005). Its great potential in biological studies was soon demonstrated by the Neanderthal Genome Project (Green et al., 2006; Noonan et al., 2006), followed by the rapidly expanding applications in various fields.

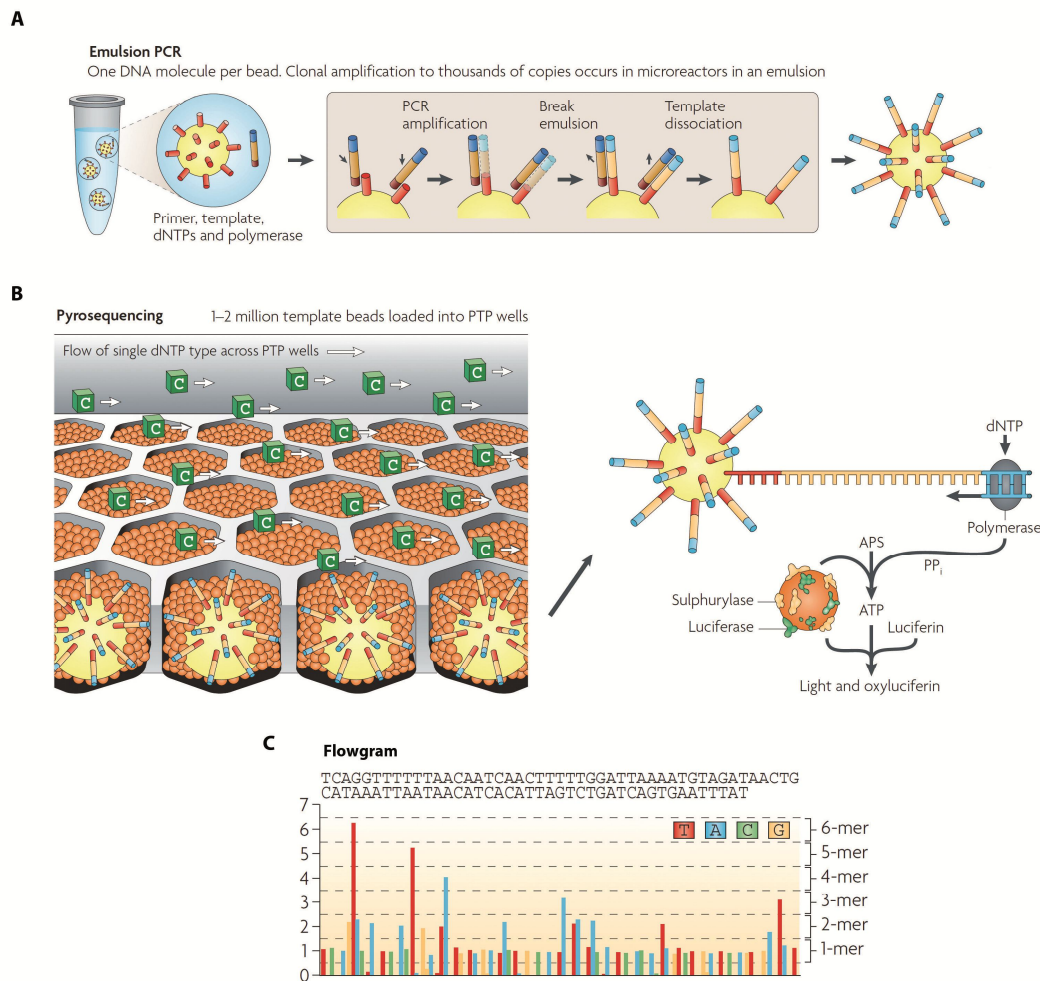


Figure 1.2 Working principles of 454 sequencing. (A). Sample amplification is carried out by emulsion PCR. A reaction mixture consisting of an oil-aqueous emulsion is created to encapsulate bead-DNA complexes into single aqueous droplets. PCR amplification is performed within these droplets to create beads containing several thousand copies of the same template sequence. **(B).** Pyrosequencing signal is generated from individual bead in PicoTiterPlate wells. DNA-amplified beads are deposited into individual PicoTiterPlate (PTP) wells. Additional beads, coupled with sulfurylase and luciferase, are added. As shown in the examples, a single type of 2'-deoxyribonucleoside triphosphate (dNTP)—cytosine—is flowing across the PTP wells. The fiber-optic slide is directly attached to a high-resolution charge-coupled device (CCD) camera, which allows detecting the light generated from each PTP well undergoing the pyrosequencing reaction. **(C).** An exemplar diagram of 454 sequencing result is shown. The light generated by the enzymatic cascade is recorded as a series of peaks called a flowgram. The output of DNA sequences is interpreted by the number of continuous identical nucleotides in proportion to the height of corresponding signal peaks. PP_i, inorganic pyrophosphate. (modified from (Metzker, 2010))

454 Sequencing is a large-scale parallel sequencing system. It has fundamentally upgraded the capacity of sequencing by the invention of multiplexing the samples by emulsion-based PCR (Dressman et al., 2003; Ghadessy et al., 2001; Tawfik and Griffiths, 1998). During the template preparation, the single-stranded DNA (ssDNA) library is immobilized onto specifically designed DNA Capture Beads, so that each bead carries only one unique ssDNA fragment. The bead-bound library is then emulsified with amplification reagents in a water-in-oil mixture, resulting in microreactors containing only one bead with one unique sample fragment. The amplification within the microreactors produces several million copies of each fragment bound to the individual bead (Margulies et al., 2005) (Figure 1.2 A).

The sequencing principle of 454 technology is based on the pyrosequencing method, that is, to detect the released pyrophosphate (PPi) during DNA synthesis through a cascade of enzymatic reactions, in the form of visible light that is proportional to the number of incorporated nucleotides. The newly developed pyrosequencing technology emerged as a competitive substitution of the traditional dideoxy chain termination technology, with its advantages to sequence at high throughput but low cost (Ronaghi et al., 1996; Ronaghi et al., 1998). 454 technology employs the typical solid-phase pyrosequencing, immobilizing DNA on beads within a three-enzyme system including *exo*⁻ DNA polymerase, ATP sulfurylase and Luciferase (Margulies et al., 2005).

Moreover, the incorporated design of a PicoTiterPlate device enables the simultaneous sequencing of the multiplexed DNA samples, by allowing only one bead per well throughout the process of sequencing (Leamon et al., 2003). As a result, a unique but enriched chemiluminescent signal is generated from each template strand and recorded by the charge-coupled device (CCD) camera within the instrument (Figure 1.2 B). These signals will be subsequently interpreted into sequence information (Margulies et al., 2005) (Figure 1.2 C).

The up-to-date 454 Sequencing machine is able to produce 1 million reads with the average length of 400 bases within 10 hours (<http://www.454.com>). The ability of producing the longest read length among all available NGS machines highlighted its applications in the *de novo* assemblies of small-size genomes, e.g. from bacteria and insects. Its short running time also encourages its utility in the other projects such as epigenetics and transcriptome studies (Metzker, 2010). However, the high error rates in the homopolymer repeats derived from the detection of non-linear light response raise the problems and limitations during the result interpretation.

1.3.3 Working principles of Solexa sequencing

Solexa was the name of the company that has commercialized the NGS machine called Genome Analyser (GA) in 2006 and was later acquired by Illumina. The working principles behind Solexa Sequencing technology are fundamentally different from 454 Sequencing, leading to the distinct features in produced results.

During template multiplexing preparation, high-density forward and reverse primers are covalently attached onto a planar, optically transparent surface, where the ssDNA sample fragments are bridge-amplified to form clusters (Bentley et al., 2008; Fedurco et al., 2006) (Figure 1.3 A). The sequencing strategy utilized by Solexa GA platform is called four-colour Cyclic Reversible Termination (CRT) (Metzker, 2010) (Figure 1.3 B and C). CRT is a cyclic method that comprises nucleotide incorporation, fluorescence imaging and cleavage (Metzker, 2005). The key feature of terminating DNA synthesis after the addition of a single nucleotide in CRT is realized by the application of 3'-blocked reversible terminators in Solexa Sequencing. Before cleaving and washing of blocking group and fluorescent dye, the four colours are detected by total internal reflection fluorescence (TIRF) imaging using two lasers with ultra-high resolution (Bentley et al., 2008) (Figure 1.3 D). In addition, the sample slide can be partitioned into eight channels, allowing simultaneous analysis of independent samples.

The Illumina/Solexa GA platform is currently dominating the NGS market (Metzker, 2010). The astonishing ability to produce nearly 2 GB sequence information per day (http://www.illumina.com/systems/genome_analyzer.ilmn) has largely promoted its diverse applications. However, the short read length of 75 bases and the most frequent error of substitutions has raised the problems during its utility in *de novo* genome sequencing.

1.3.4 Small RNA sequencing by NGS

The production of enormous amount of low-cost short reads makes the NGS platforms very powerful in many applications. Among them, NGS was soon employed for small RNA sequencing since the length limitations in NGS can be ideally ignored when only very short pieces of sequences are desired. The sequencing of small RNA libraries was therefore performed in diverse organisms and cell conditions, largely promoting the studies in miRNA field (Morozova et al., 2009).

The sample preparation of small RNA sequencing involves one more step of reverse transcription, comparing to the DNA samples. In short, the extracted RNA is first size-fractionated according to the length desired, normally by polyacrylamide gel electrophoresis (PAGE). Then, the small RNAs are ligated with 5' and 3' adaptors,

while there might be slightly modified strategies of using different DNA and RNA adaptors. The small RNAs are subsequently reverse transcribed with the universal primer to the 3' adaptor to build the cDNA library, before the regular sample multiplexing PCR and automated sequencing steps are conducted (Berninger et al., 2008).

Among the huge numbers of reads produced by NGS, people found that, not only the sequence information of the small RNAs could be retrieved, but also the quantification information of individual small RNA was reserved, represented by the abundance of the reads in the library (Wang et al., 2009b). Therefore, NGS soon gained the advantage over the classical small RNA cloning with its less hand-on work, less sample amount demanded, but much more sequence information produced. Meanwhile, NGS of small RNAs also became a competitive substitute of miRNA microarrays, for the reason that the design of the microarrays excludes the information from the unknown sequences, while NGS technologies generates data with integrity (Sharma and Vogel, 2009).

Nevertheless, NGS technologies applied in small RNA sequencing have some inherent problems, mostly derived from the sample preparation stage. The adaptor ligation, reverse transcription and PCR multiplexing all might introduce the bias of the effectively detectable sequences into the final result (Metzker, 2010). Consequently, the idea of direct RNA sequencing without the need to convert RNA into cDNA is also being actively carried out by some companies (Ozsolak et al., 2009), and will likely join the competition of NGS technologies in near future.

1.3.5 Analysis tools for NGS data

The emergence of the revolutionary NGS technologies first excited people with its huge set of data, which, however, turned out to be a big challenge soon after. The enormous amount of the short sequences demanded a more efficient annotation strategy, comparing to the process of traditional sequencing data. Different problems arose during the analysis of the diverse NGS applications, especially the *de novo* assembly and the fast reference alignment, and people have been seeking the optimized solutions with much effort (McPherson, 2009).

The analysis tools for NGS data have been developed by the platform-designing companies, as well as many laboratories and service companies. However, there are not many tools publicly available so far. In the field of small RNA sequencing, some of the data processing programs became available during the recent two years (Fahlgren et al., 2009; Friedlander et al., 2008; Hackenberg et al., 2009; Pantano et

al., 2010; Wang et al., 2009a). Most of them were released as interactive web-servers, some of which also provided stand-alone versions. The main strategies employed by these programs have subtle differences. Some of them, e.g., miRanalyzer and SeqBuster, first align all the sequences to the whole genome, annotate the sequences according to the genome loci, and directly predict the novel miRNA genes by folding the flanking sequences of the un-annotated sequences (Hackenberg et al., 2009; Pantano et al., 2010). The other programs, like miRExpress, usually annotate the sequences according to the established miRNA databases at first, as one solution to accelerate the whole process (Berninger et al., 2008; Wang et al., 2009a). Apart from the miRNA frequency data as the outcome in common, some programs provide additional information from novel miRNA gene candidates to frequent miRNA variants. Nevertheless, none of these programs has become a well-established popular tool in the RNA community. Many aspects still need to be improved, such as the flexibility of the applied genomes and databases, the simplicity in the result format, and the friendliness of the interface.

1.4 Aim of the Thesis

The advent of NGS in miRNA field promoted many labs to re-visit miRNA expressions in many physiological and pathological processes. The application of NGS in small RNA studies allows a detailed identification of all miRNA gene candidates in the genomes of various species. Furthermore, it provides the information of miRNA expression profiles. Here, NGS was employed to analyze EBV and MHV-68 infected cells. This was the first time that NGS was utilized for miRNA studies in γ -herpesviruses so far. The aim of the study in this thesis is, first, to identify and validate potential novel miRNA genes from these viral genomes by NGS technologies; second, to study cellular miRNA profiles upon virus infection, and third to characterize the interesting miRNA target genes that might contribute to the physiological and pathological processes during virus infection. To facilitate the analysis of NGS data, an automated software was designed and developed, which can be further utilized for other NGS data. Additional information gained during the analysis processes revealed the possible mis-annotations existing in the miRNA registry database, suggesting that the definition and characterization of novel miRNA genes has to be performed with much more caution.

2. RESULT

2.1 NGS Data Processing Software

The enormous amount of the read sequences produced by NGS technologies demands an automated tool for analysis, for the reason that manual analyzing procedures are no more possible to handle the huge data set. To fully employ the sequencing ability, the barcode system was designed so that different samples can be pooled and sequenced at the same time. Barcode is the sample-specific tag of a few nucleotides in the adaptor sequence. After converting the sequencing signal to the nucleo-base sequence, the raw data generated from NGS usually include additional information, e.g., barcodes, 5' and 3' adaptors, which have to be first processed before the actual sequences are extracted for analysis (Figure 2.1). The recognition of barcode sequences helps to sort the read sequences from different samples. During sequences annotation, the miRNA gene information constitutes the most significant result of the small RNA libraries, while the annotation to other non-coding RNAs (ncRNAs) and genomic sequences reserves the information of degradation products and novel miRNA candidates. The sequences of novel miRNA candidates are further

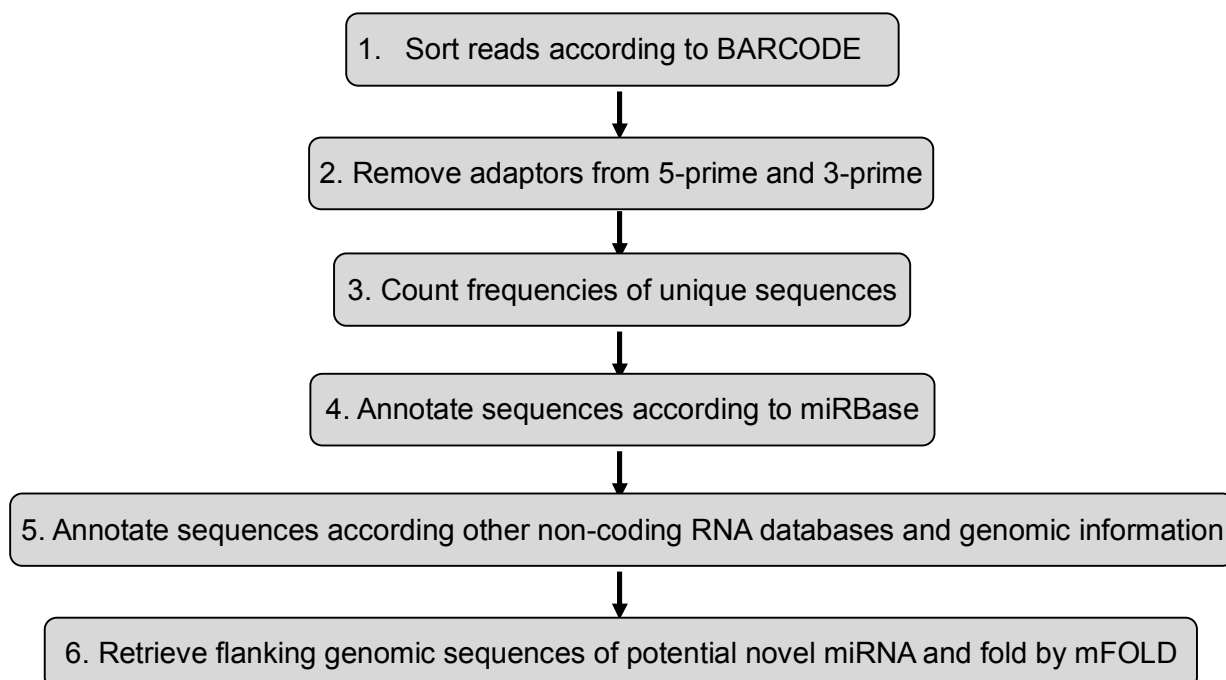


Figure 2.1 Flow chart of NGS data analysis procedures. The step-by-step procedures to process NGS data from raw sequences to final gene annotations and frequency counting are depicted here. All the sequencing data studied in this thesis are analyzed based on this process.

analyzed by retrieving flanking genomic sequences and folding by RNA folding program mFOLD (Zuker, 2003) (Figure 2.1). Based on these working procedures, an automated software was designed and developed for the analysis of all NGS data involved in this thesis.

There was no software available for analysis of NGS data of small RNA libraries when this project began. It was urged to develop an analysis tool, not only capable of handling the data set step by step as basic functions, but also able to provide interactive platforms so that the results can be produced in the way of interest. To this purpose, an interactive software has been developed by using BASIC language of RealBasic (<https://www.realsoftware.com>). Step 1 to Step 5 of the working procedures in Figure 2.1 can be realized by the software, with much flexibility, as all functions shown in the software main window (Figure 2.2 A). There are many interactive input windows in the different functions of the software, where the genomes of interest, the barcodes, and the parameters during annotations can be assigned (Figure 2.2 B to D).

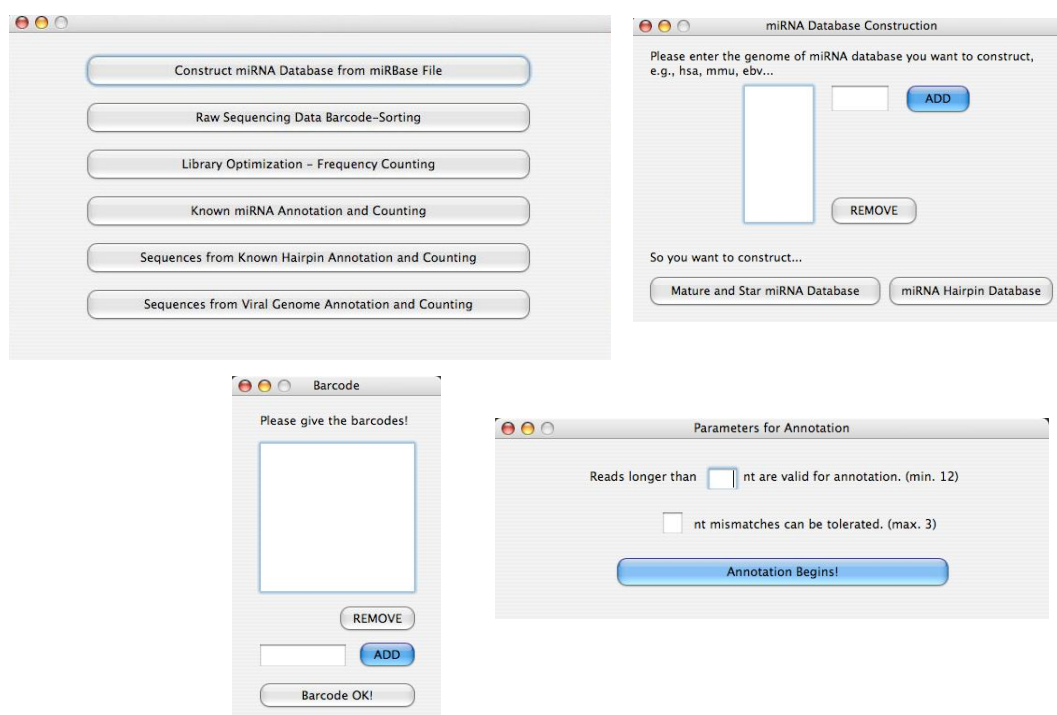


Figure 2.2 Interactive platforms of developed software for NGS data analysis. (A). Main window of the software is shown. The main functions of the software are described on the interactive buttons. **(B).** The input window for the construction of desired miRNA database is shown. The genome names of interest can be added to the list in the window. **(C).** The input window for barcode sorting is shown. The barcodes can be added to the list in the window. **(D).** The parameter window for annotation is shown. Different parameters can be assigned as desired.

The sequence annotation is carried out on the basis of direct alignment, while the sequence information, gene annotation and mismatch number are all reserved for further analysis. The main function of the software is to annotate NGS data by miRNA gene information from miRBase. A result data set with all miRNA count numbers is automatically generated. Furthermore, the information of miRNA hairpin sequences, other ncRNAs and genomic sequences, can be produced as desired.

The development of this software has largely facilitated the analysis of small RNA NGS data.

2.2 Analysis of Small RNA Libraries from EBV-infected NPC Samples

The small RNA cloning and NGS approach was first applied to the Nasopharyngeal Carcinoma (NPC) samples. NPC cells are known to be constantly associated with Epstein-Barr Virus (EBV) (Wei and Sham, 2005). Before this study, EBV genome was elucidated to harbor 23 miRNA genes, clustered in BHRF1 and BART regions (Cai et al., 2006; Grundhoff et al., 2006; Pfeffer et al., 2005). To explore the roles of EBV miRNAs as well as cellular miRNAs in NPC pathogenesis, 454 sequencing technology was utilized to study NPC samples together with control tissues.

2.2.1 Small RNA cloning and sequencing from NPC and control samples

Small RNAs were cloned and sequenced from EBV-positive NPC samples as well as control tissues (GEO number GSE14738). Biopsies were taken from the nasopharynx

Table 2.1 Sequence distribution of small RNA libraries from NPC samples.

	NPC-1	Control-1	NPC-2	Control-2
Total reads	25223	16249	22636	19052
Mapped to human genome	21668	1874	13445	3330
Mapped to EBV genome	1014	34	1217	0
Reads of known miRNAs	20019	1269	5980	1445
Human miRNAs	19262	1242	4889	1445
EBV miRNAs	757	27	1085	0
Reads of human ncRNAs	2317	616	8412	1843
human rRNAs	1294	462	7185	1456
human tRNAs	156	90	392	117
human other ncRNAs	867	64	835	270

in an area where there was clinical evidence of tumor, and control tissues were taken from clinically normal mucosa from the opposite side of the nasopharynx of the same patient. In total, four samples were generated from two patients.

Altogether, 25,223 sequence reads were obtained for NPC sample 1 (NPC-1) and 22,636 reads were obtained for NPC sample 2 (NPC-2) that were further grouped according to their origins (Table 2.1). For control tissues, there were 16,249 (Control-1) and 19,052 (Control-2) sequences generated. Interestingly, only in the NPC tissue, it was possible to map 50% of the sequences to the human or the EBV genome. The libraries obtained from control tissues contained only a minor portion of human- or EBV-derived sequences. The majority of the sequences were derived from bacterial genomes, probably due to the bacterial flora in the throat of the patients or the contamination of the samples. About 20,000 sequences of NPC-1 and about 6,000 sequences of NPC-2 were identified as known cellular or viral miRNAs. Notably, the libraries from NPC-2 and Control-2 contained significant numbers of other ncRNAs, which may indicate sample-specific lower RNA quality (Table 2.1).

2.2.2 Identification of novel EBV miRNA genes

Then, the data sets were analyzed for novel miRNA candidates. First, the sequences that match the EBV genome but have not yet been annotated functionally were investigated. Three different small RNAs were found derived from two individual

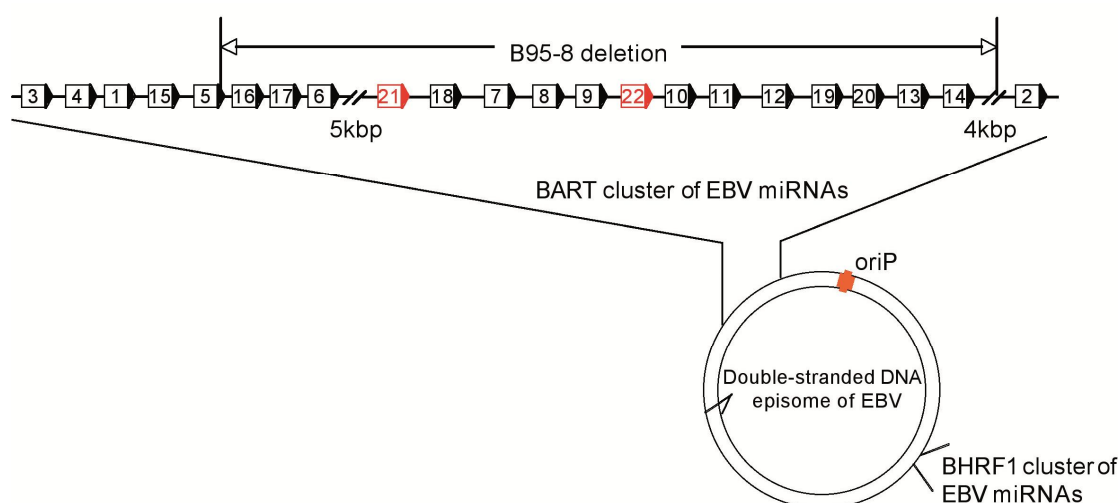


Figure 2.3 Schematic locations of putative novel EBV miRNAs in BART miRNA cluster of EBV genome. Each box with an arrow indicates an EBV miRNA precursor and its transcription direction. The putative new miRNA precursors are depicted in red. The numbers in the boxes represent the names of the BART miRNAs. The genomic localization of the BHRF1 and BART clusters are indicated schematically in the double-stranded episome. oriP, origin of replication.

Table 2.2 Novel candidate miRNAs of novel precursors identified from NPC samples.

Candidate miRNA ^a	Stem-loop structures of putative miRNA precursors ^b	dG ^b (kcal/mol)	Genomic location ^c	Conservation of Stem-loop
<i>ebv-mir-BART21-5P</i>	<pre> UU AAG A AGU GGGCUGGGUA CACUAGUG GCAACUA CAC U </pre>	- 40.4	145514-145534	rLCV ^d
<i>ebv-mir-BART21-3P</i>	<pre> UU CCG C CAG CCUGGCCUAU GUGGUCAC UGUUGAU GUG A </pre>	- 40.4	145548-145569	rLCV
<i>ebv-mir-BART22</i>	<pre> G C AG UA GUCACAG UGCUAGACC UGG UUG -AACC -AG \ CAGUGUU AUGAUCUGG ACU AAC UUGG UC C G U GA A C AC </pre>	- 35.8	147203-147225	

- Names of the putative new miRNA sequences are according to the submission to miRBase (<http://www.mirbase.org>).
- RNA secondary structure prediction and free energy calculation have been done using mFOLD version 3.2. The miRNA sequences are underlined. Due to the characteristics of 454 sequencing, the putative miRNA sequences might extend to the additional "A" at the end. The actual size of the stem-loop has not been experimentally determined.
- The genomic locations of EBV miRNAs are referring to the positions in EBV genome (GenBank accession number AJ507799).
- rLCV, Rhesus lymphocryptovirus.

precursors that fold into hairpins and originate from the EBV BART region (Figure 2.3, Table 2.2). These miRNA candidates were named as *ebv-mir-BART21* and *ebv-mir-BART22* according to the submission to the miRBase. Interestingly, *ebv-mir-BART21* is conserved in Rhesus lymphocryptovirus, a common model system in the primates for EBV infection (Table 2.2). Furthermore, the star sequences from *ebv-mir-BART4* and *ebv-mir-BART5*, which have not been reported in the miRBase before, were also detected in NPC samples, suggesting that some viral star miRNAs might be functional as well (Table 2.3).

Table 2.3 Numbers of novel EBV miRNA reads in the libraries.

Name	Sequence	Reads in libraries			
		NPC-1	Control-1	NPC-2	Control-2
<i>ebv-mir-BART21-5P</i>	UCACUAGUGAAGGCAACUAAC ^a	26	1	9	0
<i>ebv-mir-BART21-3P</i>	CUAGUUGUGCCCACUGGUGUUU ^a	10	1	6	0
<i>ebv-mir-BART22</i>	UUACAAAGUCAUGGUCUAGUAGU	201	1	80	0
<i>ebv-mir-BART4*</i>	CACAUCACGUAGGCCACCAGGUGU	6	0	9	0
<i>ebv-mir-BART5*</i>	GUGGGCCCGUGUUCACCU ^a	0	0	1	0

- Due to the characteristics of 454 sequencing, the putative miRNA sequences might have additional "A" at the end.

2.2.3 Identification of novel human miRNA genes

In addition, efforts were also made in order to find novel human miRNAs, by analyzing the pool of unknown sequences which match the human genome. Indeed, three new miRNA genes were identified. Two of them were annotated as hsa-mir-1301 and hsa-mir-1307, while this work was in progress. The third one was named as hsa-mir-2110 according to the submission to the miRBase (Table 2.4). Hsa-mir-1301 is located in an intergenic region, whereas hsa-mir-1307 and hsa-mir-2110 reside in the 5' UTRs of protein coding genes (Table 2.4). Additionally, six unidentified miRNA star sequences that derive from known miRNA genes and have not been cloned before were also found in the libraries (Table 2.5).

Table 2.4 Novel candidate human miRNAs of novel precursors identified from NPC samples.

Candidate miRNA ^a	Stem-loop structures of putative miRNA precursors ^b	dG ^b (kcal/mol)	Genomic location ^c	Conservation of Stem-loop
<i>hsa-mir-1301</i>	<pre> G -CC GU GGGGAUUGUG GGGGUCGCU -CUAGGCA GCAGCA -CU G CUCCUGACAC CUUCAGUGAGGGUCCGU CGUUGUAGG C A CGA GGU </pre>	- 47.2	2p23.3	mmu ^d
<i>hsa-mir-1307</i>	<pre> CCA U A - U C UC UG ACUGCCUA AUC CGACCGG CC CGACCGG UCG UG C UGGCGGAU UGG GCUGGCU GG GC -GGCU AGC AC U AGA U GC U C UA CG </pre>	- 39.6	10q24.33	ptr ^d , mml ^d
<i>hsa-mir-2110</i>	<pre> UU C U G UC CAGGGGU GGGGAAA GGCCGC --UGAG GA GCG \ GUUCUCA CUCCUUU CUGGCG ACUC UU UGU G CC U CC U G CG </pre>	- 34.1	10q25.3	

- Names of the putative new miRNA sequences are according to the submission to miRBase (<http://www.mirbase.org>).
- RNA secondary structure prediction and free energy calculation have been done using mFOLD version 3.2. The miRNA sequences are underlined. Due to the characteristics of 454 sequencing, the putative miRNA sequences might extend to the additional "A" at the end. The actual size of the stem-loop has not been experimentally determined.
- The genomic locations of human miRNAs are referring to the positions in human chromosomes according to the assembly from GenBank.
- mmu, *Mus musculus* (mouse); ptr, *Pan troglodytes* (chimpanzee); mml, *Macaca mulatta* (monkey).

Table 2.5 Numbers of novel human miRNA reads in the libraries.

Name	Sequence	Reads in libraries			
		NPC-1	Control-1	NPC-2	Control-2
hsa-mir-1301	UUGCAGCUGCCUGGGAGUG ^a	15	1	5	0
hsa-mir-1307	ACUCGGCGUGGGCUCGGUCGUGG	22	8	79	22
hsa-mir-2110	UUGGGGAAACGGCCGCUGAGUG ^a	3	1	2	3
hsa-mir-103-2*	AGCUUCUUACAGUGCUGCCUUG	12	1	15	1
hsa-mir-205*	GAUUUCAGUGGAGUGAAGUUC ^a	15	3	9	5
hsa-mir-196b*	UCGACAGCACGACACUGCCUUC ^a	0	1	0	0
hsa-mir-224*	AAAUGGUGCCCUAGUGACUAC ^a	0	0	2	0
hsa-mir-365-2*	AGGGACUUUCAGGGGCAGCUGU	0	0	1	0
hsa-mir-449b*	CAGCCACAACUACCCUGCCACU	1	0	0	0

a. Due to the characteristics of 454 sequencing, the putative miRNA sequences might have additional "A" at the end.

2.2.4 Validation of novel EBV miRNAs

In order to further validate the expression of the novel miRNA candidates, Northern blotting was performed in the EBV-positive cell lines Jijoye, EREB2.5, C666.1, and BL41/B95.8 as well as the EBV-negative B cell line BL41 (Figure 2.2). Probes specific to the two arms of ebv-mir-BART21 as well as ebv-mir-BART22 were readily

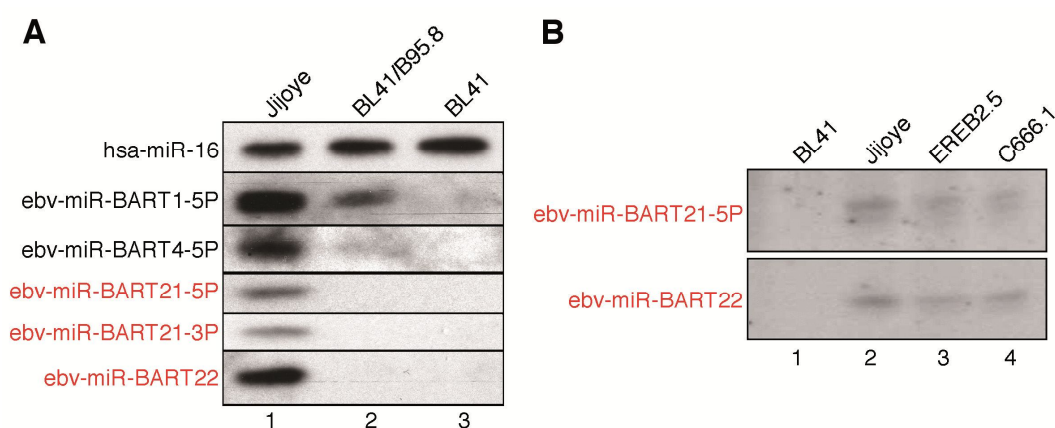


Figure 2.4 Expression analysis of novel EBV miRNAs by Northern blotting. **(A)**. Total RNAs from EBV-positive Jijoye (lane 1) and BL41/B95.8 (lane 2) cells and EBV-negative BL41 cells (lane 3) were blotted onto nylon membranes and hybridized with probes complementary to hsa-mir-16, ebv-mir-BART1-5p, ebv-mir-BART4-5p, ebv-mir-BART21-5p, ebv-mir-BART21-3p, and ebv-mir-BART22. Novel EBV miRNAs are highlighted in red. **(B)**. Total RNAs from BL41 (lane 1), Jijoye (lane 2), EREB2.5 (lane 3), and C666.1 (lane 4) cells were blotted onto a nylon membrane and hybridized with probes complementary to ebv-mir-BART21-5p and ebv-mir-BART22.

detectable in Jijoye, EREB2.5, and C666.1 cells, whereas no signal was observed in BL41/B95.8 and BL41 cells. Notably, the BL41/B95.8 cell line carries a deletion within the BART region where the two novel miRNAs are located (Figure 2.3). The C666.1 cell line originated from an NPC, and its miRNA pattern closely resembles the EBV miRNA pattern in NPC tissues. It is therefore a model cell line for NPC pathogenesis (Cheung et al., 1999).

To further confirm the existence of the new EBV miRNAs in NPC samples, six undifferentiated NPC samples and one control tissue were taken to measure the expression levels of novel miRNAs. HEK 293 cells served as a negative control (Figure 2.5). Since the amount of extracted RNA from the tissues was very low, the RNAs were polyadenylated and reverse transcribed (Hurteau et al., 2006), generating cDNA from miRNA suitable for qRT-PCR validation. GAPDH mRNA was taken for normalization. The background signal from the control tissue sample was set to 1 for calculation. On that basis, all six NPC samples gave strong signals for one known EBV miRNA (ebv-mir-BART1-5p) and three new EBV miRNAs (ebv-mir-BART21-5p, ebv-mir-BART21-3p, and ebv-mir-BART22) tested, indicating that the new EBV miRNAs can be detected in a number of NPC samples.

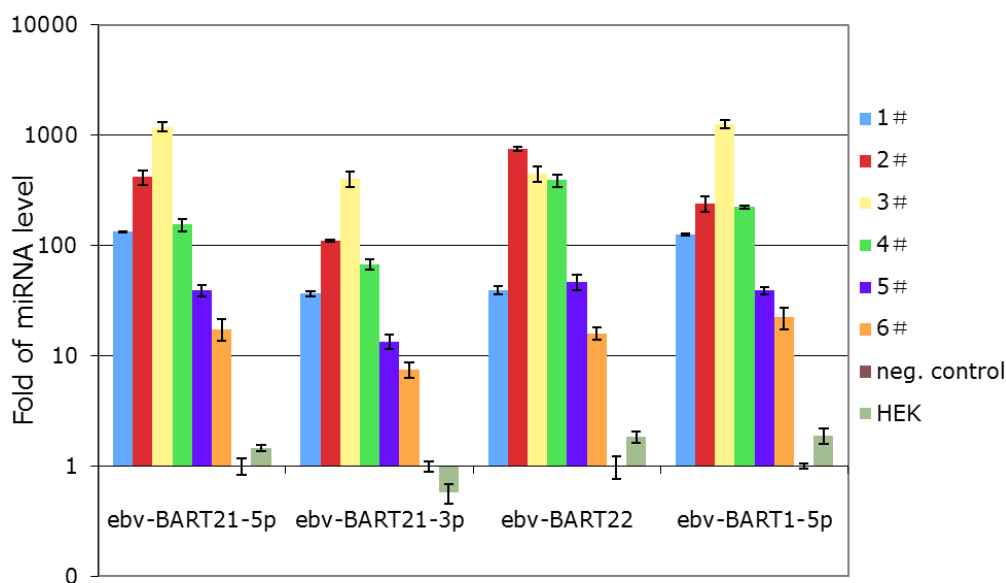


Figure 2.5 Verification of novel EBV miRNA expressions in several NPC samples by qRT-PCR. Total RNA was extracted from six undifferentiated NPC samples (1# to 6#), one tumor negative control tissue samples (neg. control) and HEK cells. Equal amount of RNA was polyadenylated and reverse transcribed using an oligo dT-adaptor primer as described (Hurteau et al., 2006). One known EBV miRNA (ebv-mir-BART1-5p) and three new EBV miRNAs (ebv-mir-BART21-5p, ebv-mir-BART21-3p, ebv-mir-BART22) levels were measured with normalization to GAPDH mRNA level. The result from the negative control tissue was set as 1. Data is shown in logarithm scale.

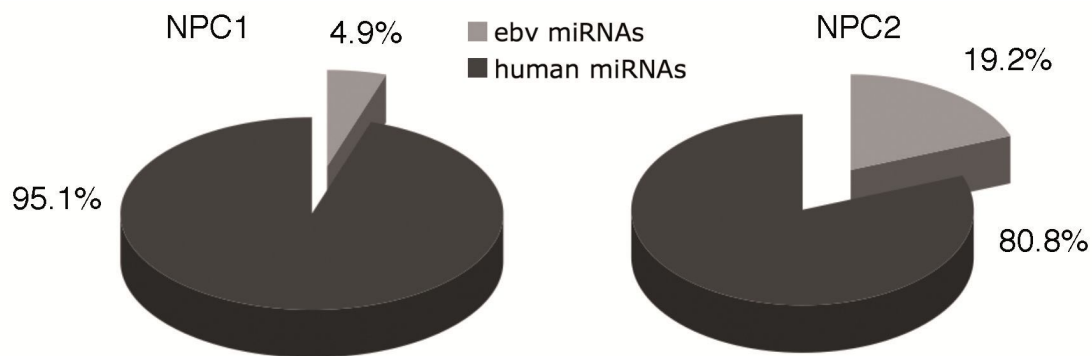


Figure 2.6 MiRNA composition in NPC samples. Schematic representation of cellular and EBV-derived miRNA fractions in NPC tissue samples is shown.

2.2.5 MiRNA expression analysis suggests an NPC-specific miRNA signature

MiRNA expression analyses revealed distinct miRNA signatures for different types of tumors (Calin and Croce, 2006). In order to establish a miRNA expression profile characteristic for NPCs, the viral and cellular miRNAs compositions were examined in detail in the individual library from NPC or control tissues.

Generally, about 5% of the NPC-1 and 19% of the NPC-2 miRNAs were identified as EBV miRNAs, indicating that viral miRNAs are highly expressed in NPCs (Figure 2.6). Notably, small numbers of EBV miRNAs were present in Control-1 as well, which might be due to a minor contamination of the control tissue with tumor tissue (Table 2.1).

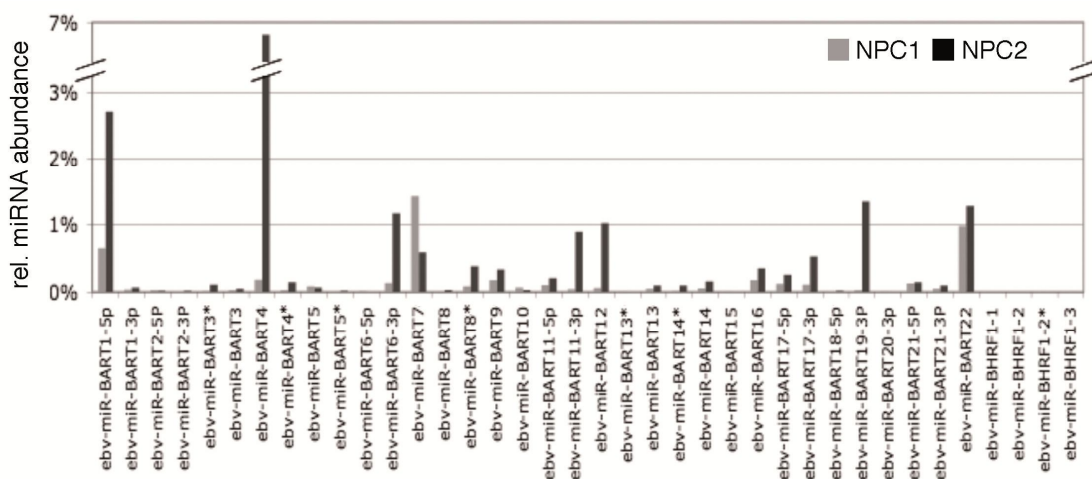


Figure 2.7 Relative abundance of EBV miRNAs in the NPC-1 and NPC-2 libraries. Individual read numbers are presented as percentages of the total miRNA reads in the libraries.

Among the EBV miRNAs, high levels of ebv-mir-BART1, ebv-mir-BART4, ebv-mir-BART6, ebv-mir-BART7, ebv-mir-BART11, ebv-mir-BART12, and ebv-mir-BART19 as well as the new EBV miRNAs ebv-mir-BART21 and ebv-mir-BART22 were found in both NPC libraries. Interestingly, no EBV miRNA from the BHRF1 cluster was detected in the libraries, suggesting that miRNAs from this region might not be involved in NPC pathogenesis (Figure 2.7).

The most abundant human miRNAs are presented in Figure 2.8. The 20 most frequently cloned miRNAs were similar between NPC and control tissues (Appendix Table I). However, hsa-mir-320, hsa-mir-17-5p, and hsa-mir-652 were less frequent in the libraries from the NPCs than in those from control tissues, suggesting that these miRNAs might be downregulated in NPC tissue. On the other hand, the read numbers for hsa-mir-23a/b (both miRNAs were indistinguishable in our sequencing data sets), hsa-mir-200c, and hsa-mir-27a/b were significantly increased in the NPC tumor samples, suggesting specific upregulation of these miRNAs. Consistent with the cloning data, hsa-mir-23a/b and hsa-mir-27a/b were known to be processed from the same primary transcript.

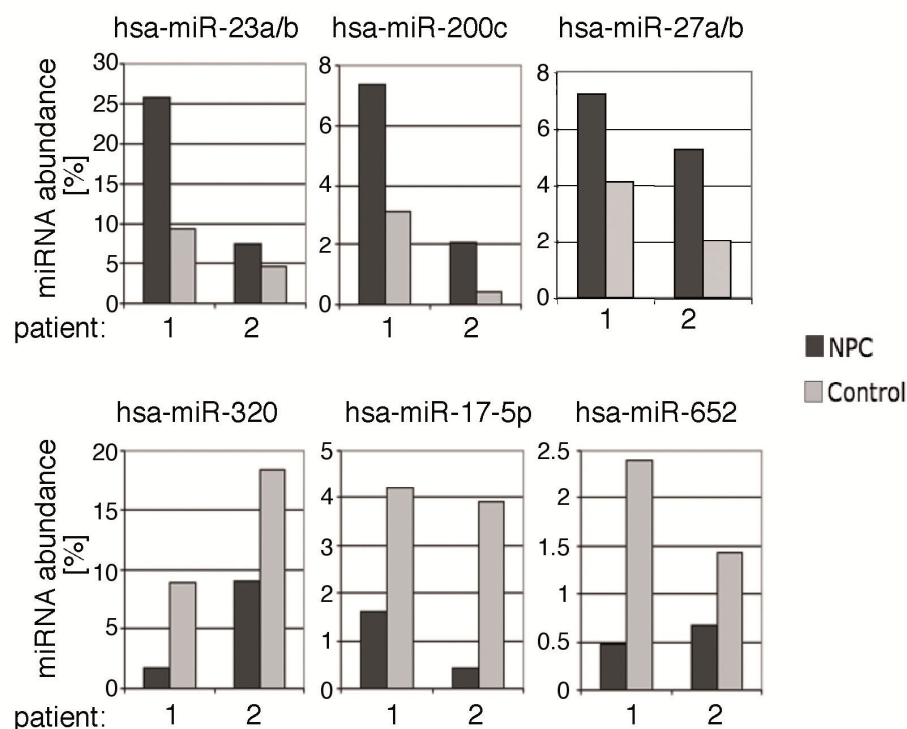


Figure 2.8 Cellular miRNA expressions in NPC and control tissue. Cellular miRNAs hsa-mir-23a/b, hsa-mir-200c, and hsa-mir-27a/b are upregulated in NPC tissues. Hsa-mir-320, hsa-mir-17-5p, and hsa-mir-652 are more abundant in small RNA libraries from control tissue samples. The criteria for miRNA selection were a 1.8-fold change in both patients and at least 1% abundance in two of the four libraries. MiRNA read numbers are shown as percentages of the total miRNA reads in the libraries.

2.2.6 Misregulated miRNAs hsa-mir-15a and hsa-mir-16 inhibit expression of tumor suppressor BRCA1

Next, the potential targets of the miRNAs that are mis-expressed in the two NPC libraries were analyzed. In both NPC samples, expressions of hsa-mir-15a and hsa-mir-16, which are derived from one primary transcript, were upregulated (Figure 2.9). Indeed, bioinformatic predictions identified target sites for hsa-mir-15a and hsa-mir-16 in the 3'UTR of the tumor suppressor BRCA1 (Breast Cancer 1) (Figure 2.10 A). Therefore, high levels of hsa-mir-15a and has-mir-16 may lead to low levels of BRCA1, resulting in low tumor suppressor activity and tumor growth in NPC cells.

In order to analyze the effects of hsa-mir-15a and hsa-mir-16 on BRCA1 expression, the BRCA1 3' UTR was fused to a firefly-renilla dual luciferase reporter. The reporter plasmid was transfected into HEK 293 cells together with 2'-O-Methylated (2'OMe-) antisense inhibitors against endogenous hsa-mir-15a or hsa-mir-16 (Meister et al., 2004a). Indeed, luciferase expression was elevated when endogenous hsa-mir-15a or hsa-mir-16 was inhibited, suggesting that BRCA1 is regulated by hsa-mir-15a and hsa-mir-16 (Figure 2.10 B).

To further validate a functional interaction of the miRNA pathway with the BRCA1 mRNA, the binding of Ago proteins to the BRCA1 mRNA was investigated. It was shown that miRNA target mRNAs can be immunoprecipitated and identified using antibodies against Ago proteins (Beitzinger et al., 2007; Easow et al., 2007; Hendrickson et al., 2008; Karginov et al., 2007). Endogenous Ago1 and Ago2 complexes were immunoprecipitated from a HEK 293 cell lysate by using Ago1- and Ago2-specific antibodies, and co-immunoprecipitated mRNAs were analyzed by qRT-PCR. As shown in Figure 2.10 C, BRCA1 mRNA was coimmunoprecipitated with

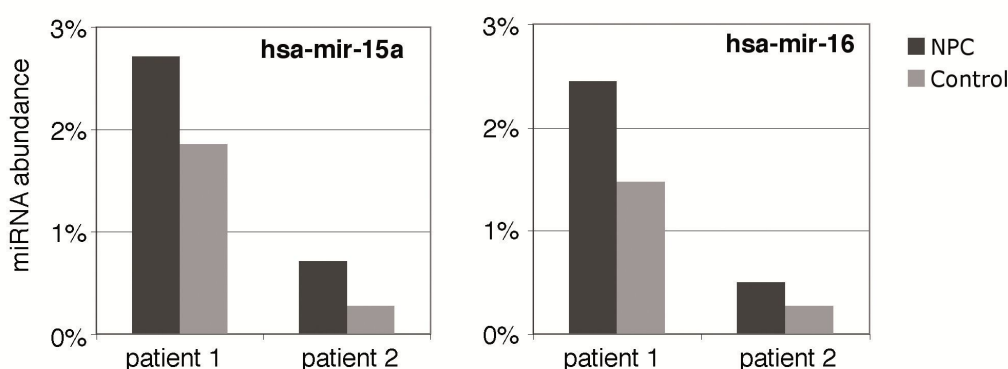


Figure 2.9 Expressions of hsa-mir-15a and hsa-mir-16 are upregulated in two NPC samples compared to healthy tissues. MiRNA read numbers are shown as percentages of the total miRNA reads in the libraries.

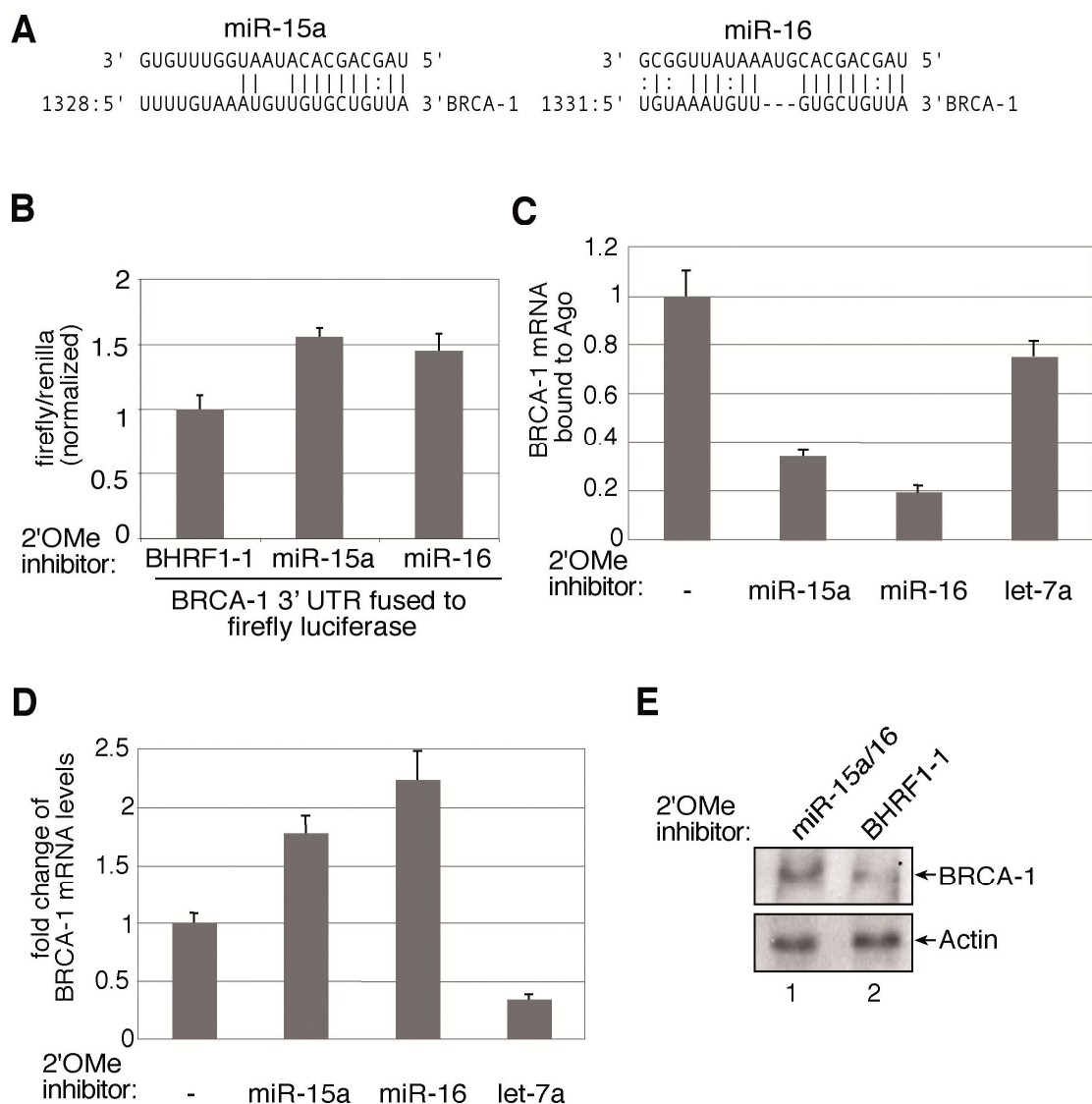


Figure 2.10 Hsa-mir-15a and hsa-mir-16 target BRCA1 mRNA. (A) Putative binding sites of hsa-mir-15a and hsa-mir-16 in the BRCA1 3'UTR predicted by Miranda (John et al., 2004). (B) A firefly luciferase reporter fused to the BRCA1 3'UTR was cotransfected with 2'OMe-antisense inhibitors against hsa-mir-15a or hsa-mir-16 into HEK 293 cells. Firefly luciferase expression was measured after 48 h and normalized to *Renilla* luciferase expression. (C) Ago1- and Ago2-containing complexes were immunoprecipitated by monoclonal antibodies from HEK 293 cell lysates transfected with miRNA inhibitors as indicated. RNAs were extracted and reverse transcribed from immunoprecipitated Ago1/2 complexes. BRCA1 mRNA incorporated into Ago1/2 complexes was measured by qRT-PCR and normalized to the GAPDH mRNA level. (D) Total RNA was extracted and reverse transcribed from HEK 293 cells transfected with miRNA inhibitors as indicated. BRCA1 mRNA levels were quantified by qRT-PCR and normalized to GAPDH mRNA levels. (E) Analysis of BRCA1 protein levels by Western blotting. Lysates of MCF-7 cells transfected with 2'OMe-antisense inhibitors to hsa-mir-15a and hsa-mir-16 (lane 1) or to ebv-mir-BHRF1-1 as a control (lane 2) were transferred to nitrocellulose membranes and analyzed by Western blotting using anti-BRCA1 antibodies.

anti-Ago1 and anti-Ago2 monoclonal antibodies. Moreover, the BRCA1 mRNA was released from Ago protein complexes when 2'OMe- inhibitors complementary to hsa-mir-15a or hsa-mir-16, which interrupt miRNA-mRNA interactions, were transfected, indicating that BRCA1 is targeted by the miRNA pathway.

Finally, BRCA1 mRNA as well as protein levels were measured in the presence or absence of hsa-mir-15a or hsa-mir-16 inhibitor. MiRNAs suppress target protein synthesis either by induction of target mRNA degradation or translational repression. The qRT-PCR reveals that, endogenous BRCA1 mRNA was robustly increased when hsa-mir-15a or hsa-mir-16 was inhibited (Figure 2.10 D). Notably, inhibition of hsa-let-7a, a miRNA that does not target BRCA1, led to a decrease of BRCA1 mRNA levels, which was most likely due to unrelated, secondary hsa-let-7a effects. Consistent with the mRNA expression data, an increase in BRCA1 protein levels was also observed when hsa-mir-15a and hsa-mir-16 were inhibited (Figure 2.10 E).

In summary, the data suggest that hsa-mir-15a and hsa-mir-16 are upregulated in NPC samples and target the tumor suppressor BRCA1.

2.2.7 Summary of results from NGS data in NPC samples

Taken together, 454 sequencing in two pairs of NPC samples with corresponding control tissues has identified two novel EBV and three novel human miRNA genes, together with a number of previously unidentified EBV and human star miRNAs. The miRNA composition has suggested a unique expression signature of NPC samples compared to healthy tissues. Among the dysregulated miRNAs, hsa-mir-15a and hsa-mir-16 were shown to be elevated in both NPC samples, and they were revealed to target the tumor suppressor BRCA1 at both mRNA and protein levels.

2.3 Analysis of Small RNA Libraries from MHV-68 infected Cell Lines

Next, the small RNA cloning and NGS approach were employed in MHV-68 infected cell lines, of which the viral miRNAs had not been well characterized. Nine miRNA genes had been so far identified in MHV-68 genome (Pfeffer et al., 2005). 454 sequencing technology was utilized in this miRNA study of MHV-68 infected cell lines compared to control cell lines, to investigate whether there were more novel MHV-68 miRNA genes, and to study miRNA profiles in differentially treated cell lines, so as to explore the roles of MHV-68 and cellular miRNAs during viral infection and life cycle.

2.3.1 Small RNA cloning and sequencing of MHV-68 infected cells

In order to validate the expression of known and to identify novel MHV-68 miRNAs, murine fibroblast NIH 3T3 cells were infected with MHV-68, which results in lytic replication (sample NIH 3T3+). Uninfected NIH 3T3 cells served as negative control (sample NIH 3T3-). In addition, S11 cells, the B lymphoma cell line persistently infected with MHV-68, were also analysed. S11 cells were either left untreated (sample S11-) or were treated with TPA (12-O-tetradecanoylphorbol-13-acetate) to induce the lytic cycle (sample S11+). Small RNAs were extracted and sequenced using 454 sequencing technology. 59922 reads were obtained from NIH 3T3-, 54135 reads from NIH 3T3+, 43035 reads from S11- and 60704 reads from S11+ after barcode sorting (GEO number GSE22938). After removal of the adapter sequences, more than 99% of the remaining reads are longer than 15 nt, which were taken for the subsequent analysis (Table 2.6).

After thorough analysis of the reads against both MHV-68 and mouse genomes, it was found that the majority of reads are miRNA sequences, while there was a minor portion derived from degradation products of other nc RNAs (Table 2.6 and Figure 2.11), indicating good quality of the small RNA libraries. Accordingly, no MHV-68 sequence was found in the NIH 3T3- sample. Nearly 10% of the reads in both the S11- and S11+ libraries were MHV-68 sequences, i.e. much more than the 0.5% in MHV-68 infected NIH 3T3 cells (Figure 2.11).

Table 2.6 Sequence distribution of small RNA libraries from MHV-68 infected cell lines.

	NIH3T3-	NIH3T3+	S11-	S11+
total reads	59922	54135	43035	60704
>15nt	59360	53920	42699	59773
MHV-68 sequences	0	276	4129	5575
MHV-68 known miRNA	0	194	3237	4425
MHV-68 novel star	0	55	370	536
MHV-68 novel miRNA	0	23	496	576
MHV-68 miRNA loop	0	1	3	2
other MHV-68 sequence	0	3	23	36
mmu sequences	53555	49407	33575	45657
mmu known miRNA	49879	46888	29977	38896
mmu noval star	190	123	78	141
mmu miRNA loop	39	12	39	59
mmu rRNA	1007	345	1324	3176
mmu tRNA	1860	1706	1540	2110
mmu ncRNA	580	333	617	1275

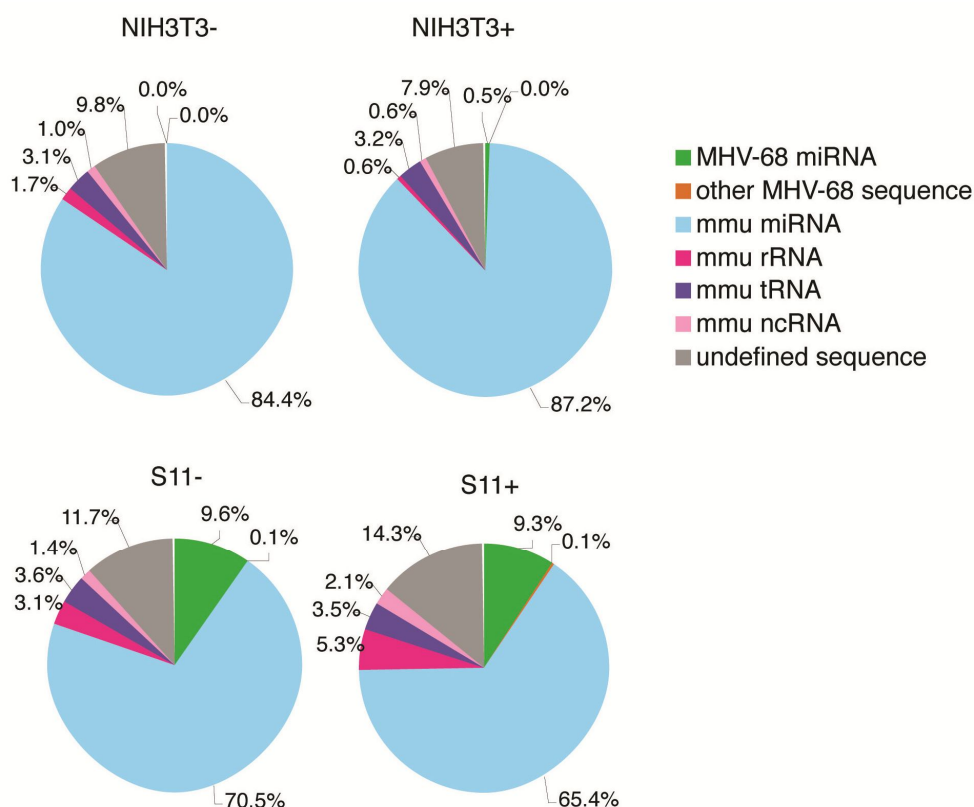


Figure 2.11 Comprehensive analysis of small RNA libraries by 454 sequencing constructed from NIH 3T3 and S11 cells. Schemes show the abundance of MGHV-68 and murine sequences (mmu) as the percentage of read numbers in NIH 3T3 and S11 small RNA libraries by 454 sequencing.

2.3.2 Identification of novel MGHV-68 miRNA genes

By analyzing the pool of MGHV-68 sequences from the small RNA libraries, a considerable number of reads did not match to known mature MGHV-68 miRNAs in miRBase v14.0. However, among them, about half of the sequences matched to known miRNA hairpins, and were thus characterized as novel star miRNAs (Table 2.6 and Table 2.7). The remaining MGHV-68 sequences were analyzed using the secondary structure prediction program mFOLD by extracting the flanking sequences from MGHV-68 genome. In this way, six novel MGHV-68 miRNA genes (termed mghv-mir-M1-10 to mghv-mir-M1-15), which give rise to 11 mature miRNAs in total, were identified (Table 2.7). Mghv-mir-M1-11 is a perfectly matched hairpin, but has only very low read numbers from both arms. The other five hairpins show common imperfect miRNA folding structure, and are biased in generating the mature miRNAs from the 3-prime arm (Table 2.7 and Table 2.8).

Table 2.7 MiRNA read numbers of known and novel viral precursors from MHV-68 infected samples.

Name ^a	Sequence	Number of reads in the libraries		
		NIH 3T3+	S11-	S11+
mghv-mir-M1-1	UAGAAAUGGCCGUACUCCUUU	35	1168	1572
mghv-mir-M1-1*	AGGAAGUGGGUCCAACUU	0	2	0
mghv-mir-M1-2	CAGACCCCCUCUCCCCUCUUU	1	36	71
mghv-mir-M1-2-5p	AGAGGGGGAGUGUGUGGUCUGU ^b	19	149	225
mghv-mir-M1-3	GAGGUGAGCAGGAGUUGCGCUU	7	29	42
mghv-mir-M1-3*	AGCGAACCCUCUGCUCACUGCCC	0	9	15
mghv-mir-M1-4	UCGAGGAGCACGUGUUAUUCUA	0	23	29
mghv-mir-M1-4*	AGAUAGCAUGUGCCGUCCUUU	0	6	7
mghv-mir-M1-5	AGAGUUGAGAUCGGGUCGUCUC	8	144	275
mghv-mir-M1-5*	AGGCAAACCCGAGCUCCUUU	29	28	84
mghv-mir-M1-6	UGAAACUGUGUGAGGUGGUUUU	1	38	101
mghv-mir-M1-6*	CAACCACCUCCACAAUUUCAG ^b	0	22	28
mghv-mir-M1-7-5p	AAAGGUGGAGGUGCGGUAACCU	11	140	231
mghv-mir-M1-7-3p	GAUAUCGCGCCACCUUUAUU	12	306	510
mghv-mir-M1-8	AGCACUCACUGGGGUUUGGUC	61	679	977
mghv-mir-M1-8*	UGACCAACCCUAAGUGAGUUUU	7	154	177
mghv-mir-M1-9	UCACAUUUGCCUGGACCUUUUU	58	674	617
mghv-mir-M1-10	UGAUUACACGGAAGGUUCUUUU	5	62	90
mghv-mir-M1-10*	UUAAGAACCCUCAGUGCAAUC ^b	1	20	12
mghv-mir-M1-11-5p	AGCUGUCAGGGGUUACAUG ^b	0	0	1
mghv-mir-M1-11-3p	UGUAACCCUCGACAGCUGUC	0	1	0
mghv-mir-M1-12	UUUGGUGUGGGAGUCCUACCCUUU	4	76	103
mghv-mir-M1-12*	AAGGGUACUCUCAUCACCAAUGU ^b	0	1	2
mghv-mir-M1-13	UAUCUCAUGUGAGCUCUUCUUU	8	254	276
mghv-mir-M1-13*	UGGGAAGAGUCUGUUGAGUGGC	0	1	4
mghv-mir-M1-14	UGCUACAGCGUGCAGAACGUUU	2	74	78
mghv-mir-M1-14*	CCCGUUCUGGAUGCUGUGGGAC ^b	3	7	8
mghv-mir-M1-15	AGCUACCCGCGUGGCCGGAGUGUUU	0	0	2

- a. The definition of miRNAs and star miRNAs of a precursor is according to the relative abundance of the reads of both arms. Names in black are the known miRNAs. Names in red are the novel star miRNAs of known precursors. Names in blue are the novel miRNAs of novel precursors.
- b. Due to the characteristics of 454 sequencing, the putative miRNA sequences might extend to the additional "A" at the end.

Table 2.8 Novel candidate MHV-68 miRNAs of novel precursors identified from MHV-68 infected samples.

Candidate miRNA ^a	Stem-loop structures of putative miRNA precursors ^b	dG ^b (kcal/mol)	Genomic location ^c
<i>mgHV-mir-M1-10*</i>	<u>UU</u> C A C GUCUG	- 21.5	262-282
<i>mgHV-mir-M1-10</i>	AAGAACC UC GUG AAUCACUU C UUUCUUGG AG CAC UUAGUGAG A	- 21.5	301-322
	<u>UU</u> A G A GUUU		
<i>mgHV-mir-M1-11-5P</i>	AG GACAGCUGUCAGGGGUUACAUGAG A	- 44.9	762-780
<i>mgHV-mir-M1-11-3P</i>	CUGUCGACAGUCCCAAUGUACUU A C	- 44.9	792-811
<i>mgHV-mir-M1-12*</i>	GUAA U AAAUUAAU	- 21.5	1722-1744
<i>mgHV-mir-M1-12</i>	GGGU---ACUCUCA CACCAAUGU A CCCA UGAGGGU- GUGGUUUCA U UUUUC UCC AACGAUG	- 21.5	1764-1788
<i>mgHV-mir-M1-13*</i>	U UGU C- UA	- 19.6	3749-3770
<i>mgHV-mir-M1-13</i>	GGGAAGAG- UC UGAG- UGGC GCG G UUUCUUCUC AG ACUC AUCG UGU G U G UGU U AA U	- 19.6	3787-3808
<i>mgHV-mir-M1-14*</i>	GCCC G G CUGA	- 28.7	5105-5126
<i>mgHV-mir-M1-14</i>	CGUUCUG AUGCUGUGG ACA A GCAAGAC UCGGACAUC UGU A UUUU G G CGUU	- 28.7	5140-5161
<i>mgHV-mir-M1-15</i>	CU -C-- CC- U U	- 15.7	5462-5486
	AG ACCCG GUGG GGAG GU U UC UGGGC CACC UCUC CA A UC CUUC CAA C G		

- Names of the putative new miRNA sequences are according to the submission to miRBase (<http://www.mirbase.org>). The definition of miRNAs and star miRNAs of a precursor is according to the relative abundance of the reads of both arms (See Table 2.7).
- RNA secondary structure prediction and free energy calculation have been done using mFOLD version 3.2. The miRNA sequences are underlined. Due to the characteristics of 454 sequencing, the putative miRNA sequences might extend to the additional "A" at the end. The actual size of the stem-loop has not been experimentally determined.
- The genomic locations of MHV-68 miRNAs are referring to the positions in MHV-68 genome (GenBank accession number NC_001826.2).

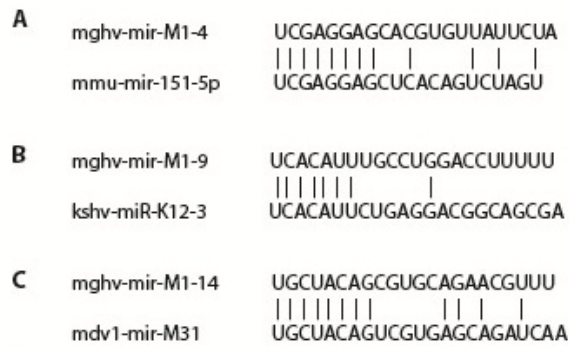


Figure 2.12 Seed sequence homology among MHV-68 miRNAs and murine or other herpesvirus miRNAs. The alignment of three MHV-68 miRNA sequences and murine or other herpesvirus miRNA sequences is shown.

Furthermore, the seed homology of the known and newly identified MHV-68 miRNAs was investigated by comparing to the miRNAs from mouse and other herpesviruses, since both Kaposi's sarcoma-associated herpesvirus (KSHV) and Marek's disease virus (MDV) have been reported to encode the functional orthologs of the oncogenic mir-155 (Skalsky et al., 2007; Zhao et al., 2009). Intriguingly, mghv-mir-M1-4 shows the same seed sequence as mmu-mir-151-5p, which has been revealed to be an important oncogenic factor during tumor invasion and metastasis (Ding et al., 2010) (Figure 2.12 A). On the other hand, mghv-mir-M1-9 and newly identified mghv-mir-M1-14 have the seed homology with two miRNAs from KSHV and MDV (Figure 2.12 B and C). This information suggests that miRNAs from different viruses or even mouse may regulate similar target mRNAs.

2.3.3 Genomic organization of novel MHV-68 miRNAs

Interestingly, like the already known nine MHV-68 miRNAs, all six novel miRNA genes are situated within the first 6 kbp at the left end of the MHV-68 genome and are located closely to the eight vtRNAs, except for mghv-mir-M1-11 (Figure 2.13).

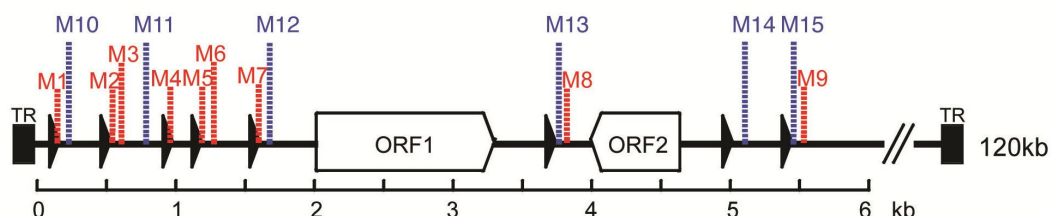


Figure 2.13 MHV-68 miRNAs are located directly after vtRNA sequences. Genomic locations of MHV-68 miRNAs are shown, modified from (Pfeffer et al., 2005). The first 6 kbp of the MHV-68 genome are depicted. Black triangles represent the 8 vtRNA sequences. M1 to M9 (in red) are the known MHV-68 miRNA precursors. M10 to M15 (in blue) are the 6 novel MHV-68 miRNA genes identified in this paper. ORF: open reading frame; TR: terminal repeat.

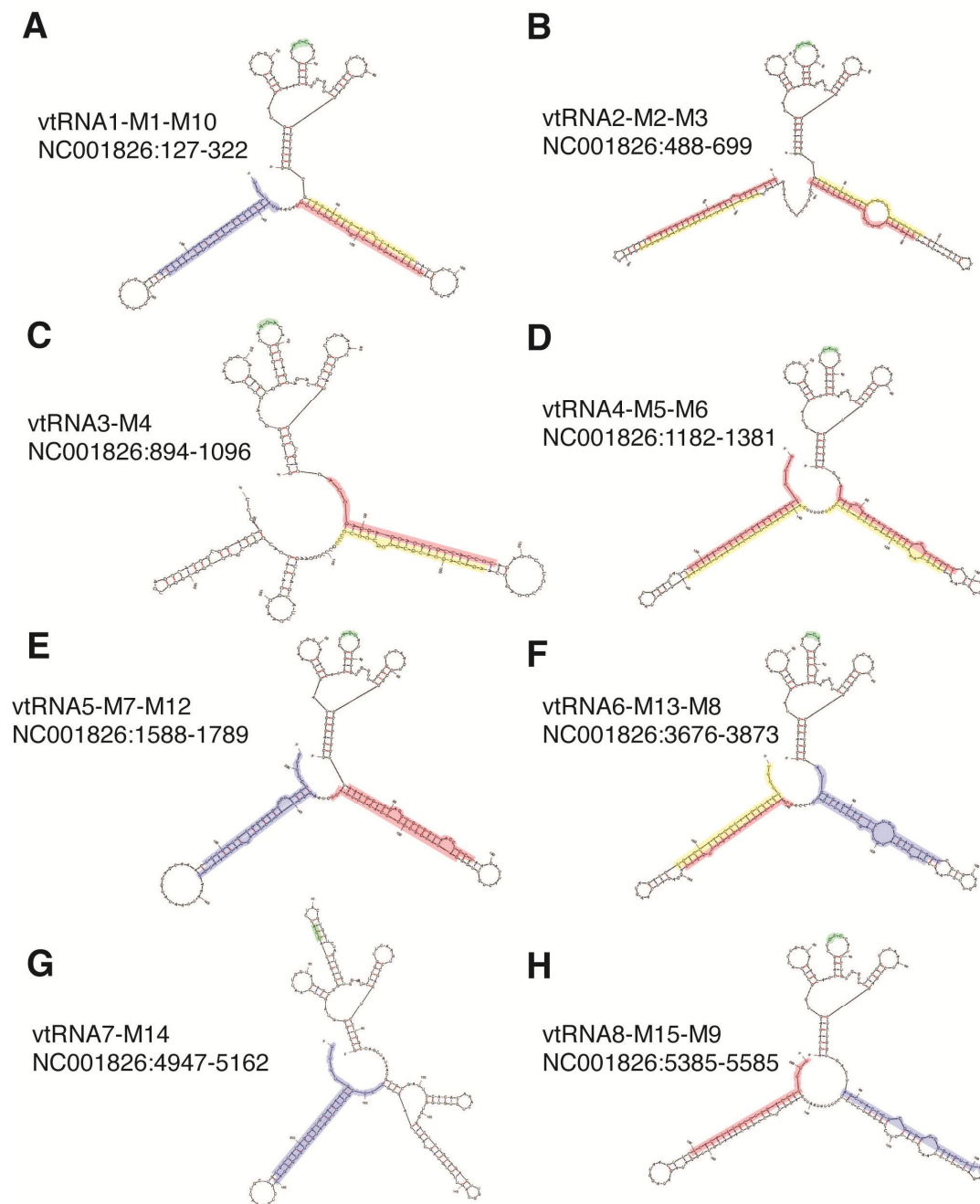


Figure 2.14 Unique vtRNA-miRNA-miRNA structures in MHV-68 genome. RNA folding structures of 8 vtRNA sequences and their subsequent miRNAs are shown. Sequences in green are the predicted anticodons of the vtRNA sequences (Bowden et al., 1997). Sequences in red are the known MHV-68 miRNAs. Sequences in yellow are the novel star miRNAs of known precursors. Sequences in blue are the novel miRNAs of novel MHV-68 miRNA precursors. The genomic locations of the sequences are annotated aside.

The novel MHV-68 miRNAs are positioned either immediately following the known miRNAs (Figure 2.14 A and E), or between the vtRNAs and known miRNAs (Figure 2.14 F and H). The vtRNA-miRNA-miRNA structure is common for six of the eight vtRNAs. There is only one miRNA hairpin structure following vtRNA3 and vtRNA7, and the other stretch was neither able to form a hairpin according to mFOLD (Figure 2.14 C and G), nor was any corresponding read found from the libraries. Furthermore, these specifically structured RNA sequences of approximately 200 nt in length all start with the conserved A/B box promoter for RNA polymerase III in the vtRNAs, and end with a poly(U) sequence which serves as the terminus for RNA polymerase III, implying that the vtRNA-miRNA-miRNA sequences are transcribed as a long primary transcript and are then processed further into mature miRNAs.

2.3.4 Validation of the novel MHV-68 miRNA expression

To further validate the existence of the novel MHV-68 miRNAs, Northern blotting was performed with RNAs isolated from S11 cells. RNAs were extracted from either total cell lysates or from lysates after immunoprecipitation (IP) with a monoclonal anti-mouse Ago2 antibody. As the negative control, immunoprecipitation were performed using an isotype-matched control antibody (anti-BrDU). Probes against the abundant mghv-mir-M1-10, mghv-mir-M1-12 and mghv-mir-M1-14 were well

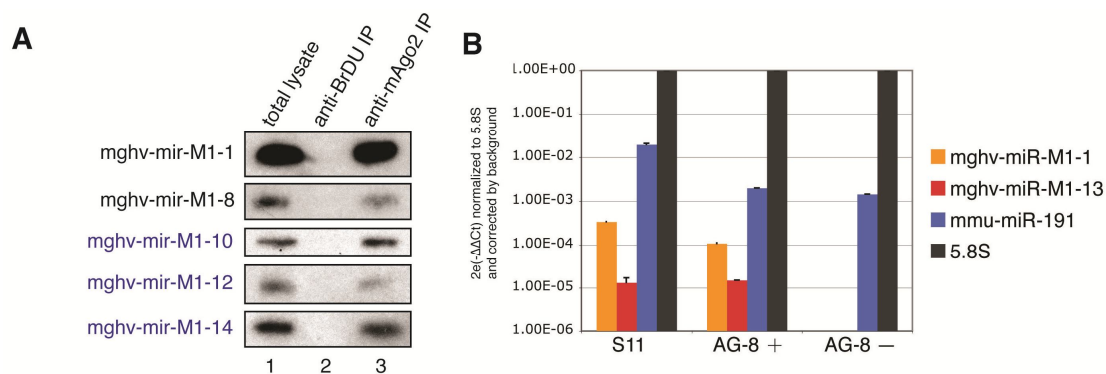


Figure 2.15 Validation of novel MHV-68 miRNAs. (A). Northern blot validation of novel MHV-68 miRNAs. RNAs were extracted from total S11 cell lysates (lane 1), anti-BrDU control IP (lane 2), and anti-mAgo2 immunoprecipitation (IP) using monoclonal antibody 6F4 (lane 3), and blotted onto a nylon membrane. Probes complementary to known or novel MHV-68 miRNAs were labelled and used for detection. Novel MHV-68 miRNAs are highlighted in blue. **(B).** Stem-loop qRT-PCR validation of the novel MHV-68 miRNA mghv-mir-M1-13. RNA was extracted from total cell lysates of S11 cells and from infected or uninfected Ag-8 cells. The latter served as a negative control. The samples were subjected to stem loop qRT-PCR as described in materials and methods. Data shown are means \pm SD of triplicate experiments. As positive control, the expressions of mghv-mir-M1-1 and cellular miRNA mmu-mir-191 are also shown.

detectable not only in total cell lysates but also in the anti-mAgo2 co-immunoprecipitated samples (Figure 2.15 A), indicating that the novel MHV-68 miRNAs, like cellular and already known MHV-68 miRNAs, are efficiently associating with functional RISC complexes. Only a very weak signal could be detected from the probe against mghv-mir-M1-13 (data not shown). However, the expression of mghv-mir-M1-13 was shown by a more sensitive stem-loop qRT-PCR (Figure 2.15 B) in both S11 cells and in Ag-8 myeloma cells 48 hours after infection with MHV-68. No MHV-68 miRNAs were detectable in uninfected Ag-8 cells, while the cellular miRNA mmu-mir-191 was detected in all three samples.

Since MHV-68 miRNAs derive from unusual precursors, it was interesting to investigate whether the MHV-68 miRNAs employ the same miRNA processing machinery as cellular miRNAs. To this end, Dicer-deficient mouse embryonic fibroblasts (*Dicer*^{-/-} MEF) were infected with MHV-68 and miRNA generation was monitored. Two independently derived *Dicer*^{-/-} MEF clones were tested. Compared to wildtype MEFs (*Dicer*^{+/+}), *Dicer*^{-/-} MEFs were not able to produce mature cellular or MHV-68 miRNAs (Figure 2.16). Thus, MHV-68 miRNAs are processed by a Dicer-dependent pathway.

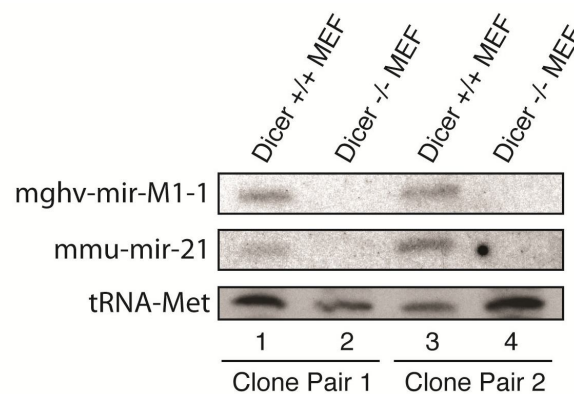


Figure 2.16 MHV-68 miRNAs are generated in a Dicer-dependent pathway. MHV-68 miRNA generation in MHV-68 infected *Dicer*^{-/-} MEFs was monitored. Two independent clones of *Dicer*^{-/-} MEFs (lane 2 and lane 4) were infected with MHV-68 in parallel with wildtype controls (lane 1 and lane 3). Total RNAs were extracted and blotted onto a nylon membrane. Probes complementary to mghv-mir-M1-1 and mmu-mir-21 were labelled and used for detection. Probing against tRNA-Met served as a loading control.

2.3.5 Cellular miRNA profiles in NIH 3T3 and S11 cells

Apart from the MHV-68 sequences, the majority of reads in the sequencing libraries were murine miRNA sequences. Annotating these sequences by miRBase v14.0, a significant number of reads derived from the other arm of known murine miRNA hairpins were found. Altogether, 61 novel murine star miRNAs were identified and registered (Table 2.9).

Table 2.9 Sequences and read numbers of murine novel star miRNAs in the sequencing libraries.

Name ^a	Sequence	Number of reads in the libraries			
		NIH3T3-	NIH3T3+	S11-	S11+
mmu-let-7a-2*	CUGUACAGCCUCCUAGCUUUC	1	1	1	0
mmu-let-7e*	CUAUACGGCCUCCUAGCUUUC	7	15	0	0
mmu-let-7f-2*	CUAUACAGUCUACUGUCUUUC	6	2	5	5
mmu-mir-100*	ACAAGCUUGUGUCUAAUAGGUAU	1	1	0	0
mmu-mir-103-1*	GGCUUCUUUACAGUGCUGCCUUG	0	5	0	0
mmu-mir-103-2*	AGCUUCUUUACAGUGCUGCCUUG	16	7	3	6
mmu-mir-107*	AGCUUCUUUACAGUGUUGCCUUG	2	2	0	1
mmu-mir-132*	AACCGUGGCUUUCGAUUGUAC	0	0	1	1
mmu-mir-134*	CUGUGGGCCACCUAGUCACC ^b	2	5	0	0
mmu-mir-143*	GGUGCAGUGCUGCAUCUCUGG	7	2	0	0
mmu-mir-152*	UAGGUUCUGUGAUACACUCCGACU	1	0	0	0
mmu-mir-155*	CUCCUACCUGUUAGCAUUAAC ^b	0	0	3	6
mmu-mir-16-2*	ACCAAUAUUAUUGUGCUGCUUU ^b	27	24	16	24
mmu-mir-181b-1*	CUCACUGAACAUAUGAAUGC ^b	2	0	0	0
mmu-mir-181c*	ACCAUCGACCGUUGAGUGGACC	5	1	0	0
mmu-mir-182*	GUGGUUCUAGACUUGCCAACU ^b	0	2	0	0
mmu-mir-190*	ACUAUAUAUCAAGCAUAUCCU ^b	1	0	0	0
mmu-mir-1948*	AUAUGAGUAUUCUGCCUAAU	1	0	0	1
mmu-mir-195*	CCAAUAUUGGCUGUGCUGCUCC ^b	0	1	0	0
mmu-mir-196a-1*	CAACGACAUCAAACCACCUGAU	0	2	0	0
mmu-mir-196b*	UCGACAGCACGACACUGCCUUC ^b	1	0	0	0
mmu-mir-1981*	CAUCUAACCCUGGCCUUUGAC ^b	1	2	0	0
mmu-mir-19b-1*	AGUUUUGCAGGUUUGCAUCCAGC	2	1	0	0
mmu-mir-210*	AGCCACUGCCCACCGCACACUG	7	1	0	0
mmu-mir-217*	CAUCAGUUCUAAUGCAUUGCCU	0	1	0	0
mmu-mir-221*	ACCUGGCAUACAAUGUAGAUUUCUGU	8	6	0	0
mmu-mir-222*	UCAGUAGCCAGUGUAGAUCU	1	1	0	0
mmu-mir-23a*	GGGUUCCUGGGGAUGGGAUUU	0	0	3	0
mmu-mir-25*	AGGCGGAGACUUGGGCAAUUGC	0	2	0	0
mmu-mir-26a-2*	CCUGUUCUUGAUUACUUGUUUC	1	1	0	0
mmu-mir-29b-2*	CUGGUUUCACAUGGUGGCUUAGAUAU	0	0	1	0

Table 2.9 (continue) Sequences and read numbers of murine novel star miRNAs in the sequencing libraries.

Name ^a	Sequence	Number of reads in the libraries			
		NIH3T3-	NIH3T3+	S11-	S11+
mmu-mir-301a*	GCUCUGACUUUUAUUGCACUACU	1	0	0	0
mmu-mir-30d*	CUUUCAGUCAGAUGUUUGCUGC	7	2	0	1
mmu-mir-32*	CAAUUUAGUGUGUGUGAUUU	2	0	0	1
mmu-mir-329*	AGAGGUUUUCUGGGUCUCUGUU	0	1	0	0
mmu-mir-34a*	AAUCAGCAAGUAUACUGCCCU ^b	11	2	22	33
mmu-mir-350*	AAAGUGCAUGCUCUUUGG ^b	2	0	0	0
mmu-mir-351*	GGUCAAGAGGCGCCUGGGAAC	2	6	0	0
mmu-mir-361*	UCCCCAGGUGUGAUUCUGAUUUUGU	1	2	2	2
mmu-mir-370*	CAGGUCACGUCUCUGCAGUU ^b	0	2	0	0
mmu-mir-379*	UAUGUAACAUGGUCCACUAACU	2	1	0	0
mmu-mir-410*	AGGUUGUCUGUGAUGAGUUCG	1	0	0	0
mmu-mir-466h-3p	UACGCACGCACACACACAC ^b	1	2	0	0
mmu-mir-466i-5p	UGUGUGUGUGUGUGUGUGUGUG	0	0	2	3
mmu-mir-466l-5p	UUGUGUGUACAUGUACAUGUAU ^b	1	0	0	0
mmu-mir-493*	UUGUACAUGGUAGGCUUUC ^b	1	0	0	0
mmu-mir-497*	CAAACCACACUGUGGUGUUAG ^b	1	0	0	0
mmu-mir-500*	AAUCCUUGCUAUCUGGGUGCUUAGU	0	0	0	1
mmu-mir-543*	AAGUUGCCCGCGUGUUUUUCG	1	0	0	0
mmu-mir-652*	CAACCCUAGGAGGGGGUGCCAUUC ^b	3	0	2	0
mmu-mir-664*	CUGGCUGGGGAAAUGACUGG ^b	1	4	0	0
mmu-mir-669a-1*	ACAUAACAUACACACACAGUAU ^b	22	6	0	0
mmu-mir-669d*	UAUACAUAACACCCAUUAUAC ^b	1	0	0	0
mmu-mir-669f-5p	AGUUGUGUGUGCAUGUGCAUGUGU	7	1	0	0
mmu-mir-670*	UUUCCUCAUAUCCAUCAGGAGUGU	0	3	0	0
mmu-mir-677*	GAAGCCAGAUGCCGUUCCUGAGAAGG	0	0	0	2
mmu-mir-700*	UAAGGCUCUCCUCCUGUGCUUGC ^b	2	1	0	0
mmu-mir-805*	AUUUAUAUGUCUUUCAAGUUCUJAG	0	1	0	0
mmu-mir-92a-1*	AGGUUGGGAUUUUGUCGCAAUGCU	1	1	0	0
mmu-mir-96*	CAAUCAUGUGUAGUGCCAAUUAU	1	0	0	0
mmu-mir-98*	CUAUACAACUJACUACUUUCCU	9	1	0	0

- a. The definition of miRNAs and star miRNAs of a precursor is according to the relative abundance of the reads of both arms (Appendix II).
- b. Due to the characteristics of 454 sequencing, the putative miRNA sequences might extend to the additional "A" at the end.

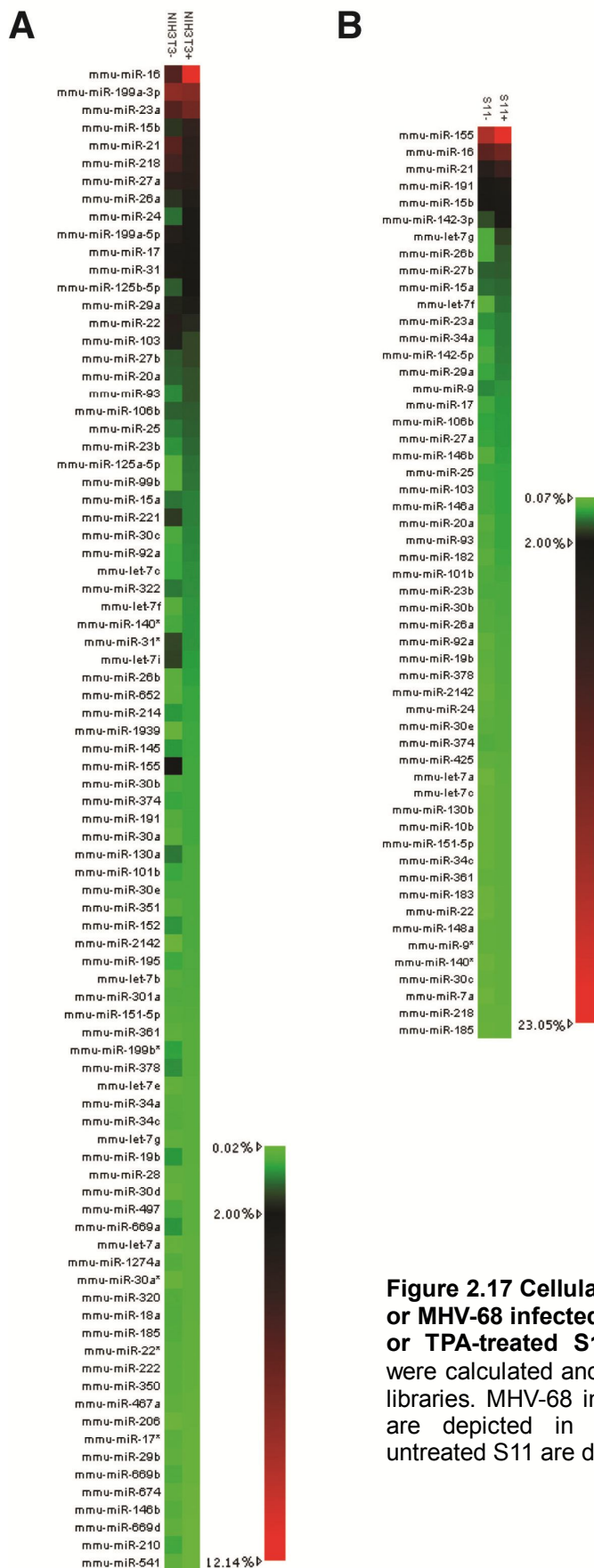


Figure 2.17 Cellular miRNA profiling of uninfected or MHV-68 infected NIH 3T3 cells and of untreated or TPA-treated S11 cells. Cellular miRNA levels were calculated and compared in the four small RNA libraries. MHV-68 infected vs. non-infected NIH 3T3 are depicted in heatmap (A). TPA-treated vs. untreated S11 are depicted in the heatmap (B).

The read numbers of annotated murine miRNAs in the libraries suggested unique miRNA expression signatures of NIH 3T3 and S11 cells (Appendix Table II). NIH 3T3- and NIH 3T3+ cells showed distinct patterns of cellular miRNA expression levels, suggesting that miRNAs may play a role in the cellular response to MHV-68 infection (Figure 2.17 A). The cellular miRNA expression profile was also analysed in TPA-induced versus non-induced S11 cells. The changes after TPA induction were only subtle (Figure 2.17 B).

Among the abundantly expressed cellular miRNAs in NIH 3T3 cells, mmu-mir-16 and mmu-mir-15b, which belong to the same miRNA family, were found to be highly upregulated after MHV-68 infection. This upregulation was further confirmed by Northern blotting (Figure 2.18 A). Mghv-mir-M1-1 was, as expected, only present in NIH 3T3+ cells, and tRNA-Met served as loading control.

In the study of cellular miRNA profiles in EBV-infected NPC samples, it has been shown that hsa-mir-15a and hsa-mir-16 are upregulated in EBV-positive nasopharyngeal carcinoma (Figure 2.9). The tumour suppressor gene BRCA1 was found to be one of the targets that are regulated by miR-15/16 (Figure 2.10). Therefore, the question whether the upregulation of mmu-mir-16 and mmu-mir-15b after MHV-68 infection might also lead to downregulation of BRCA1 in the MHV-68

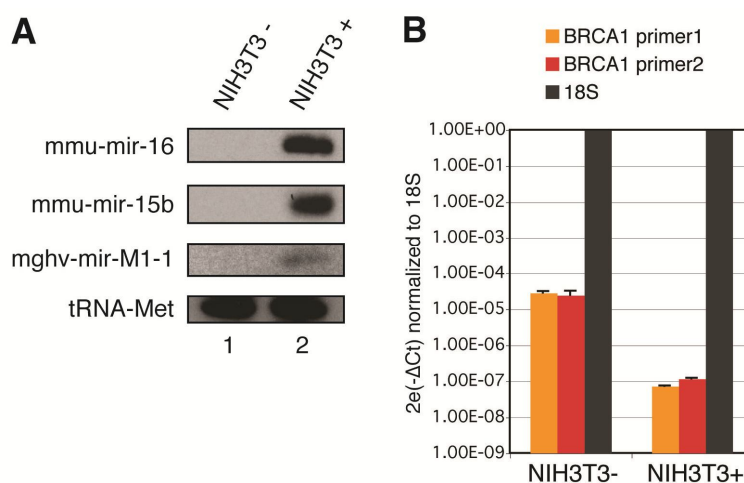


Figure 2.18 miR-15/16 upregulation was observed in MHV-68 infected NIH 3T3 cells. (A). Northern blot validation of cellular miRNAs upregulated after infection of NIH 3T3 cells. Total RNAs were extracted from uninfected (lane 1) or MHV-68 infected NIH 3T3 cells (lane 2). RNAs were blotted onto a nylon membrane and detected by labelled probes complementary to mmu-mir-16, mmu-mir-15b and mghv-mir-M1-1. Probing against tRNA-Met served as a loading control. **(B).** Downregulation of BRCA1 in MHV-68 infected NIH 3T3 cells. To analyse the expression of BRCA1, RNA was isolated from uninfected and MHV-68 infected NIH 3T3 cells 48h after infection and subjected to qRT-PCR using primers specific for BRCA1 and 18S RNA. Data shown are means + SD of triplicate determinations.

model system was further investigated. As shown in Figure 2.18 B, BRCA1 expression was indeed reduced when NIH 3T3 cells were infected with MHV-68, compared to uninfected cells, suggesting that miR-15/16 upregulation and the subsequent BRCA1 downregulation might be a common feature of γ -herpesvirus infection.

2.3.6 Summary of results from NGS data in MHV-68 infected cells

In summary, 454 sequencing has been carried out in two pairs of model cell lines, *i.e.* the MHV-68 infected versus non-infected NIH 3T3 cells and TPA-treated versus untreated S11 cells. Six novel MHV-68 miRNA genes, generating 11 mature miRNAs in total, were identified and validated. Furthermore, the accomplishment of the MHV-68 miRNA set revealed a unique vtRNA-miRNA-miRNA structure in MHV-68 genome. On the other hand, these RNA polymerase III promoter driven transcripts still employ a Dicer-dependent pathway in the biogenesis of MHV-68 miRNAs. Moreover, the analysis of cellular miRNAs in the small RNA sequencing libraries has suggested the expression signature of NIH 3T3 and S11, after the treatment of MHV-68 infection and TPA induction, respectively. The MHV-68 infection in NIH 3T3 cells led to the upregulation of mmu-mir-15b and mmu-mir-16, and the downregulation of BRCA1 expression, which was similar to the consequences of EBV infection in NPC samples, implying a common effect of γ -herpesvirus infection.

2.4 Mis-annotation of MicroRNA Genes in miRBase

By using miRBase as the reference database in our miRNA studies, we found that some miRNA sequences of interest turned out to be the pieces of the other non-coding RNAs (ncRNAs). Therefore, we set out to systematically check all the murine and human miRNA sequences in the database for the mis-annotation. To better distinguish between the mis-annotated miRNAs and the alternatively generated miRNAs from the other ncRNAs, the small RNA libraries by Solexa sequencing accessible through the GEO database, provided by Babiarz *et al.* in the study of Dgcr8 and Dicer dependency in the production of small RNAs (Babiarz *et al.*, 2008), were re-analysed. Surprisingly, the study elucidated that, a considerable number of miRNA genes might have been mis-annotated in the current version of miRBase.

2.4.1 Examination of murine miRNA genes

To systematically analyze the known miRNA genes, the newest version (v15.0) of miRBase, which was just released in April 2010, was downloaded. The most commonly used murine and human miRNA sequences were extracted for a close examination. These miRNA sequences were compared with the other ncRNA gene sequences, including ribosomal RNA (rRNA) genes (Benson et al., 2008), transfer RNA (tRNA) genes (Chan and Lowe, 2009), small nuclear and small nucleolar RNA (snRNA and snoRNA) genes (Szymanski et al., 2003) and the mitochondrial genome sequence (Benson et al., 2008). Since at least snoRNA and tRNA sequences have been reported to produce miRNAs in an alternative pathway (Babiarz et al., 2008; Ender et al., 2008), the finding that some miRNA sequences fully matched to the other ncRNAs was not sufficient to define that these miRNA sequences have been mis-annotated.

Babiarz *et al.* have generated the small RNA libraries from wildtype, Dicer1 knockout and Dgcr8 knockout mouse embryonic stem cells (wt, Dicer1^{-/-}, Dgcr8^{-/-} mESCs) for Solexa sequencing, to study the dependency of these two processor proteins in the production of small RNAs (Babiarz et al., 2008). These libraries were ideal to distinguish the small RNA sequences as miRNAs or the degradation pieces of ncRNAs. Dicer dependency was considered as an important criteria to define a miRNA gene annotation (Ambros et al., 2003). To the knowledge known so far, the Dgcr8-containing microprocessors could be bypassed in the production of miRNAs from mirtrons (miRNAs produced from intron sequences), snoRNAs and tRNAs, but Dicer is dependent in the processing of all miRNAs, only with the exception of mir-451, according to the recent report that, its conserved short hairpin is specifically cleaved by Ago2 (Cifuentes et al., 2010).

For this purpose, Solexa sequencing data of these three libraries were retrieved through the publicly accessible GEO database (GEO number GSE20384), and re-analyzed using the reference of miRBase v15.0. Since it was noticed that, in the large amount of reads produced by Solexa sequencing, the read with errors of nucleotide substitution tend to accumulate especially in the highly abundant reads, the reads with one mismatch in the hit to miRNA sequences were also reserved, in addition to the fully matched reads for further analysis (Appendix Table III and IV).

As expected, 325 murine miRNA genes (mature miRNA and its star miRNA, or same mature miRNA from different precursors, was counted as one miRNA gene) showed nice dependencies on both Dicer1 and Dgcr8, characterized by that, the read numbers of these miRNAs were much more in the wt mESCs libraries than in the

Table 2.10 Read numbers of mentioned murine miRNA entries in three small RNA libraries.

miRNA ^a	wt		Dicer1 ^{-/-}		Dgcr8 ^{-/-}	
	mismatch0 ^b	mismatch1 ^b	mismatch0	mismatch1	mismatch0	mismatch1
mmu-mir-451	111	11	127	4	115	21
mmu-mir-590-3p	0	0	0	0	0	0
mmu-mir-590-5p	0	0	0	0	0	0
mmu-mir-664	14	0	1	0	171	21
mmu-mir-685	13	3	53	2	16	2
mmu-mir-689	19	1	33	11	25	7
mmu-mir-696	2	1	1	1	4	2
mmu-mir-712	5	1	1	0	12	1
mmu-mir-712*	658	66	40	3	306	18
mmu-mir-714	3	1	12	0	3	0
mmu-mir-715	4	2	2	0	2	0
mmu-mir-720	861	118	1440	83	1975	196
mmu-mir-1274a	67	575	305	1659	196	1678
mmu-mir-1937a	273	38	872	67	877	94
mmu-mir-1937b	25	2	192	21	175	23
mmu-mir-1937c	1	2	0	1	2	4
mmu-mir-1944	343	31	657	30	867	67
mmu-mir-1957	0	75	0	270	0	355
mmu-mir-1959	116	143	169	261	221	355
mmu-mir-1971	0	5	0	0	1	254
mmu-mir-1981	37	3	0	0	2770	110
mmu-mir-2132	90	31	256	62	536	147
mmu-mir-2133	41	11	334	46	232	47
mmu-mir-2134	27	3	12	3	40	6
mmu-mir-2135	514	110	304	37	501	79
mmu-mir-2138	827	133	1091	95	1172	196
mmu-mir-2140	71	8	49	1	77	7
mmu-mir-2141	1257	164	1174	68	1779	152
mmu-mir-2142	8946	1125	12243	1268	14705	1808
mmu-mir-2143	662	120	3721	214	3199	275
mmu-mir-2144	532	77	777	61	995	120
mmu-mir-2145	206	26	591	69	821	94
mmu-mir-2146	489	65	353	22	515	45

- a. Names of miRNA entries are according to miRBase v14.0 and v15.0. Names in red are probably mis-annotated miRNAs. Names in blue are the dead miRNA entries removed from miRBase v15.0. Names in black are normal miRNAs.
- b. "Mismatch" refers to the mismatch existed in the alignment of library reads to miRNA sequences. "Mismatch0" means no mismatch. "Mismatch1" means one nucleotide mismatch. The read numbers with one nucleotide mismatch are shown in grey.

Table 2.11 Probably mis-annotated murine miRNA genes that match to other ncRNAs or do not match in murine genome.

miRNA	Sequence	matched RNA
(fully matched)		
mmu-mir-689	CGUCCCCGCUCGGCGGGGUCC	murine 28S rRNA
mmu-mir-2132	GGCGGGUGUUGACGCGAUG	
mmu-mir-2134	GUCUUGGGAAACGGGGUGC	
mmu-mir-2135	AGAGGUCUUGGGGCCGAAAC	
mmu-mir-2138	AAGGGAACGGGCUUGGCGGAAU	
mmu-mir-2140	AGGUGCAGAUCUUGGUGGU	
mmu-mir-2141	AGGAGGUGUCAGAAAAGUU	
mmu-mir-2146	GUGGAGAAGGGUUGCAUGUG	
mmu-mir-2133	GUCCCGCGGGGCCCGAAGCGUU	murine 18S rRNA
mmu-mir-2145	AGCAGGGUCGGGCCUGGUU	murine 5S rRNA
mmu-mir-696	GCGUGUGCUUGCUGUGGG	murine 45S pre-rRNA
mmu-mir-714	CGACGAGGGCCGGUCGGUCGC	
mmu-mir-715	CUCCGUGCACACCCCCGCGUG	
mmu-mir-720	AUCUCGCUGGGGCCUCCA	murine tRNA-Thr(TGT) ^a
mmu-mir-1937a	AAUCCCGGACGAGCCCCCA	murine tRNA-Pro(AGG) ^a
mmu-mir-1937b	AUCCCGGACGAGCCCCCA	
mmu-mir-1944	CUCUGUGCUGAAUGUCAAGUUCUGAUU	murine Snord43 snoRNA
(with one nucleotide mismatch or gap)		
mmu-mir-1274a	UCAGGUCCCUGUUCAGGCGCCA	murine tRNA-Lys(TTT) ^a
mmu-mir-1937c	AUCCCGGAAGAGCCCCCA	murine tRNA-Pro(AGG) ^a
mmu-mir-1939	UCGAUUCCCUGCCAAUGCAC	murine tRNA-Gly(CCC) ^a
mmu-mir-1957	CAGUGGUAGAGCAUAUGAC	murine tRNA-Cys(GCA) ^a
mmu-mir-1959	GGGGAUGUAGCUCAGUGGAG	murine tRNA-Ala(AGC) ^a
(not matched to murine genome)		
mmu-mir-590-5p	GAGCUUAUUCAUAAAAGUGCAG	
mmu-mir-590-3p	UAAUUUUUAUGUAUAAGCUAGU	

- a. There might be more than one tRNA sequences that match to this miRNA, due to the characteristics of tRNA sequences..

Dicer1^{-/-} and Dgcr8^{-/-} mESCs libraries, normally ten-fold or even higher (Appendix Table III). This was similar to what Babiarz *et al.* have observed when miRBase v10.0 was utilized. 131 murine miRNA sequences have no reads or extremely low numbered reads in all three libraries. This might be due to the tissue-specific expression of these miRNAs and were not followed up. 20 miRNA sequences have nearly no reads in Dicer1^{-/-} library, but have much more reads in the Dgcr8^{-/-} mESCs library than in the wt mESCs library. These included all of the mirtrons, snoRNA and tRNA-generated miRNAs known so far, and leave the interesting question to study the processing pathways of the rest of them. The remaining 38 miRNA sequences, which have abundant and similar read numbers in all three libraries, were the most suspicious candidates that could have been mis-annotated. Mir-451 was one of these Dicer1- and Dgcr8- independent sequences, but none of the rest sequences showed the similarity to its specific hairpin structure.

To further test the hypothesis, the dead miRNA entries that have just been removed from the miRBase v15.0 due to mis-annotation were tested. Mmu-mir-2142, mmu-mir-2143 and mmu-mir-2144 were reported to be pieces of rRNA genes, while mmu-mir-685 was reported to be the piece of ncRNA RNase P. The examination of these four sequences in all three sequencing libraries resulted in similar read numbers (Table 2.10), indicating that the independencies from Dicer1 and Dgcr8 in production can be served as the useful evidence in defining whether the miRNA sequences have been mis-annotated, and were actually the degradation products of the other ncRNAs.

First, rRNA-matched murine miRNA sequences were checked. Surprisingly, eight murine miRNAs were found to be matched to murine 28S rRNA sequence, one miRNAs matched to 18S rRNA sequence and one miRNA matched to 5S rRNA sequences (Table 2.11). All of these ten miRNA sequences showed independencies from Dicer1 and Dgcr8 with similar or higher read numbers in both knockout mESCs libraries than in the wt mESCs libraries (Table 2.10). Mouse rRNAs were known to be produced as a 45S rRNA long transcript (Perry, 1976). There were four more miRNAs found to be matched in the additional 45S rRNA regions (Table 2.11). However, different from the other three miRNAs, mmu-mir-712 showed largely reduced read number in Dicer1^{-/-} mESCs library, implying that it might be an interesting miRNA derived from an alternative pathway (Table 2.10). Of note, mmu-mir-689, mmu-mir-696, mmu-mir-714 and mmu-mir-715 have been challenged for the annotation of miRNA genes in another Dicer knockout models (Calabrese *et al.*, 2007).

Next, tRNA gene sequences were examined. The tRNA sequences might not be efficiently annotated in the small RNA sequencing libraries, due to the fact that, the mature tRNAs are modified with the addition of a “CCA” tail (Xiong and Steitz, 2006), but this feature was not reflected in most of the tRNA databases and might also be ignored when the genomic sequence is utilized. Indeed, three murine miRNA sequences were found to be matched to the tRNA sequences with “CCA” in addition (Table 2.11). All of them showed both Dicer1 and Dgcr8 independencies (Table 2.10). Moreover, additional five murine miRNA sequences were found that they have one mismatch to the tRNA sequences (Table 2.11). The detailed analysis in the sequencing libraries revealed that, the perfect match to these miRNA sequences were much less than the sequences with one mismatch (Table 2.10), which turned out to be perfectly matched to the related tRNAs (data not shown), and both read numbers are dispensable of Dicer1 and Dgcr8. The speculation was that, although the error rate of about 1% in NGS is not much higher than the traditional Sanger Sequencing, the ability to produce huge volume of data by NGS is accompanied by the production of many sequences with errors. On the other hand, the principle behind many NGS data annotation programs was first to align the read sequences to the perfectly matched genome loci. It is not surprising when these short sequences with errors were able to find some hits elsewhere in the genome. Furthermore, the hairpin folding condition was stringent enough. These might be reasons for the possible mis-annotation of these miRNA sequences. Since the identification of novel miRNA genes by NGS nowadays does not require further Northern Blotting validation as necessity during the registration to the miRNA database, and it is also difficult to clarify the processing pathways of the low-abundant miRNAs. The actual sequences of identified miRNAs were not very well controlled.

Then, the miRNA sequences were searched for matching to the other ncRNAs, and two murine miRNAs were found (Table 2.11). Among them, mmu-mir-664, matched to one H/ACA snoRNA, got much lower read number in Dicer1^{-/-} mESCs library, than the Dgcr8^{-/-} and wt mESCs libraries, implying a similar processing pathway to the mmu-mir-1839 from H/ACA 45 snoRNA. Mmu-mir-1944, which is matched to Snord43 snoRNA and abnormally long of 27 nt, and has high read numbers in all three libraries (Table 2.10), is probably mis-annotated.

Interestingly, mmu-mir-1971, which is especially short with only 18 nt was also noticed. It might be the truncated form of mmu-mir-1981 with one mismatch generated during sequencing procedures (Figure 2.19). Mmu-mir-1971 itself nearly got no reads from all three libraries (Table 2.10).

```

mmu-mir-1971  5'  GUAAAGGCUGGGCUGAGA
                |||||
mmu-mir-1981  5'  GUAAAGGCUGGGCUUAGACGUGGC

```

Figure 2.19 Alignment of the murine miRNA which is a possible truncated form of an abundant miRNA. One probably mis-annotated murine miRNA is aligned with its corresponding miRNA.

Furthermore, the sequence of mmu-mir-590, which was supposed as an ortholog of hsa-mir-590, got no hit at all in the current assembly of murine genome from GenBank. Nor does the miRBase provide any genomic information of this miRNA gene, as it does for most of the other miRNA genes (Table 2.11).

Taken together, there are 24 murine miRNA genes that have to be carefully looked over and re-considered for their definition as miRNA genes. In addition, when analyzing closely at individual read sequence, the sequences matched to these suspicious miRNA genes always showed diversity of start, termini and length, with a length preferably shorter than 20 nt of “tRNA-derived” mis-annotated miRNAs or around 25 nt of other “ncRNA-derived” mis-annotated miRNAs (data not shown). This is obviously distinguished from the classical miRNAs, which showed a distinct pattern of start and termini, with the length mainly around 20 to 22 nt.

2.4.2 Examination of human miRNA genes

Although there is no human Dicer or Dgcr8 knockout samples available so far, the large homology between human genome and murine genome leads to the possibility of utilizing these mESCs small RNA libraries for the examination of human miRNAs as well. For this purpose, the three libraries were re-analysed again using the reference of human miRNAs from miRBase v15.0 (Appendix Table IV), and meanwhile searched for the identity of human miRNAs to human ncRNA sequences.

As a result, eleven human miRNA sequences were found matched perfectly to diverse human ncRNA sequences, together with six miRNA sequences harbouring one mismatch to ncRNA sequences (Table 2.13). Most of these mis-annotated miRNAs showed independencies from Dicer1 and Dgcr8 in production, while the rest got no read from all three libraries (Table 2.12).

Of note, two miRNA genes were also found to perfectly match human mitochondrial genome sequence (Table 2.13). Hsa-mir-1973 is aligned to the mitochondrial 16S rRNA and showed independencies from Dicer1 and Dgcr8 in the read numbers, while hsa-mir-4284 is aligned to the mitochondrial Phe tRNA gene and has no read in all three murine libraries.

Table 2.12 Read numbers of mentioned human miRNA entries in three small RNA libraries.

miRNA ^a	wt		Dicer1 ^{-/-}		Dgcr8 ^{-/-}	
	mismatch0 ^b	mismatch1 ^b	mismatch0	mismatch1	mismatch0	mismatch1
hsa-mir-106b*	168	41	0	1	0	0
hsa-mir-107	631	91	0	0	0	1
hsa-mir-145	317	36	35	3	18	4
hsa-mir-185	643	123	0	0	0	0
hsa-mir-23a	8307	960	84	4	70	5
hsa-mir-720	866	119	1465	86	1996	210
hsa-mir-766	0	0	0	0	0	0
hsa-mir-935	24	2	0	0	0	0
hsa-mir-1246	8	11	26	6	27	7
hsa-mir-1247	6	1	2	0	0	0
hsa-mir-1248	64	12	173	4	258	18
hsa-mir-1249	12	1	0	1	0	3
hsa-mir-1260	5	698	1	3314	2	3862
hsa-mir-1260b	143	11	723	29	719	56
hsa-mir-1274a	101	21	515	22	289	41
hsa-mir-1274b	660	95	1807	110	1724	191
hsa-mir-1280	12	15	27	85	94	128
hsa-mir-1290	0	21	0	34	0	54
hsa-mir-1291	0	0	0	0	0	0
hsa-mir-1308	1555	5658	10237	21398	5165	20376
hsa-mir-1826	376	313	625	176	616	194
hsa-mir-1973	6	2	3	0	16	5
hsa-mir-1975	0	0	0	0	0	0
hsa-mir-1979	27	301	151	1670	180	1284
hsa-mir-3074	9	0	0	0	0	0
hsa-mir-3182	0	18	0	81	0	67
hsa-mir-3195	0	8	0	1	0	6
hsa-mir-4284	0	0	0	0	0	0
hsa-mir-4286	250	108	482	187	554	229
hsa-mir-4289	1	14	0	0	0	0
hsa-mir-4306	0	11	0	0	0	0
hsa-mir-4317	0	7	0	0	0	0
hsa-mir-4318	0	22	0	0	0	0
hsa-mir-4323	0	0	0	0	0	0
hsa-mir-4328	0	4	0	0	0	1

- a. Names of miRNA entries, according to miRBase v15.0. Names in red are probably mis-annotated miRNAs. Names in black are normal miRNAs.
- b. "Mismatch" refers to the mismatch existed in the alignment of library reads to miRNA sequences. "Mismatch0" means no mismatch. "Mismatch1" means one nucleotide mismatch. The read numbers with one nucleotide mismatch are shown in grey.

Table 2.13 Probably mis-annotated human miRNA genes that match to other ncRNAs.

miRNA	Sequence	matched RNA
(fully matched)		
hsa-mir-720	UCUCGCUGGGGCCUCCA	human tRNA-Thr(TGT) ^a
hsa-mir-1274a	GUCCUGUUCAGGCGCCA	human tRNA-Lys(TTT) ^a
hsa-mir-1274b	UCCUGUUCGGGCGCCA	human tRNA-Lys(TTT) ^a
hsa-mir-1280	UCCCACCGCUGCCACCC	human tRNA-Leu(AAG) ^a
hsa-mir-1308	GCAUGGGUGGUUCAGUGG	human tRNA-Gly(GCC) ^a
hsa-mir-4286	ACCCACUCCUGGUACC	human tRNA-Leu(TAA) ^a
hsa-mir-1246	AAUGGAUUUUUGGAGCAGG	human U2 snRNA
hsa-mir-1248	ACCUUCUUGUAUAAGCACUGUGCUAAA	human H/ACA box 81 snoRNA
hsa-mir-1291	UGGCCUGACUGAAGACCAGCAGU	human H/ACA box 34 snoRNA
hsa-mir-1975	CCCCACAACCGCGCUUGACUAGCU	human RNY5 scRNA
hsa-mir-1979	CUCCACUGCUUCACUUGACUA	human RNY3 scRNA
hsa-mir-1973	ACCGUGCAAAGGUAGCAUA	human mitochondrial 16S rRNA
hsa-mir-4284	GGGCUCACAUCACCCCAU	human mitochondrial tRNA-Phe
(with one nucleotide mismatch or gap)		
hsa-mir-1826	AUUGAUCAUCGACACUUCGAACGCAAU	human 5.8S rRNA
hsa-mir-3195	CGCGCCGGGCCCGGCUU	human 28S rRNA
hsa-mir-1260	AUCCCACCUCUGCCACCA	human tRNA-Leu(AGG) ^a
hsa-mir-1260b	AUCCCACCACUGCCACCAU	human tRNA-Leu(AGG) ^a
hsa-mir-3182	GCUUCUGUAGUGUAGUC	human tRNA-Val(CAC) ^a
hsa-mir-1290	UGGAUUUUUGGAUCAGGGA	human U2-snRNA-related

a. There might be more than one tRNA sequences that match to this miRNA, due to the characteristics of tRNA sequences.

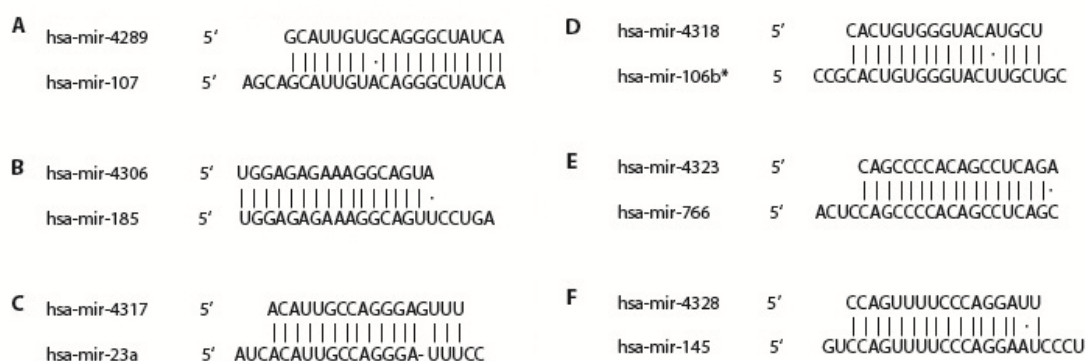


Figure 2.20 Alignment of human miRNAs which are possible truncated form of abundant miRNAs. Six probably mis-annotated human miRNAs are aligned with their corresponding miRNAs.

Moreover, six human miRNA genes were found to be the possible truncated form of the abundantly expressed human miRNAs, with one mismatch or one gap (Figure 2.20). These six miRNA sequences, however, are all abnormally short with the length of only 17 to 19, which does not seem to qualify them as normal miRNA genes.

As a result, 25 human miRNA genes have been probably mis-annotated.

At last, among the huge information emerged during the analysis, four human miRNA sequences were found to get significant read numbers in the wt mESCs library, but largely reduced numbers in both *Dicer1*^{-/-} and *Dgcr8*^{-/-} mESCs libraries (Table 2.12). The orthologs of these miRNAs in murine genome have not been reported before. The loci of these sequences were searched in murine genome, and their flanking sequences were all shown to form nice hairpin structures (Table 2.14). Among them, the hairpin of *mmu-mir-3074* turned out to be the reverse complementary transcript of the pre-miRNA *mmu-mir-24-1*, which is the same case as *hsa-mir-3074* and *hsa-mir-24-1*. Thus, there are four novel murine miRNA candidates identified.

2.4.3 Summary of examination of mis-annotated miRNAs in miRBase

Taken together, 24 murine miRNA genes and 25 human miRNA genes in the current version of miRBase are probably mis-annotated. Most of them might actually be the degradation products of other ncRNAs. The rapid development of the sequencing technologies has promoted the studies in miRNA field, especially the identification of novel miRNA genes. However, this analysis has raised the question whether all of the miRNA genes in the current database have been correctly annotated. People should

Table 2.14 Novel murine miRNA candidates of known human miRNA orthologs.

Candidate miRNA ^a	Stem-loop structures of putative miRNA precursors ^b	dG ^b (kcal/mol)	Genomic location ^c
<i>mmu-mir-935</i>	<pre> C C G A CCC C CAUCC GGCGG GG GCGG CGGC GUGGCGGGAGCGG CU GGC U UCGCC -CU-CGCC- GCCG CAU<u>CGCCUUCGCC</u> GA CCG C C AUU C UCUGC </pre>	- 55.6	7A1
<i>mmu-mir-1247</i>	<pre> -C- A C C UU C ACGUU U GGC-CG CGGGCGC CC GUC CG CGU CCCGG GC C CCG GU GCCCGCG GG CAG GC GCA GGGCC--C--CG U A CAA A U A U- A UC </pre>	- 42.0	12F1
<i>mmu-mir-1249</i>	<pre> GU A U CAA CUA UUGC GG-GGAGGAGGG GGGGA GGGC GUUCC U AGCG CC <u>CUUCUCCC-CCCCU</u> <u>CCCG--CAAGG</u> G GUU A U UCC </pre>	- 45.9	15E2
<i>mmu-mir-3074</i>	<pre> -A U U A GC- GUGUG GCUCG CUCC GU CCUGCUGA CUGA CAGU A UGGGC GAGG CA <u>GGAUGACU</u> <u>GACU</u> GUCA A GG C C C AUA AGAGUA </pre>	- 36.2	13B3

- Names of the putative new miRNA sequences are according to their orthologs in human miRNAs retrieved from miRBase (<http://www.mirbase.org>).
- RNA secondary structure prediction and free energy calculation have been done using mFOLD version 3.2. The miRNA sequences are underlined. The actual size of the stem-loop has not been experimentally determined.
- The genomic locations of murine miRNAs are referring to the positions in murine chromosomes according to the assembly from NCBI (<http://www.ncbi.nlm.nih.gov/mapview/>).

be careful when defining a novel miRNA gene according to NGS data. Meanwhile, the database might take more responsibility during the acceptance of novel miRNA genes. More strict evidence other than NGS data might also be necessary.

3. DISCUSSION

3.1 Advantages of developed software for NGS data analysis

The advent of NGS technologies has started a new era in the analysis of genome as well as gene expression profiles. Its amazing ability of producing enormous amount of short sequences at fast speed and low cost has inspired biologists with various applications in many research areas, including studies in the small RNA field. However, the obstacles stand between the huge set of data and the significant useful information. The specific characteristics of NGS data – the large number and the short length of the reads – demanded alternative methods for processing and alignment, other than those being commonly applied in Sanger sequencing. This will remain as the biggest challenge, before the potential of NGS can be fully evaluated and utilized (McPherson, 2009).

In this study, we decided to use NGS to investigate the miRNAs important for γ -herpesvirus infection, which had not been carried out before. The short lengths of NGS reads were ideal for the studies of miRNAs, and would reserve as much sequence information as possible for further analysis. However, at the time when this project started, there was no analysis tool publicly available for NGS data. So an automated software has been designed and developed for the analysis of NGS data used in this study (Figure 2.2).

With the development of NGS applications, a couple of data processing programs were developed during the recent two years (Fahlgren et al., 2009; Friedlander et al., 2008; Hackenberg et al., 2009; Pantano et al., 2010; Wang et al., 2009a). Compared to these complicated programs, the software used in this study still shows some advantages.

First of all, the stand-alone software is easy to handle. Most of the other accessible programs only provide online versions. The large size of NGS data files has made them difficult for data transferring. The stand-alone software can directly process the data and save the results on the personal computers. Furthermore, the small program size and no need for installation make it easily sharing among the users to analyse desired NGS data.

Second, this automated software has comprised much flexibility in the analysis of NGS data. Customized miRNA database and genome sequences can be applied as desired. This feature can not only keep pace with the newest version of the miRNA database from miRBase, but also enable the flexibility in the analyses of the

sequences corresponding to different viral genomes in this study, which is still not possible in the other programs. Compared to the pre-set settings of the other online programs, these basic but powerful functions of this software have realized all the demanded analyses in this study. Meanwhile, the parameters for the quality of sequence alignment can also be adjusted as desired, so that the results have been generated in the well-controlled processes.

Third, this software uses slightly different strategies than most of the other programs in the analysis of small RNA NGS data (Figure 2.1). While the other programs first align all the sequences to the whole genomes, and define the miRNA abundance according to the reads corresponding to the gene loci, the software used in this study first aligns the sequences against the miRNA database, and directly defines the miRNA read numbers. The purpose behind was to facilitate the analysis of the huge dataset on the personal computers, by minimizing the size of target database. As a result, it was possible to analyse a single NGS library within several days, without the demand for a specialized powerful computer system. The experiences gained during NGS data analysis revealed that, a small RNA library of good quality contained at least 80% of the sequences generated from known miRNA genes. So the direct alignment to the miRNA database is effective and time-saving.

Fourth, the use of this software can avoid the mistakes derived from the alignment to the whole genome. As shown in Result 2.4, a number of miRNA genes have been probably mis-annotated, some of which might derive from ncRNA pieces or truncated miRNAs with one mismatch. The design of this software can provide the results of alignment to miRNA or ncRNA databases with desired number of mismatched nucleotides. The exclusion of these reads with mismatches will avoid the improper annotation of miRNA genes.

Meanwhile, all the information, including read numbers, read length, gene annotations and mismatch numbers, are all reserved in the result files, providing the possibility for the further analysis of interest, for instance, the analysis of variations in the 5 prime and 3 prime of miRNA reads.

As illustrated by the small RNA libraries applied to NGS that are involved in the study of this thesis, the development of this software led to the convenient and powerful analysis of NGS data. And it will benefit further NGS libraries of interest in the small RNA research.

3.2 Identification of novel gammaherpesvirus miRNAs

The identification of the novel gene category of miRNAs was the profoundly significant issue in biological study during the past decade. These small regulatory non-coding RNA genes, processed from imperfect pairing hairpin precursors, were first identified in the little model organism of worm (Lee et al., 1993; Wightman et al., 1993). Several years later, the study of miRNAs explosively expanded into various species of invertebrates, vertebrates, as well as plants. Consequently, also viruses were analysed and the question whether virus can also encode miRNA genes was successfully addressed for the first time in 2004 (Pfeffer et al., 2004). In their study, small RNA cloning in the EBV/B95.8 infected B lymphoma cell line resulted in the identification of five EBV miRNAs in total. However, the deletion region carried in the genome of EBV/B95.8 has resulted in the underestimation of miRNA gene numbers in EBV genome.

Later on, the identification of viral miRNAs has been successfully carried out in a number of γ -herpesviruses, by classical small RNA cloning, or computational prediction (Cai et al., 2005; Cai et al., 2006; Grundhoff et al., 2006; Pfeffer et al., 2005), leading to the characterization of a number of miRNA clusters existing in the γ -herpesvirus genomes. As the investigations began to focus on the functions of viral miRNAs, the advent of NGS technologies with more sensitive and powerful sequencing ability allowed the possibility to re-examine the viral genomes for the previously ignored miRNA genes.

When the study of this thesis started, there was no report of NGS application to γ -herpesviruses related models. So the small RNA libraries were constructed from several EBV and MHV-68 related samples and analysed by 454 sequencing. As a result, two novel EBV miRNA precursors and six novel MHV-68 miRNA precursors have been successfully identified in this study. Some of these miRNAs showed significant expression levels with high read numbers in the sequencing libraries and clear bands in the Northern blotting, indicating the effectiveness of NGS in novel miRNA identification compared to the classical small RNA cloning and sequencing method. Of note, the identification of novel EBV miRNAs in this study was performed with the amount-restricted NPC samples from the patients. Almost all EBV miRNAs from the BART region, including the two novel EBV miRNAs, were readily detected in the sequencing libraries, highlighting the great capability of NGS in handling low quantity samples.

During the analysis, 454 sequencing has produced enormous amount of reads including both viral and cellular sequences. Among the huge information, the

identification of novel miRNA genes has been carefully carried out and strictly controlled, so as to avoid the possible mistakes in the gene annotations, as illustrated in Result 2.4. The sequences, other than the known miRNA genes, have been seriously checked for their genome loci and sequence uniformity. The sequences that matched to other ncRNAs, and showed the diversity in start, termini and length were considered as degradation products from ncRNAs, and ignored in the analysis of novel miRNA candidates. Only those sequences, which had a distinct pattern of accumulative sequences with 20 to 23 nt, were analysed with their flanking sequences from the genome for the folding of the hairpin structure. Most of the identified novel miRNAs were successfully validated by means of Northern blotting or qRT-PCR. These rules were strictly applied to the identification work of EBV and MHV-68 miRNAs, as well as the cellular miRNAs from the human genome.

Interestingly, several reports that were released at a similar time or later than this study have confirmed the characterized novel miRNA genes, but no further novel miRNA gene in EBV and MHV-68 has been identified or suggested (Reese et al., 2010; Walz et al., 2010). These were very supportive evidence that the miRNA gene sets of EBV and MHV-68 have probably been completed.

As consequences, the characterization of novel miRNA genes as well as the completion of miRNA gene sets will promote the studies of miRNA functions in EBV and MHV-68 infection and pathogenesis processes.

3.3 Genome organization and evolutionary conservation of gammaherpesvirus miRNAs

The first report of miRNA genes in EBV genome has answered the question, whether or not the small size of viral genome is capable of encoding miRNA genes as well (Pfeffer et al., 2004). Five years thereafter, more than 200 viral miRNA genes have so far been identified. Intriguingly, all of these viral miRNA genes were identified in the genomes of dsDNA viruses, the majority of which were herpesviruses (Skalsky and Cullen, 2010). No miRNA gene has been found in RNA virus yet. There might be several speculations for this interesting observation. RNA viruses, comprising 70% of all viruses, show much higher mutation rates than do the DNA viruses because of the error rate of the enzymes involved in RNA replication (Baron et al., 1991). This might interfere with the existence of specifically structured miRNA precursor genes in the RNA virus genome. In contrast, the relative stability of dsDNA virus genomes was able to reserve miRNA genes during evolution. Meanwhile, the unique ability of dsDNA

viruses, particularly the herpesviruses, to establish the long-term, latent infections, means that these viruses need to block the protective host innate or adaptive immune responses while minimizing the expression of potentially antigenic viral proteins. As a result, the tiny miRNA genes with regulatory functions could be an effective device to overcome these obstacles. Furthermore, the accessibility of these particular nuclear DNA viruses to the nuclear miRNA-processing machinery enables the biogenesis of the viral miRNAs. Of note, there is no viral protein characterized to be involved in the viral miRNA generation or regulatory pathways, depicting a solely cellular environment which the dsDNA viral miRNAs have nicely incorporated and utilized.

The group of γ -herpesviruses have been mostly studied for viral miRNAs, with more than 100 miRNA genes identified so far from five model γ -herpesviruses infecting human, primates and mouse (Table 1.1). Interestingly, miRNA genes in the γ -herpesvirus genomes are all organized as clusters. For instance, EBV miRNAs, including the two novel miRNAs identified in this study, were clustered in BHRF1 and BART regions, respectively. The three BHRF1 miRNA genes were exclusively detectable during the latency III-infected lymphoblast and induced lytic replication (Cai et al., 2006; Xing and Kieff, 2007), and were absent in the NPC samples, too. The BART transcript, of which the protein product has been seeking for long but always failed, was then revealed to harbor 22 miRNA genes, grouped in two sub-clusters. The BART miRNAs were demonstrated to be produced from a long transcript, while the processing of pre-miRNAs from the primary transcript occurs prior to completion of the splicing reaction (Edwards et al., 2008). Similarly, MHV-68 miRNAs were also clustered in the first 6 kbp region of the genome. The completion of MHV-68 miRNA gene set and the detailed analysis of the unique vtRNA-miRNA-miRNA structures in this study have elucidated its specific organization. The feature that two miRNAs locate closely adjacent in the genome with only several nucleotides in between was nearly never seen in the other species. Meanwhile, these vtRNA-miRNA-miRNA pieces were probably transcribed as separate transcripts of approximately 200 nt, under the regulation of RNA polymerase III promoter (Bogerd et al., 2010). The compactness of the viral miRNA gene organization, illustrated by the little intergenic sequences and the shared promoter regions, has nicely reflected the restricted size of viral genomes for the goodness during evolution.

On the other hand, γ -herpesviruses miRNAs showed much diversity in their sequences. There are a considerable number of miRNA genes that are highly conserved among animals or plants. These are normally abundantly expressed miRNAs with important regulatory functions, indicating the indispensable roles of miRNA genes during evolution. However, the homology among γ -herpesviruses

miRNAs is very limited. The genomes of the γ -herpesviruses shared some similarities in the organization of ORFs (Simas and Efstathiou, 1998), but the overall identity of their genome sequences is not high. Recently, a global analysis has been performed among all the known and computationally predicted miRNA genes from the γ -herpesviruses (Walz et al., 2010). Surprisingly, only two pairs of viral genomes produced viral miRNAs with homology. One pair was EBV and rLCV, which shared 60% identity in the genome sequences. All of the three EBV BHRF1 miRNA precursors, and 19 of the 22 BART miRNA precursors, including the ebv-mir-BART21 identified in this study, found their orthologs in rLCV genome, while the other 13 rLCV miRNA precursors were not conserved. Another pair was rhesus rhadinovirus (RRV) and the closely related Japanese macaque herpesvirus (JMHV). They shared at least nine conserved miRNA precursors. The analysis of MHV-68 miRNA genes in this study has also confirmed the limitation in the sequence homology (Figure 2.12). Only one MHV-68 miRNA was found to have the same seed sequence as a KSHV miRNA, however, the little identity in the remaining nucleotides do not qualify them as orthologs. The limited conservations among γ -herpesvirus miRNA sequences implied their later and independent derivation processes during evolution of the viruses, which might be an interesting and significant aspect in studying the overall origination of miRNA genes.

3.4 EBV and tumorigenesis

EBV infection is benign and uneventful in the majority of humans, nevertheless, its presence in a spectrum of malignancies, varying from the T cell and B cell lymphomas in the immune system to the epithelial carcinomas in the nasopharynx and stomach, implies its role in the tumorigenesis processes (Kutok and Wang, 2006).

The transforming events initiated by EBV have been studied through different aspects. Now the upcoming roles of miRNA regulation might be another significant component of this puzzle.

A couple of cellular miRNAs have been revealed to be induced by EBV in the lymphoid malignancies, such as mir-146a and mir-155 (Cameron et al., 2008b; Gatto et al., 2008; Rahadiani et al., 2008). In this study, the NPC samples analyzed by NGS provided the opportunity to systematically depict the miRNA regulation for the first time in the EBV-related epithelial carcinomas.

Like other tumours, the NPC samples were characterized by distinct miRNA expression profiles. In particular, hsa-mir-23a/b, hsa-mir-200c, and hsa-mir-27a/b were significantly upregulated, whereas hsa-mir-320, hsa-mir-17-5p, and hsa-mir-652

were downregulated in the NPC samples compared to the healthy control tissues (Figure 2.8). Bioinformatic predictions suggested that hsa-mir-23a and hsa-mir-23b, which are the most abundant miRNAs in the NPC samples, may regulate the tumour suppressors ITGB1 (integrin-beta1), LIG4 (ATP-dependent DNA ligase IV), and SAFB (scaffold attachment factor B). It was tempting to speculate that other upregulated miRNAs might target tumour suppressors as well. Indeed, it was exemplified in this study that, the expression of hsa-mir-15a and hsa-mir-16 were elevated in the NPC samples, and both miRNAs can target BRCA1, a tumour suppressor gene important for breast carcinoma (Wang, 2007). Interestingly, miR-15a and miR-16 have been implicated in cancers before. In B cell lymphocytic leukemia, miR-15a and miR-16 expression is downregulated, and it has been suggested that both miRNAs target the oncogene bcl-2 (B cell lymphoma 2) (Cimmino et al., 2005). The dual role of the miRNAs indicated the complexity and tissue specificity in the miRNA functions. On the other hand, miR-15 and miR-16 induction and BRCA1 downregulation were observed similarly in MHV-68 infected NIH 3T3 cells (Figure 2.18). Notably, there was a report that NIH 3T3 cells, when ectopically expressed an RNA transcript that was antisense to the BRCA1 mRNA and thus inhibited the expression level of BRCA1 protein, showed accelerated and anchorage-independent growth as well as tumorigenicity in nude mice (Rao et al., 1996). Taken together, this suggested a common feature during the γ -herpesviruses infection which might contribute to the transformation of host tissues.

In addition, the expression levels of EBV encoding miRNAs were also well depicted in this study. Almost all miRNAs from the BART cluster were readily detected in the NPC samples. Several BART miRNAs, including the newly identified ebv-mir-BART21 and ebv-mir-BART22, were abundantly expressed (Figure 2.7), suggesting that these miRNAs may have important functions in maintaining the virus in NPC tissues. Of note, no miRNA originating from the BHRF1 region was found in the data sets, in line with the observation of the EBV-positive gastric cancer samples (Kim do et al., 2007), while in contrast to the situation in the latency III-infected B cell lymphoblasts (Cai et al., 2006; Xing and Kieff, 2007). The differences in the EBV latency stages and corresponding miRNA expression sets might further inspire the studies of tumorigenesis processes in EBV-related epithelial carcinomas and lymphomas.

3.5 MHV-68 miRNA expression signatures

In this study, NGS was also applied to cell lines infected with MHV-68, which is a powerful model virus infecting murine cells, to globally investigate the viral and cellular miRNA expression patterns.

Almost all MHV-68 miRNAs were detectable in the two infected cell lines that have been sequenced (Table 2.7). Overall, the persistently infected S11 cells showed a much higher MHV-68 miRNA expression level than the lytically infected NIH 3T3 cells (Figure 2.11). Mghv-mir-M1-1, mghv-mir-M1-8 and mghv-mir-M1-9 were the three most abundant miRNAs in both cell lines. Mghv-mir-M1-5* was more abundant than mghv-mir-M1-5 in infected NIH 3T3 cells, while in S11 cells, mghv-mir-M1-5 was expressed at a higher level. Such different MHV-68 miRNA expression patterns might be suggestive for distinct functions during lytic and persistent/latent infection.

By Northern blotting, the expression of three (mghv-mir-M1-10, mghv-mir-M1-12 and mghv-mir-M1-14) of the six novel MHV-68 miRNAs were well demonstrated. Although found with a comparable read number in NGS data sets, mghv-mir-M1-13 was hardly detectable by Northern blotting. This might be due to its low GC content. However, the expression of mghv-mir-M1-13 was shown by a more sensitive stem-loop qRT-PCR. This is consistent with a recent report that reverse ligation-mediated RT-PCR (RLM-RT-PCR) is able to detect mature MHV-68 miRNAs with at least 100-fold higher sensitivity than Northern blotting (Diebel et al., 2010). The expression of mghv-mir-M1-11 and mghv-mir-M1-15 with extremely low read numbers in NGS data was too low to be detected by either Northern Blotting or stem-loop qRT-PCR.

MHV-68 miRNAs are among the minor portion of miRNAs that are under the regulation of RNA Polymerase III. It has been recently shown that the generation of MHV-68 miRNAs is dependent on the A/B boxes in the vtRNA sequences as well as the presence of tRNase Z and Dicer, but not on Drosha (Bogerd et al., 2010; Diebel et al., 2010). By infecting the Dicer-deficient MEFs with MHV-68, it was confirmed that MHV-68 miRNAs are processed by a Dicer-dependent pathway (Figure 2.16). Importantly, while Bogerd et al. (Bogerd et al., 2010) showed Dicer-dependency by siRNA-mediated knockdown of Dicer in human (HeLa) cells transfected with an MHV-68 miRNA expression plasmid, this study demonstrated it by infection of authentic host cells (*Dicer*^{-/-} and *Dicer*^{+/+} MEFs) with MHV-68.

The vtRNAs were identified and characterized more than ten years ago and were shown to be non-amino-acetylated (Bowden et al., 1997). However, their function still remains unknown. With the characterization of MHV-68 miRNA organization, it might be speculated that the vtRNA sequences remained as remnants during evolution, and

serve now as the promoter sequences for the generation of MHV-68 miRNAs. How the differential expression of MHV-68 miRNAs is regulated, and the significance of the existence of the vtRNA-miRNA-miRNA structures, will be interesting to further investigate.

MHV-68 miRNAs were shown to be efficiently associating with the RISC complexes by immunoprecipitation using a monoclonal anti-mouse Ago2 antibody, implying that they are functional as cellular miRNAs (Figure 2.15 A). However, the functions of MHV-68 miRNAs are still to be explored. By matching the seed sequences of MHV-68 miRNAs, they are predicted to target both viral and cellular proteins. The abundance of MHV-68 miRNAs might also suggest that they could function by occupying the cellular RISC machinery, thus interfering with the normal cellular miRNA pathways. The attenuated but not lethal phenotype of a spontaneous MHV-68 mutant virus lacking the first 9.5 kbp of the genome, including all vtRNAs and miRNAs, indicated that the vtRNAs and miRNAs are not absolutely essential for lytic replication and for the establishment and maintenance of latency (Clambey et al., 2002).

Apart from MHV-68 miRNAs, the small RNA libraries also allowed the analysis of the expression signatures of cellular miRNAs in non-infected versus infected NIH 3T3 cells (Figure 2.17). The upregulation of mmu-mir-15b and mmu-mir-16, and the downregulation of their correlated target protein BRCA1 were further validated.

Altogether, NGS application of small RNAs expressed in lytically infected NIH 3T3 cells and in persistently infected S11 cells provided the first comprehensive overview of both MHV-68 and cellular miRNA expression in infected cells, and completely defined the miRNA coding potential of MHV-68. These data would aid to fully explore the functions of γ -herpesvirus miRNAs.

3.6 Further application of NGS in miRNA studies

The application of NGS technologies in miRNA studies has been exemplified in various reports, including the study of this thesis. Its advantages of producing enormous amount of short reads with low cost and fast speed, not only possess the powerful and sensitive sequencing capability that is able to reserve as much sequence information as possible from little amount of samples, but also provide the possibility to analyse the miRNA expression levels represented by sequence frequencies in the libraries at the same time. The identification of novel miRNA genes and the profiling of cellular miRNA expressions performed in this thesis all relied and were benefited from these advanced technologies. However, several problems came

into sight and waited for some better solutions, before NGS would exert more significant functions.

First, the identification of novel miRNA genes by NGS has led to the possible mis-annotations of some miRNA genes in the database, as illustrated in Result 2.4. This problem was noticed when a miRNA gene was observed to be strongly induced during MHV-68 infection in NIH 3T3 cells. Later on, the close examination revealed that this so-called miRNA gene was actually a piece of rRNA. It was not surprising that rRNA degradation product accumulated during the virus infection.

Thus, the interference of the mis-annotated miRNA genes during research has driven the systematic examination of ncRNA-matched human and murine miRNAs. The result was surprising. More than 20 miRNA genes were found to be suspiciously mis-annotated in both human and murine miRNA sets, constituting more than 2% of the miRNA genes in the current version of miRBase release. Almost all of these mis-annotated miRNA genes derived from NGS projects. The direct alignment of the reads to the genome sequence, together with the subsequent folding of the suggestive novel miRNA genes, which were performed automatically by NGS data processing programs, might be the reason for the generation of these mis-annotated miRNA genes. A standardized and well-controlled program, which can reasonably meet the needs during small RNA NGS data analysis and be popularly shared among the investigators in miRNA field, might be beneficial to avoid such problems. The difficulties of validating low abundant miRNAs by any method led to the registration of these mis-annotated miRNA genes in the database without careful control. To solve these problems in the future, more strict criteria, such as the validation of novel miRNA expression from the suggested precursor sequence in artificial vectors, might be necessary.

Second, the miRNA profiling, which has been performed by many NGS projects nowadays, is only semi-quantitative. The many steps during the sample preparation, especially the primer ligation, reverse transcription and sample amplification steps, not only make the absolute quantification impossible, but introduce the biases to the samples that might further disturb the interpretation of the sequencing results as well. This might be the reason that some sequencing results cannot be validated by other method. Meanwhile, there also exists the difference of the results among different NGS platforms. Recently, a systematic study has been performed under well control to compare the results from microarrays, NGS platform and qRT-PCR method (Git et al., 2010). The study suggested serious consideration of the differences in the results generated from these common methods applied in miRNA profilings. Furthermore, the lack of a proper internal normalization control among the small RNA data makes the

miRNA absolute quantification impossible, too. The application of the synthetic small RNA samples might be a solution, however, the correlations might vary according the miRNA concentration (Fahlgren et al., 2009; Willenbrock et al., 2009).

As consequences, the development of the direct RNA sequencing method, namingly RNA-seq, which does not demand the conversion of RNAs to cDNAs and sample amplification, was very attractive and regarded as the solutions to the second problem mentioned above (Wang et al., 2009b). The direct depiction of the real RNA world would probably revolutionize studies in miRNA field.

Taken together, the miRNA world, which has just been under the exploration for about ten years, still has many mysteries to be further investigated. The great potential of NGS technologies, largely promoting miRNA studies during the past five years, was well illustrated in this thesis by the identification of novel miRNA genes from γ -herpesviruses, and significant profilings of cellular miRNAs. NGS technologies will for sure continue to benefit the researches in miRNA field in the future, with improvements in the applications.

4. MATERIALS & METHODS

4.1 Materials

4.1.1 Chemicals and enzymes

Unless stated otherwise, all chemicals were purchased from *Amersham Bioscience* (Buckinghamshire, UK), *Biorad* (Hercules, USA), *Merck* (Darmstadt, Germany), *Qiagen* (Hilden, Germany), *Roche* (Penzberg, Germany), *Roth* (Karlsruhe, Germany) and *Sigma-Aldrich* (Munich, Germany). Radioactive chemicals were provided by *Perkin Elmer* (Waltham, USA). Enzymes were delivered from *New England Biolabs* (Ipswich, USA) and *Fermentas* (Burlington, Canada).

4.1.2 Plasmid

pMIR-TK-RNL is referred in short as pMIR in this work. It is modified from the commercially available pMIR-REPORT plasmid by *Ambion* (Austin, USA) (Beitzinger et al., 2007). It encodes for the *Phototinus pylaris* luciferase (in this work termed firefly). The original CMV promoter was replaced by HSV-TK promoter which was PCR-cloned from pRL-TK plasmid (*Promega*, Madison, USA). A *Renilla reniformis* luciferase (in this work termed renilla) under the control of a SV40 promoter and a poly(A) site was PCR-amplified from pRL-SV40 plasmid (*Promega*, Madison, USA) and inserted into SspI site of pMIR-REPORT. The firefly coding sequence is flanked by a multiple cloning site (MCS) at its 3' end, allowing for the introduction of regulatory sequences into the 3'UTR. The plasmid carries an ampicillin resistance.

4.1.3 Antibodies

α -HA	<i>Abcam</i> (Cambridge, USA)
α -human Ago1 (4B8)	monoclonal, rat hybridoma supernatant (Beitzinger et al., 2007)

α -human Ago2 (5D4)	monoclonal, rat hybridoma supernatant (Beitzinger et al., 2007)
α -mouse Ago2 (6F4)	monoclonal, rat hybridoma supernatant
α -human RmC (16D2)	monoclonal, rat hybridoma supernatant
α -BRCA1	#MS110, Merck (Darmstadt, Germany)
α - β -actin	Abcam (Cambridge, USA)
α -mouse IgG	peroxidase conjugated, Sigma-Aldrich (Munich, Germany)

4.1.4 Tissue samples

NPC samples Biopsies were taken from the nasopharynx in an area where there was clinical evidence of tumor, and control tissues were taken from clinically normal mucosa from the opposite side of the nasopharynx in the same patient.

4.1.5 Bacterial strains, virus stock and cell lines

Bacterial strains: *E. coli* XL1 blue

Virus stock: wildtype MHV-68 (clone G2.4), kindly provided by Dr. A. Nash (University of Edinburgh, Edinburgh, UK)

Cell lines: Ag-8
 BL41
 BL41/B95.8
 C666.1
 Dicer^{+/+} MEF (Parameswaran et al., 2010)
 Dicer^{-/-} MEF (Parameswaran et al., 2010)
 EREB2.5
 HEK
 Jijoye
 MCF7
 NIH 3T3
 S11, kindly provided by Dr. J.P. Stewart (University of Liverpool, Liverpool, UK)

4.1.6 Cell culture media

For the cultivation of BL41, BL41/95.8, EREB2.5, Jijoye cell lines:

RPMI 1640 medium with L-glutamine (<i>PAA</i> , Pasching, Austria)	500mL
fetal bovine serum (<i>Biochrom</i> , Berlin, Germany)	10%
penicillin/streptomycin (<i>PAA</i> , Pasching, Austria)	1%

For the cultivation of C666.1 cell line:

RPMI 1640 medium with L-glutamine	500mL
fetal bovine serum	10%
penicillin/streptomycin	1%
HEPES (<i>Sigma-Aldrich</i>)	25mM

For the cultivation of Ag-8, S11 cell lines:

RPMI 1640 medium with L-glutamine	500mL
fetal bovine serum	10%
penicillin/streptomycin	1%
2-Mercaptoethanol (<i>Sigma-Aldrich</i>)	50µM

For the cultivation of HEK, NIH 3T3 cell lines:

DMEM medium with L-glutamine (<i>PAA</i> , Pasching, Austria)	500mL
fetal bovine serum	10%
penicillin/streptomycin	1%

For the cultivation of Dicer^{+/+} MEF, Dicer^{-/-} MEF cell lines:

DMEM medium with L-glutamine	500mL
fetal bovine serum	10%
penicillin/streptomycin	1%
HEPES	10mM

For the cultivation of MCF7 cell lines:

DMEM medium with L-glutamine	500mL
fetal bovine serum	10%
penicillin/streptomycin	1%
bovine insulin (<i>Sigma-Aldrich</i>)	18µg/mL

4.1.7 Buffers and solutions

LB (lysogeny broth) media	1% (w/v)	Bacto Trypton
	0.5% (w/v)	NaCl
	0.5% (w/v)	Yeast extract
Phosphate buffered saline (PBS)	137 mM	NaCl
	2.7 mM	KCl
	4.3 mM	Na ₂ HPO ₄
	1.4 mM	KH ₂ PO ₄ adjust pH to 7.5
HEPES 2x for Calcium phosphate transfection	274 mM	NaCl
	54.6 mM	HEPES
	1.5 mM	Na ₂ HPO ₄ adjust pH to 7.1
Cell lysis buffer	150 mM	KCl
	25 mM	Tris pH 7.5
	2 mM	EDTA
	1 mM	NaF
	0.5%	NP-40
	0.5mM	ABESF (add freshly)
	0.5mM	DTT (add freshly)
RIPA buffer-300	50 mM	Tris pH7.5
	300 mM	NaCl
	1%	Triton X 100
	1%	Sodium deoxycholate
	0.1%	SDS
Protease K buffer, 2x	300 mM	NaCl
	200 mM	Tris pH 7.5
	25 mM	EDTA
	2%	SDS

1x TBE buffer	89 mM	Tris-BASE
	89 mM	boric acid
	2.5 mM	EDTA
DNA loading dye 5x	15 g	Saccharose
	50 ml	H ₂ O
	0.025%	Xylene cyanol
20x SSC	3 M	NaCl
	0.3 M	Sodium citrate
		adjust pH to 7.0
EDC cross-link solution	0.13 M	1-Methylimidazole (pH 8)
	0.16 M	EDC
50x Denhardt's solution	1%	Albumin fraction V
	1%	Polyvinylpyrrolidon K30
	1%	Ficoll 400
Hybridization solution	7.5 ml	20x SSC
	21.0 ml	10% SDS
	0.6 ml	1 M Na ₂ HPO ₄ pH 7.2
	0.6 ml	50x Denhardt's solution
	3 mg	Salmon Sperm DNA
Northern blotting wash solution I	25%	20x SSC
	1%	SDS
Northern blotting wash solution II	5%	20x SSC
	1%	SDS
RNA loading dye 1x	90%	Formamide
	0.025%	Xylene cyanol
	0.025%	Bromophenol blue in 1x TBE

Denaturing polyacrylamide gels for northern blotting

15%	10%	SequaGel Buffer (<i>national diagnostics</i> , Atlanta USA)
	60%	SequaGel Concentrate
	30%	SequaGel Diluent
	0.1%	APS
	0.05%	TEMED

SDS running buffer	200 mM	Glycin
	25 mM	Tris-BASE
	0.1% (w/v)	SDS

Towbin-blotting buffer	40 mM	Glycin
	50 mM	Tris-BASE
	0.037% (w/v)	SDS
	20%	Methanol

Western blotting wash buffer	30 mM	Tris-BASE
	150 mM	NaCl
	0.25%	Tween-20
		adjust PH to 7.5

Chemiluminescence detection	100 mM	Tris pH 8.5
	1.2 mM	Luminol in 10 ml
	0.68%	p-cumaric acid in 150 μ l
		H ₂ O ₂ (30%) 11 μ l
		mix all components before use

Protein sample buffer 5x	400 mM	Tris/HCl pH 6.8
	5 mM	EDTA
	0.01%	Bromphenol blue
	50%	Glycerin
	1% (w/v)	SDS

Polyacrylamide gels for SDS-PAGE

5% stacking gel	5%	Acrylamide 37,5:1
	75 mM	Tris pH 6.8
	0.1 %	SDS
	0.1 %	APS
	0.05%	TEMED
10% separation gel	10%	Acrylamide 37.5:1
	400 mM	Tris pH 8.0
	0.1%	SDS
	0.1%	APS
	0.05%	TEMED
Renilla buffer	2.2 mM	EDTA
	220 mM	K ₂ PO ₄ pH 7.2
	0.44 mg/ml	BSA
	1.1 M	NaCl
	1.3 mM	NaN ₃
	1.43 μM	Coelenterazine (P.J.K., Kleinblitterdorf, Germany) (add freshly)
Firefly buffer	470 μM	D-luciferin (P.J.K., Kleinblitterdorf, Germany)
	530 μM	ATP (P.J.K., Kleinblitterdorf, Germany)
	270 μM	Coenzyme A (P.J.K., Kleinblitterdorf, Germany)
	20 mM	Tricine
	5.34 mM	MgSO ₄ pH 7.2
	0.1 mM	EDTA
	33.3 mM	DTT
		(add freshly)

4.2 Methods

4.2.1 Molecular biological methods

4.2.1.1 General methods

Any less detailed descriptions of molecular biological standard methods (DNA/RNA gel-electrophoresis, -extraction, -precipitation and the determination of concentrations of nucleic acids, PCR, etc.) were performed as described in Sambrook et al. (Sambrook et al., 1989) or according to the manufacturers' instructions, respectively. There, one can also find the composition of not listed buffers and solutions.

The isolation of plasmid-DNA from *E. coli* was carried out by using Plasmid MiniKit I[®] (*Omega BioTek*, Darmstadt, Germany) or NucleoBond[®] XtraMidi-Kit (*Macherey Nagel*, Düren, Germany), respectively. For the elution of DNA fragments from agarose gels, the NucleoSpin[®]-Kit (*Macherey Nagel*, Düren, Germany) was used.

4.2.1.2 Cloning of 3'UTRs from cDNA library into pMIR-TK-RNL

pMIR-TK-RNL miRNA reporter plasmids which express the firefly luciferase ORF fused to a cleavage site complementary to a small RNA or a regulatory 3'UTR sequence and renilla luciferase as a transfection control were generated from pMIR-REPORT as described above (Beitzinger et al., 2007)

3'UTRs were amplified by polymerase chain reaction (PCR). As template, cDNA library of HEK cells was used. PCR amplification was performed by the Phusion[™] polymerase (*Finnzymes*, Espoo, Finland). PCR products were digested with restriction enzymes *SacI* and *NaeI* and cloned into MCS of the reporter plasmid pMIR-TK-RNL.

The DNA oligos used as primers for PCR amplifications are as followed:

(human) BRCA1-3'UTR:

forward: 5'- GCTGAGCTCCTGCAGCCAGCCACAGGTACAGAGCC -3'

reverse: 5'- CGCTGCCGCGAAGTGTTTGCTACCAAGTTTATTTGCAGTG -3'

4.2.1.3 RNA Extraction from tissue samples or cultured cells

a) Total RNA extraction (mRNA and miRNAs)

Extraction of RNA was performed following the TriFast[®] protocol (*Qiagen*, Erlangen, Germany). Briefly, tissue samples were frozen by liquid nitrogen and squeezed to powders by grinder. Grinded tissue samples or cultured cells were homogenized by

pipetting up and down several times in an appropriate amount of TriFast. Samples were incubated for a few minutes at room temperature to let nucleoprotein complexes dissociate. 200 μ l chloroform per 1 ml TriFast were added. The samples were mixed for 20 seconds and centrifuged for 20 minutes at full speed and 4°C in a desk top centrifuge resulting in the dissociation of organic and aqueous phase. The upper phase (approx. 500 μ l) was pipetted into a new sterile reaction tube containing 1 ml isopropanol for the precipitation of mRNA. If miRNA was desired, the upper phases were distributed into three tubes, which were further filled up with absolute ethanol. RNA was precipitated at -20°C overnight. After pelleting the RNA for 15 minutes by centrifugation at full speed at 4°C, isopropanol or absolute ethanol was removed thoroughly and the pellet washed with 80% ethanol. After pelleting and removing the ethanol, the RNA was air-dried for 5 minutes and was dissolved at 70°C in an appropriate amount of ddH₂O.

b) RNA extraction of immunopurified complexes and input samples

Cells were usually lysed in 1ml lysis buffer per 15 cm plate. For input samples, usually 100 μ l lysate (generally 1/10 of lysate used for immunoprecipitation) was digested in 200 μ l 2x proteinase K buffer containing 40 mg Proteinase K. RNA from immunopurified samples was directly isolated from antibody coupled beads by adding 200 μ l 2x proteinase K buffer containing 40 mg Proteinase K. Proteinase K digestion was performed for 20 minutes at 65°C, followed by two times phenol/chloroform/iso-amylalcohol extractions. For subsequent RNA precipitation, the aqueous phase was mixed with three volumes (miRNAs) or two volumes (mRNAs) of absolute ethanol and incubated at -20°C. After pelleting the RNA for 30 minutes by centrifugation at 17'000g at 4°C, ethanol was removed thoroughly and the pellet was air-dried for 5 -10 minutes. RNA was dissolved at 70°C in an appropriate amount of ddH₂O.

4.2.1.4 Ago complex purification

Desired cells were lysed in cell lysis buffer and centrifuged at 10,000 g for 10 min at 4°C. For immunoprecipitation (IP) of endogenous Ago complexes, 100 μ l Protein G Sepharose (*GE Healthcare*, Munich, Germany) was washed with PBS and incubated with 2ml of hybridoma supernatant of monoclonal antibody anti-human-Ago1(4B8), anti-human-Ago2(5D4), or anti-Rmc, respectively, at 4°C with gentle agitation overnight. After several wash steps with PBS, beads were incubated with cell lysates for 3 h at 4°C. After incubation, beads were washed five times using RIPA-300 buffer. RNA was isolated with 40 mg Proteinase K in 200 μ l Proteinase K buffer followed by

phenol/chloroform/iso-amylalcohol extractions and ethanol precipitation. For the immunoprecipitation with purified monoclonal antibody anti-mouse-Ago2(6F4) and commercial antibody anti-HA, 10µg/ml of respective antibody was first mixed with cell lysates under constant rotation at 4°C for 3h. Protein G Sepharose beads were added to the lysates and the rotation continued for 1h. The washing of beads and precipitation of RNAs were performed as described above.

4.2.1.5 RNA polyacrylamide gel electrophoresis

For the detection of miRNA species, denaturing RNA polyacrylamide gel-electrophoresis was performed using the SequaGel[®] System Kit (*National Diagnostics*, Atlanta, USA). The acrylamide concentration was 15%. Before loading, the samples were provided with 2x dye and denatured for 5 min at 95°C. The gel was pre-run for 10-15 min at 10W. 1x TBE was used as running buffer. Samples were loaded after rinsing each pocket with buffer and the gel was run 28W.

4.2.1.6 Northern blotting

After adding formamide loading dye, the RNAs were separated by electrophoresis usually on a 15% denaturing polyacrylamide gel and transferred to Hybond-N membrane (*Amersham Bioscience*, Buckinghamshire, UK) by semidry blotting for 30 min with 20 V. H₂O was used to pre-wet three sheets of Whatman, the membrane and another three sheets of Whatman on top of the gel. After blotting was completed, the damp membrane was removed and placed with RNA side face up on top of a Whatman paper saturated in freshly prepared cross-linking EDC solution (Pall et al., 2007). Wrapped in Saran, the membrane was incubated for 1 h at 50 °C. After cross-linking the membrane was rinsed in excess RNase-free distilled water and dried. Pre-hybridization was performed in hybridization solution for 1 h at 45°C, before a 5'-³²P-labeled probe (see below) was added for hybridization overnight at 45°C. Subsequently, the membrane was washed in 10-min intervals twice with wash solution I and once with wash solution II. Exposure to Kodak BioMax MS films was performed with an intensifying screen (*Kodak*, Stuttgart, Germany) at -80°C.

For Northern probe preparation, 10 pmol of synthetic DNA-oligonucleotides (*Metabion*, Martinsried, Germany) reverse complementary to the appropriate miRNA were radio-labeled in a T4-Polynucleotide kinase (*Fermentas*, Burlington, Canada) reaction in the presence of [γ -³²P]-ATP (*Perkin Elmer*, Waltham, USA) according to standard

protocols. Subsequently, the probe was purified by gel filtration using MicroSpin G-25 columns (*GE Healthcare*, Munich, Germany).

The following probes for Northern blotting were used:

hsa-mir-16: 5'- CGCCAATATTTACGTGCTGCTA -3'
 ebv-mir-BART1-5p: 5'- CACAGCACGTCACCTTCCACTAAGA -3'
 ebv-mir-BART4: 5'- AGCACACCAGCAGCATCAGGTC -3'
 ebv-mir-BART21-5p: 5'- GTTAGTTGCCTTCACTAGTGA -3'
 ebv-mir-BART21-3p: 5'- AACACCAGTGGGCACA ACTAG -3'
 ebv-mir-BART22: 5'- ACTACTAGACCATGACTTTGTA -3'
 mmu-mir-15b: 5'- TGTA AACCATGATGTGCTGCTA -3'
 mmu-mir-16: 5'- CGCCAATATTTACGTGCTGCTA -3'
 mmu-mir-21: 5'- TCAACATCAGTCTGATAAGCTA -3'
 mghv-mir-M1-1: 5'- AAAGGAAGTACGGCCATTTCTA -3'
 mghv-mir-M1-8: 5'- GACCAAACCCCCAGTGAGTGCT -3'
 mghv-mir-M1-10: 5'- AAAGAACCTTCCGTGTAATCA -3'
 mghv-mir-M1-12: 5'- GCGTCGGGACCCGGGA -3'
 mghv-mir-M1-13: 5'- AAAGGGGTAGGACTCCCACACCAAA -3'
 mghv-mir-M1-14: 5'- AAAGAAGAGCTCACATGAGATA -3'
 tRNA-Met: 5'-TGGTAGCAGAGGATGGTTTTCGATCCATCGACCTCTG -3'

4.2.1.7 Reverse transcription and qRT-PCR of mRNA detection

RNA was isolated as described above and dissolved in 12 µl H₂O. RNA was first treated with DNaseI to remove DNA contaminations using the following reaction mix: 12 µl RNA, 1.5 µl DNaseI buffer (*Fermentas*), 1 µl DNaseI (*Fermentas*) and 0.5 µl RiboLock (*Fermentas*). DNaseI digest was performed for 30 minutes at 37° C. Afterwards the enzyme was inactivated for 10 minutes at 70° C and reaction was cooled on ice. Then, cDNA synthesis was performed in a final 30 µl reaction using First Strand cDNA Synthesis-Kit from (*Fermentas*), according to the manufacturer's protocol, using oligo(dT) as primers.

Quantitative real-time reverse transcription-PCR (qRT-PCR) was performed using MESA Green qPCR Mastermix Plus for SYBR green assay with fluorescein (*Eurogentec*, Seraing, Belgium) and carried out on a MyiQ single-color real-time PCR detection system (*Bio-Rad*, Hercules, USA) with supplied software. The qRT-PCR reactions were set up as 25 µl reactions: 12.5 µl MESA GREEN qPCR kits for SYBR® Assay, 0.5 µl, forward RT-primer (10 µM), 0.5 µl reverse RT-primer (10 µM), 11.5 µl cDNA (1:5 or 1:10 diluted). The glyceraldehyde-3-phosphate dehydrogenase

(GAPDH) mRNA or 18S rRNA level was used for normalization. Error bars are derived from three individual measurements.

The following primers for mRNA qRT-PCR were used:

(human)BRCA1, forward: 5'- TAAGCCAGAATCCAGAAGGC -3'

(human)BRCA1, reverse: 5'- GGGATGACCTTTCCACTCCT -3'

(human)GAPDH, forward: 5'- AATGGAAATCCCATCACCATCT -3'

(human) GAPDH, reverse: 5'- CACCCCACTTGATTTTGG -3'

(mouse)BRCA1-primer1, forward: 5'- TTGTGAGCGTTTGAATGAGG -3'

(mouse)BRCA1-primer1, reverse: 5'- CTGTCCTTCAAGGTGGCATT -3'

(mouse)BRCA1-primer2, forward: 5'- CAAGGCGAGAGCTAGAAGGA -3'

(mouse)BRCA1-primer2, reverse: 5'- AATGTGGGCTGGCTCTTTAG -3'

(mouse)18S rRNA, forward: 5'- CGGCTACCACATCCAAGGAA -3'

(mouse)18S rRNA, reverse: 5'- GCTGGAATTACCGCGGCT -3'

4.2.1.8 Reverse transcription and qRT-PCR of miRNA detection

Mature miRNAs were modified and validated as described (Hurteau et al., 2006). Total RNA was extracted as described above. Poly(A) tail was added to 1.0 µg RNA using Poly(A) Tailing Kit (*Ambion*, Austin, USA). The Adaptor-primer AACGAGACGACGACAGACTTTTTTTTTTTTTTTTTTV was used in reverse transcription using First Strand cDNA synthesis Kit (*Fermentas*). qRT-PCR was performed using MESA Green qPCR Mastermix Plus for SYBR Assay with fluorescein (*Eurogentec*, Seraing, Belgium), and carried out on MyiQ™ Single Color Real-Time PCR Detection System (*Bio-Rad*, Hercules, USA) with supplied software. GAPDH mRNA level was used for normalization. Error bars are derived from three individual measurements.

The following primers for poly(A)-tailed miRNA qRT-PCR were used:

Universal PCR primer: 5'- AACGAGACGACGACAGACTTTT -3'

ebv-BART1-5p: 5'- TCTTAGTGGAAGTGACGTGCTGT -3'

ebv-mir-BART21-5p: 5'- TCACTAGTGAAGGCAACTAAC -3'

ebv-mir-BART21-3p: 5'- CTAGTTGTGCCCACTGGTGTTT -3'

ebv-mir-BART22: 5'- TACAAAGTCATGGTCTAGTAGT -3'

(human)GAPDH: 5'- CCATCAATAAAGTACCCTGTGCTCAACC -3'

4.2.1.9 Reverse transcription and stem-loop qRT-PCR of miRNA detection

Real-time quantification of miRNAs by stem-loop qRT-PCR was carried out as described (Chen et al., 2005). Total RNA was isolated using the miRneasy Kit (*Qiagen*, Hilden, Germany) according to manufacturer's protocol. 1 µg of RNA was reverse-transcribed using Superscript II reverse transcriptase (*Invitrogen*, Carlsbad, USA). qPCR was performed using POWER SYBR GREEN MASTER MIX (*Applied Biosystems*, Darmstadt, Germany) on the 7300 platform (*Applied Biosystems*, Darmstadt, Germany). The 5.8S rRNA level was used for normalization. Error bars are derived from three individual measurements.

The following primers for miRNA stem-loop qRT-PCR were used:

(SLP = stem-loop RT primer; qP = qPCR primer)

The universal primer: 5'- GTGCAGGGTCCGAGGT -3'

mmu-mir-191, SLP:

5'-GTTGGCTCTGGTGCAGGGTCCGAGGTATTTCGCACCAGAGCCAACCAGCTG-3'

mmu-mir-191, qP: 5'- CGGCAACGGAATCCCAAAG -3'

mghv-mir-M1-1, SLP:

5'-GTTGGCTCTGGTGCAGGGTCCGAGGTATTTCGCACCAGAGCCAACAAAGGA -3'

mghv-mir-M1-1, qP: 5'- CGGCTAGAAATGGCCGTACT -3'

mghv-mir-M1-13, SLP:

5'-GTTGGCTCTGGTGCAGGGTCCGAGGTATTTCGCACCAGAGCCAACAAAGAA -3'

mghv-mir-M1-13, qP: 5'- CGCGTATCTCATGTGAGCTC -3'

(mouse)5.8S rRNA, SLP:

5'-GTTGGCTCTGGTGCAGGGTCCGAGGTATTTCGCACCAGAGCCAACAGCGAC-3'

(mouse)5.8S rRNA, qP: 5'- GCCCGCCTGTCTGAGC -3'

4.2.1.10 Western blotting

For western blotting, protein sample buffer was added to lysates. The proteins were analyzed by 10% SDS-PAGE followed by semidry western blotting using 1x Towbin blotting buffer onto a nitrocellulose membrane (*GE Healthcare*, Munich, Germany). The membrane was blocked by 5% milk in wash buffer. The primary antibodies were incubated with the membrane with recommended concentrations at 4°C under gentle shaking overnight. After three times 10 minutes washing with wash buffer, the secondary antibodies were incubated with the membrane with recommended concentrations at room temperature for 1h under gentle shaking. The membrane was washed again for three times with wash buffer, before the development by

chemiluminescence reagent. The signals were detected by ECL Hyperfilm (*GE Healthcare*, Munich, Germany).

4.2.1.11 Generation of small RNA libraries for 454 sequencing

Small RNA cloning was carried out by Vertis Biotechnology (Weihenstephan, Germany) and has been described earlier (Tarasov et al., 2007). Small RNA species were isolated from the desired tissue samples or cells using the mirVana miRNA isolation kit (*Applied Biosystems*, Darmstadt, Germany). The small RNAs were separated on a denaturing 12.5% polyacrylamide gel stained with SYBR green II. After passive elution, RNAs with a length of 15 to 30 bases were concentrated by ethanol precipitation and dissolved in water. Next, RNAs were poly(A) tailed using poly(A) polymerase. An adaptor was ligated to the 5'-phosphate of the miRNAs: (5' end adaptor [43 nucleotides]: 5'-GCCTCCCTCGCGCCATCAGCTNNNNGACCTTGGCTGTCACTCA -3'). NNNN represents a "barcode" sequence. Then, first strand cDNA synthesis was performed using an oligo(dT) linker primer [3'-end oligo(dT) linker primer (61 nt), 5'-GCCTTGCCAGCCCGCTCAGACGAGACATCGCCCCGC(T)₂₅-3'] and Moloney murine leukemia virus RNaseH reverse transcriptase. The resulting cDNAs were PCR amplified in 22 cycles, using the high-fidelity Phusion polymerase (*Finnzymes*, Espoo, Finland). Amplification products (120 to 135 bp) were confirmed by polyacrylamide gel electrophoresis (PAGE) analysis. All cDNA pools in one project were mixed in equal amounts and subjected to gel fractionation. The 120 to 135 bp fraction was electro-eluted from 6% PAA gels. After isolation with Nucleospin extract II (*Macherey Nagel*, Düren, Germany), cDNA pools were dissolved in 5 mM Tris-HCl, pH 8.5, at a concentration of 10 ng/l and used in single-molecule sequencing. Massively parallel sequencing was performed by 454 Life Sciences (Branford, USA), using a Genome Sequencer 20 system. The complete sequencing data is submitted and available at the Gene Expression Omnibus.

The barcodes used in sequencing and GEO accession number of the libraries are:

Result 2.2:

EBV-infected NPC samples and control tissues (GEO accession number GSE14738)

NPC-1: barcode CAAT

Control-1: barcode ATCG

NPC-2: barcode ACTA

Control-2: barcode AGGT

Result 2.3:

MHV-68 infected cells (GEO accession number GSE22938)

uninfected NIH 3T3 cells: barcode ACTA

infected NIH 3T3 cells: barcode AGGT

S11 cells: barcode ATCG

TPA induced S11 cells: barcode CAAT

4.2.2 Cellular biological methods**4.2.2.1 Culturing of mammalian cells**

Mammalian cell lines were cultured in different medium as mentioned above (4.1.6). The cells are cultured at 37°C in an atmosphere containing 5% CO₂. Adherent cell lines Dicer^{+/+} MEF, Dicer^{-/-} MEF, HEK, MCF7 and NIH 3T3 cells were grown in culture plates of different sizes. Non-adherent cell lines BL41, BL41/95.8, EREB2.5, Jijoye, AG-8 and S11 were grown in culture flasks of different sizes. Adherent cell line C666.1 was grown in flask collagen I (*Biocoat BD*, Franklin Lakes, USA). To split the adherent cells, after medium was aspirated off, cells were washed once with PBS (pH 7.5) and detached by Trypsin-EDTA (*PAA*, Pasching, Austria) treatment, with the exception of C666.1 which was detached by Acutase (*PAA*, Pasching, Austria).

4.2.2.2 Virus infection and lytic cycle induction

NIH 3T3 cells, MEFs and Ag-8 cells were infected with wildtype MHV-68 at an MOI of 1. The original stock of MHV-68 (clone G2.4) was obtained from Dr. A. Nash (University of Edinburgh, Edinburgh, UK). Working stocks of virus were prepared as previously described (Adler et al., 2000). Cells were harvest 48h after infection.

MHV-68 constantly infected S11 cells were treated with TPA (20 ng/ml) for 48h to induce the lytic cycle.

4.2.2.3 2'OMe- miRNA inhibitor transfection

If not used for luciferase assays, 2' O-Methylated miRNA inhibitors were transfected with Lipofectamine RNAiMax (*Invitrogen*, Carlsbad, USA) according to the manufacturer's protocol 2 days prior to the harvest of the cells.

The following 2' OMe miRNA inhibitors were used:

hsa-mir-15a: 5'- TGTAACCATATGTGCTGCTA -3'

hsa-mir-16: 5'- CGCCAATATTTACGTGCTGCTA -3'

hsa-let-7a: 5'- AACTATACAACCTACTACCTCA -3'

ebv-mir-BHRF1-1: 5'- AACTCCGGGGCTGATCAGGTTA -3'

4.2.2.4 Cotransfection of 2' OMe- inhibitors and luciferase reporter constructs

The day before transfection, cells were plated sub-confluently on a 48-well plate. Co-transfection for luciferase assays were performed with 100 ng pMIR-TK-RNL 3'UTR and 20 pmol 2'OMe-miRNA-inhibitor per 2×10^4 cells in a 96-well plate using Lipofectamine 2000 (*Invitrogen*, Carlsbad, USA) according to the manufacturer's protocol.

4.2.2.5 Luciferase assay

Luciferase activity was measured 48h post transfection using a dual luciferase reporter system as described by the manufacturer (*Promega*, Madison, USA). *Firefly* luciferase expression was normalized to *Renilla* luciferase expression. Error bars are derived from four individual measurements.

4.2.3 Computational methods

4.2.3.1 Sequence analysis of 454 sequencing libraries

Base calling and quality trimming of sequence chromatograms were done by the publicly available Phred software (Ewing and Green, 1998; Ewing et al., 1998). The adapter sequences and poly(A) tails were removed from the sequences. The remaining sequences that are longer than 15 nt were subjected to later analysis. Sequences were annotated according to miRBase (Griffiths-Jones, 2004), tRNA database (Chan and Lowe, 2009), non-coding RNA database (Szymanski et al., 2003), EBV (AJ507799) and MHV68 (NC_001826.2) genome sequence from GenBank. The automated analysis of the sequences in the libraries was carried out by VBA programming in Microsoft Excel, or the developed stand-alone program.

The retrieved sequences other than the known miRNAs were then subjected to a search for putative novel miRNA sequences. Genomic regions containing inserts with 100 nt flanks were retrieved from GenBank to calculate RNA secondary structures by mFOLD (Zuker, 2003). Only regions that folded into hairpins and contained an insert in one of the hairpin arms were considered as putative novel miRNA sequences.

The relative abundance of miRNAs was calculated as the percentage of individual miRNA read numbers in total miRNA read numbers from each library. The heatmap of the expression profiles were generated using Mayday platform (Battke et al., 2010).

4.2.3.2 Programming method

The stand-alone software designed and developed in this project for the analysis of NGS data was using BASIC language by the RealBasic Program (<https://www.realsoftware.com>). The software was developed and compiled for the Operating System of Mac, but is also possible to be converted to the version fitting for Windows or Linux Operating system.

ABBREVIATIONS

3' UTR	3' untranslated region
5' UTR	5' untranslated region
Ago	Argonaute
BALF5	BamHI fragment A containing the fifth leftward ORF
BART	BamHI fragment A rightward transcript
BHRF1	BamHI fragment H rightward open reading frame 1
bp	base pair
BRCA1	breast cancer 1
cDNA	complementary DNA
CRT	cyclic reversible termination
DNA	deoxyribonucleic acid
dNTP	2'-deoxyribonucleoside triphosphate
ds	double-stranded
EBV	Epstein-Barr virus
GA	Genome Analyzer
GEO	Gene Expression Omnibus
hAgo	human Argonaute
hsa	<i>Homo sapiens</i>
IP	immunoprecipitation
kbp	kilo base pair
KSHV	Kaposi's sarcoma-associated herpesvirus
mAgo	murine Argonaute
MCS	multiple cloning sites
MDV	Marek's disease virus
MEF	mouse embryonic fibroblast
mESC	mouse embryonic stem cell
mghv	mouse gammaherpesvirus 68 (= Murid herpesvirus 4)
MHV-68	mouse gammaherpesvirus 68 (= Murid herpesvirus 4)
miRNA	microRNA
mmu	<i>Mus musculus</i>
ncRNA	non-coding RNA
NGS	next generation sequencing

NPC	nasopharyngeal carcinoma
nt	nucleotides
ORF	open reading frame
P-bodies	processing bodies
PAGE	polyacrylamide gel electrophoresis
PCR	polymerase chain reaction
Pol	polymerase
pre-miRNA	precursor microRNA
pri-miRNA	primary microRNA
PTP	PicoTitrePlate
qRT-PCR	quantitative real time polymerase chain reaction
RISC	RNA induced silencing complex
rLCV	Rhesus lymphocryptovirus
RNA	ribonucleic acid
rRNA	ribosomal RNA
scRNA	small cytoplasmic RNA
SD	standard deviation
snoRNA	small nucleolar RNA
snRNA	small nuclear RNA
ss	single-stranded
stRNA	small temporal RNA
TPA	12-O-tetradecanoylphorbol-13-acetate
tRNA	transfer RNA
wt	wild type
vtRNA	viral transfer RNA

FIGURE INDEX

- Figure 1.1** Model of miRNA-guided post-transcriptional regulation of gene expression.
- Figure 1.2** Working principles of 454 sequencing.
- Figure 1.3** Working principles of Solexa sequencing.
- Figure 2.1** Flow chart of NGS data analysis procedures.
- Figure 2.2** Interactive platforms of developed software for NGS data analysis.
- Figure 2.3** Schematic locations of putative novel miRNAs in BART miRNA cluster of EBV genome.
- Figure 2.4** Expression analysis of novel EBV miRNAs by Northern blotting.
- Figure 2.5** Verification of novel EBV miRNA expressions in several NPC samples by qRT-PCR.
- Figure 2.6** MiRNA composition in NPC samples.
- Figure 2.7** Relative abundance of EBV miRNAs in the NPC-1 and NPC-2 libraries.
- Figure 2.8** Cellular miRNA expressions in NPC and control tissue.
- Figure 2.9** Expressions of hsa-mir-15a and hsa-mir-16 are upregulated in two NPC samples compared to healthy tissues.
- Figure 2.10** Hsa-mir-15a and hsa-mir-16 target BRCA1 mRNA.
- Figure 2.11** Comprehensive analysis of small RNA libraries by 454 sequencing constructed from NIH 3T3 and S11 cells.
- Figure 2.12** Seed sequence homology among MHV-68 miRNAs and murine or other herpesvirus miRNAs.
- Figure 2.13** MHV-68 miRNAs are located directly after vtRNA sequences.
- Figure 2.14** Unique vtRNA-miRNA-miRNA structures in MHV-678 genome.
- Figure 2.15** Validation of novel MHV-68 miRNAs.
- Figure 2.16** MHV-68 miRNAs are generated in a Dicer-dependent pathway.
- Figure 2.17** Cellular miRNA profiling of uninfected or MHV-68 infected NIH 3T3 cells and of untreated or TPA-treated S11 cells.
- Figure 2.18** miR-15/16 upregulation was observed in MHV-68 infected NIH 3T3 cells.
- Figure 2.19** Alignment of the murine miRNA which is a possible truncated form of an abundant miRNA.
- Figure 2.20** Alignment of human miRNAs which are possible truncated form of abundant miRNAs.

TABLE INDEX

- Table 1.1** Numbers of miRNA precursors in herpesviruses.
- Table 2.1** Sequence distribution of small RNA libraries from NPC samples.
- Table 2.2** Novel candidate miRNAs of novel precursors identified from NPC samples.
- Table 2.3** Numbers of novel EBV miRNA reads in the libraries.
- Table 2.4** Novel candidate human miRNAs of novel precursors identified from NPC samples.
- Table 2.5** Numbers of novel human miRNA reads in the libraries.
- Table 2.6** Sequence distribution of small RNA libraries from MHV-68 infected cell lines.
- Table 2.7** MiRNA read numbers of known and novel viral precursors from MHV-68 infected samples.
- Table 2.8** Novel candidate MHV-68 miRNAs of novel precursors identified from MHV-68 infected samples.
- Table 2.9** Sequences and read numbers of murine novel star miRNAs in the sequencing libraries.
- Table 2.10** Read numbers of mentioned murine miRNA entries in three small RNA libraries.
- Table 2.11** Probably mis-annotated murine miRNA genes that match to other ncRNAs or do not match in murine genome.
- Table 2.12** Read numbers of mentioned human miRNA entries in three small RNA libraries.
- Table 2.13** Probably mis-annotated human miRNA genes that match to other ncRNAs.
- Table 2.14** Novel murine miRNA candidates of known human miRNA orthologs.

REFERENCES

- (2004). Finishing the euchromatic sequence of the human genome. *Nature* **431**, 931-945.
- Adler, H., Messerle, M., Wagner, M., and Koszinowski, U.H. (2000). Cloning and mutagenesis of the murine gammaherpesvirus 68 genome as an infectious bacterial artificial chromosome. *J Virol* **74**, 6964-6974.
- Ambros, V., Bartel, B., Bartel, D.P., Burge, C.B., Carrington, J.C., Chen, X., Dreyfuss, G., Eddy, S.R., Griffiths-Jones, S., Marshall, M., *et al.* (2003). A uniform system for microRNA annotation. *RNA* **9**, 277-279.
- Ashihara, E., Kawata, E., and Maekawa, T. (2010). Future prospect of RNA interference for cancer therapies. *Curr Drug Targets* **11**, 345-360.
- Babiarz, J.E., Ruby, J.G., Wang, Y., Bartel, D.P., and Blelloch, R. (2008). Mouse ES cells express endogenous shRNAs, siRNAs, and other Microprocessor-independent, Dicer-dependent small RNAs. *Genes Dev* **22**, 2773-2785.
- Barbarotto, E., Schmittgen, T.D., and Calin, G.A. (2008). MicroRNAs and cancer: profile, profile, profile. *Int J Cancer* **122**, 969-977.
- Baron, S., Jennings, P.M., and Peterson, J.W. (1991). *Medical microbiology*, 3rd ed edn (New York ; London, Churchill Livingstone).
- Barth, S., Pfuhl, T., Mamiani, A., Ehse, C., Roemer, K., Kremmer, E., Jaker, C., Hock, J., Meister, G., and Grasser, F.A. (2008). Epstein-Barr virus-encoded microRNA miR-BART2 down-regulates the viral DNA polymerase BALF5. *Nucleic Acids Res* **36**, 666-675.
- Battke, F., Symons, S., and Nieselt, K. (2010). Mayday--integrative analytics for expression data. *BMC Bioinformatics* **11**, 121.
- Behm-Ansmant, I., Rehwinkel, J., Doerks, T., Stark, A., Bork, P., and Izaurralde, E. (2006). mRNA degradation by miRNAs and GW182 requires both CCR4:NOT deadenylase and DCP1:DCP2 decapping complexes. *Genes Dev* **20**, 1885-1898.
- Beitzinger, M., Peters, L., Zhu, J.Y., Kremmer, E., and Meister, G. (2007). Identification of human microRNA targets from isolated argonaute protein complexes. *RNA Biol* **4**, 76-84.
- Benson, D.A., Karsch-Mizrachi, I., Lipman, D.J., Ostell, J., and Wheeler, D.L. (2008). GenBank. *Nucleic Acids Res* **36**, D25-30.
- Bentley, D.R., Balasubramanian, S., Swerdlow, H.P., Smith, G.P., Milton, J., Brown, C.G., Hall, K.P., Evers, D.J., Barnes, C.L., Bignell, H.R., *et al.* (2008). Accurate whole human genome sequencing using reversible terminator chemistry. *Nature* **456**, 53-59.
- Berninger, P., Gaidatzis, D., van Nimwegen, E., and Zavolan, M. (2008). Computational analysis of small RNA cloning data. *Methods* **44**, 13-21.
- Bernstein, E., Caudy, A.A., Hammond, S.M., and Hannon, G.J. (2001). Role for a bidentate ribonuclease in the initiation step of RNA interference. *Nature* **409**, 363-366.
- Blaskovic, D., Stancekova, M., Svobodova, J., and Mistrikova, J. (1980). Isolation of five strains of herpesviruses from two species of free living small rodents. *Acta Virol* **24**, 468.
- Bogerd, H.P., Karnowski, H.W., Cai, X., Shin, J., Pohlers, M., and Cullen, B.R. (2010). A mammalian herpesvirus uses noncanonical expression and processing mechanisms to generate viral MicroRNAs. *Mol Cell* **37**, 135-142.
- Borchert, G.M., Lanier, W., and Davidson, B.L. (2006). RNA polymerase III transcribes human microRNAs. *Nat Struct Mol Biol* **13**, 1097-1101.
- Boss, I.W., Plaisance, K.B., and Renne, R. (2009). Role of virus-encoded microRNAs in herpesvirus biology. *Trends Microbiol* **17**, 544-553.
- Bowden, R.J., Simas, J.P., Davis, A.J., and Efstathiou, S. (1997). Murine gammaherpesvirus 68 encodes tRNA-like sequences which are expressed during latency. *J Gen Virol* **78** (Pt 7), 1675-1687.

- Busson, P., Keryer, C., Ooka, T., and Corbex, M. (2004). EBV-associated nasopharyngeal carcinomas: from epidemiology to virus-targeting strategies. *Trends Microbiol* 12, 356-360.
- Cai, X., Lu, S., Zhang, Z., Gonzalez, C.M., Damania, B., and Cullen, B.R. (2005). Kaposi's sarcoma-associated herpesvirus expresses an array of viral microRNAs in latently infected cells. *Proc Natl Acad Sci U S A* 102, 5570-5575.
- Cai, X., Schafer, A., Lu, S., Bilello, J.P., Desrosiers, R.C., Edwards, R., Raab-Traub, N., and Cullen, B.R. (2006). Epstein-Barr virus microRNAs are evolutionarily conserved and differentially expressed. *PLoS Pathog* 2, e23.
- Calabrese, J.M., Seila, A.C., Yeo, G.W., and Sharp, P.A. (2007). RNA sequence analysis defines Dicer's role in mouse embryonic stem cells. *Proc Natl Acad Sci U S A* 104, 18097-18102.
- Calin, G.A., and Croce, C.M. (2006). MicroRNA signatures in human cancers. *Nat Rev Cancer* 6, 857-866.
- Cameron, J.E., Fewell, C., Yin, Q., McBride, J., Wang, X., Lin, Z., and Flemington, E.K. (2008a). Epstein-Barr virus growth/latency III program alters cellular microRNA expression. *Virology* 382, 257-266.
- Cameron, J.E., Yin, Q., Fewell, C., Lacey, M., McBride, J., Wang, X., Lin, Z., Schaefer, B.C., and Flemington, E.K. (2008b). Epstein-Barr virus latent membrane protein 1 induces cellular MicroRNA miR-146a, a modulator of lymphocyte signaling pathways. *J Virol* 82, 1946-1958.
- Chan, P.P., and Lowe, T.M. (2009). GtRNAdb: a database of transfer RNA genes detected in genomic sequence. *Nucleic Acids Res* 37, D93-97.
- Chen, C., Ridzon, D.A., Broomer, A.J., Zhou, Z., Lee, D.H., Nguyen, J.T., Barbisin, M., Xu, N.L., Mahuvakar, V.R., Andersen, M.R., *et al.* (2005). Real-time quantification of microRNAs by stem-loop RT-PCR. *Nucleic Acids Res* 33, e179.
- Cheung, S.T., Huang, D.P., Hui, A.B., Lo, K.W., Ko, C.W., Tsang, Y.S., Wong, N., Whitney, B.M., and Lee, J.C. (1999). Nasopharyngeal carcinoma cell line (C666-1) consistently harbouring Epstein-Barr virus. *Int J Cancer* 83, 121-126.
- Cho, W.C. (2007). OncomiRs: the discovery and progress of microRNAs in cancers. *Mol Cancer* 6, 60.
- Choy, E.Y., Siu, K.L., Kok, K.H., Lung, R.W., Tsang, C.M., To, K.F., Kwong, D.L., Tsao, S.W., and Jin, D.Y. (2008). An Epstein-Barr virus-encoded microRNA targets PUMA to promote host cell survival. *J Exp Med* 205, 2551-2560.
- Cifuentes, D., Xue, H., Taylor, D.W., Patnode, H., Mishima, Y., Cheloufi, S., Ma, E., Mane, S., Hannon, G.J., Lawson, N.D., *et al.* (2010). A novel miRNA processing pathway independent of Dicer requires Argonaute2 catalytic activity. *Science* 328, 1694-1698.
- Cimmino, A., Calin, G.A., Fabbri, M., Iorio, M.V., Ferracin, M., Shimizu, M., Wojcik, S.E., Aqeilan, R.I., Zupo, S., Dono, M., *et al.* (2005). miR-15 and miR-16 induce apoptosis by targeting BCL2. *Proc Natl Acad Sci U S A* 102, 13944-13949.
- Clambey, E.T., Virgin, H.W.t., and Speck, S.H. (2002). Characterization of a spontaneous 9.5-kilobase-deletion mutant of murine gammaherpesvirus 68 reveals tissue-specific genetic requirements for latency. *J Virol* 76, 6532-6544.
- Croce, C.M. (2009). Causes and consequences of microRNA dysregulation in cancer. *Nat Rev Genet* 10, 704-714.
- Cullen, B.R. (2009). Viral and cellular messenger RNA targets of viral microRNAs. *Nature* 457, 421-425.
- Cummins, J.M., and Velculescu, V.E. (2006). Implications of micro-RNA profiling for cancer diagnosis. *Oncogene* 25, 6220-6227.
- Diebel, K.W., Smith, A.L., and van Dyk, L.F. (2010). Mature and functional viral miRNAs transcribed from novel RNA polymerase III promoters. *RNA* 16, 170-185.
- Ding, J., Huang, S., Wu, S., Zhao, Y., Liang, L., Yan, M., Ge, C., Yao, J., Chen, T., Wan, D., *et al.* (2010). Gain of miR-151 on chromosome 8q24.3 facilitates tumour cell migration and spreading through downregulating RhoGDIa. *Nat Cell Biol* 12, 390-399.
- Dressman, D., Yan, H., Traverso, G., Kinzler, K.W., and Vogelstein, B. (2003). Transforming single DNA molecules into fluorescent magnetic particles for detection and enumeration of genetic variations. *Proc Natl Acad Sci U S A* 100, 8817-8822.

- Easow, G., Teleman, A.A., and Cohen, S.M. (2007). Isolation of microRNA targets by miRNP immunopurification. *RNA* 13, 1198-1204.
- Edwards, R.H., Marquitz, A.R., and Raab-Traub, N. (2008). Epstein-Barr virus BART microRNAs are produced from a large intron prior to splicing. *J Virol* 82, 9094-9106.
- Ender, C., Krek, A., Friedlander, M.R., Beitzinger, M., Weinmann, L., Chen, W., Pfeffer, S., Rajewsky, N., and Meister, G. (2008). A human snoRNA with microRNA-like functions. *Mol Cell* 32, 519-528.
- Epstein, M.A., and Barr, Y.M. (1965). Characteristics and Mode of Growth of Tissue Culture Strain (Eb1) of Human Lymphoblasts from Burkitt's Lymphoma. *J Natl Cancer Inst* 34, 231-240.
- Epstein, M.A., Henle, G., Achong, B.G., and Barr, Y.M. (1965). Morphological and Biological Studies on a Virus in Cultured Lymphoblasts from Burkitt's Lymphoma. *J Exp Med* 121, 761-770.
- Ewing, B., and Green, P. (1998). Base-calling of automated sequencer traces using phred. II. Error probabilities. *Genome Res* 8, 186-194.
- Ewing, B., Hillier, L., Wendl, M.C., and Green, P. (1998). Base-calling of automated sequencer traces using phred. I. Accuracy assessment. *Genome Res* 8, 175-185.
- Fahlgren, N., Sullivan, C.M., Kasschau, K.D., Chapman, E.J., Cumbie, J.S., Montgomery, T.A., Gilbert, S.D., Dasenko, M., Backman, T.W., Givan, S.A., *et al.* (2009). Computational and analytical framework for small RNA profiling by high-throughput sequencing. *RNA* 15, 992-1002.
- Fedurco, M., Romieu, A., Williams, S., Lawrence, I., and Turcatti, G. (2006). BTA, a novel reagent for DNA attachment on glass and efficient generation of solid-phase amplified DNA colonies. *Nucleic Acids Res* 34, e22.
- Friedlander, M.R., Chen, W., Adamidi, C., Maaskola, J., Einspanier, R., Knespel, S., and Rajewsky, N. (2008). Discovering microRNAs from deep sequencing data using miRDeep. *Nat Biotechnol* 26, 407-415.
- Garcia-Blanco, M.A., and Cullen, B.R. (1991). Molecular basis of latency in pathogenic human viruses. *Science* 254, 815-820.
- Gatto, G., Rossi, A., Rossi, D., Kroening, S., Bonatti, S., and Mallardo, M. (2008). Epstein-Barr virus latent membrane protein 1 trans-activates miR-155 transcription through the NF-kappaB pathway. *Nucleic Acids Res* 36, 6608-6619.
- Ghadessy, F.J., Ong, J.L., and Holliger, P. (2001). Directed evolution of polymerase function by compartmentalized self-replication. *Proc Natl Acad Sci U S A* 98, 4552-4557.
- Git, A., Dvinge, H., Salmon-Divon, M., Osborne, M., Kutter, C., Hadfield, J., Bertone, P., and Caldas, C. (2010). Systematic comparison of microarray profiling, real-time PCR, and next-generation sequencing technologies for measuring differential microRNA expression. *RNA* 16, 991-1006.
- Godshalk, S.E., Bhaduri-McIntosh, S., and Slack, F.J. (2008). Epstein-Barr virus-mediated dysregulation of human microRNA expression. *Cell Cycle* 7, 3595-3600.
- Green, R.E., Krause, J., Ptak, S.E., Briggs, A.W., Ronan, M.T., Simons, J.F., Du, L., Egholm, M., Rothberg, J.M., Paunovic, M., *et al.* (2006). Analysis of one million base pairs of Neanderthal DNA. *Nature* 444, 330-336.
- Gregory, R.I., Yan, K.P., Amuthan, G., Chendrimada, T., Doratotaj, B., Cooch, N., and Shiekhattar, R. (2004). The Microprocessor complex mediates the genesis of microRNAs. *Nature* 432, 235-240.
- Griffiths-Jones, S. (2004). The microRNA Registry. *Nucleic Acids Res* 32, D109-111.
- Griffiths-Jones, S., Grocock, R.J., van Dongen, S., Bateman, A., and Enright, A.J. (2006). miRBase: microRNA sequences, targets and gene nomenclature. *Nucleic Acids Res* 34, D140-144.
- Griffiths-Jones, S., Saini, H.K., van Dongen, S., and Enright, A.J. (2008). miRBase: tools for microRNA genomics. *Nucleic Acids Res* 36, D154-158.
- Grundhoff, A., Sullivan, C.S., and Ganem, D. (2006). A combined computational and microarray-based approach identifies novel microRNAs encoded by human gamma-herpesviruses. *RNA* 12, 733-750.
- Hackenberg, M., Sturm, M., Langenberger, D., Falcon-Perez, J.M., and Aransay, A.M. (2009). miRanalyzer: a microRNA detection and analysis tool for next-generation sequencing experiments. *Nucleic Acids Res* 37, W68-76.
- Hammond, S.M., Bernstein, E., Beach, D., and Hannon, G.J. (2000). An RNA-directed nuclease

- mediates post-transcriptional gene silencing in *Drosophila* cells. *Nature* **404**, 293-296.
- He, L., Thomson, J.M., Hemann, M.T., Hernando-Monge, E., Mu, D., Goodson, S., Powers, S., Cordon-Cardo, C., Lowe, S.W., Hannon, G.J., *et al.* (2005). A microRNA polycistron as a potential human oncogene. *Nature* **435**, 828-833.
- Hendrickson, D.G., Hogan, D.J., Herschlag, D., Ferrell, J.E., and Brown, P.O. (2008). Systematic identification of mRNAs recruited to argonaute 2 by specific microRNAs and corresponding changes in transcript abundance. *PLoS One* **3**, e2126.
- Hock, J., Weinmann, L., Ender, C., Rudel, S., Kremmer, E., Raabe, M., Urlaub, H., and Meister, G. (2007). Proteomic and functional analysis of Argonaute-containing mRNA-protein complexes in human cells. *EMBO Rep* **8**, 1052-1060.
- Hurteau, G.J., Spivack, S.D., and Brock, G.J. (2006). Potential mRNA degradation targets of hsa-miR-200c, identified using informatics and qRT-PCR. *Cell Cycle* **5**, 1951-1956.
- Hutvagner, G., and Zamore, P.D. (2002). A microRNA in a multiple-turnover RNAi enzyme complex. *Science* **297**, 2056-2060.
- Jackson, A.L., and Linsley, P.S. (2010). Recognizing and avoiding siRNA off-target effects for target identification and therapeutic application. *Nat Rev Drug Discov* **9**, 57-67.
- John, B., Enright, A.J., Aravin, A., Tuschl, T., Sander, C., and Marks, D.S. (2004). Human MicroRNA targets. *PLoS Biol* **2**, e363.
- Karginov, F.V., Conaco, C., Xuan, Z., Schmidt, B.H., Parker, J.S., Mandel, G., and Hannon, G.J. (2007). A biochemical approach to identifying microRNA targets. *Proc Natl Acad Sci U S A* **104**, 19291-19296.
- Kasinski, A.L., and Slack, F.J. (2010). Potential microRNA therapies targeting Ras, NFkappaB and p53 signaling. *Curr Opin Mol Ther* **12**, 147-157.
- Kent, O.A., and Mendell, J.T. (2006). A small piece in the cancer puzzle: microRNAs as tumor suppressors and oncogenes. *Oncogene* **25**, 6188-6196.
- Khvorova, A., Reynolds, A., and Jayasena, S.D. (2003). Functional siRNAs and miRNAs exhibit strand bias. *Cell* **115**, 209-216.
- Kim do, N., Chae, H.S., Oh, S.T., Kang, J.H., Park, C.H., Park, W.S., Takada, K., Lee, J.M., Lee, W.K., and Lee, S.K. (2007). Expression of viral microRNAs in Epstein-Barr virus-associated gastric carcinoma. *J Virol* **81**, 1033-1036.
- Kutok, J.L., and Wang, F. (2006). Spectrum of Epstein-Barr virus-associated diseases. *Annu Rev Pathol* **1**, 375-404.
- Lagos-Quintana, M., Rauhut, R., Lendeckel, W., and Tuschl, T. (2001). Identification of novel genes coding for small expressed RNAs. *Science* **294**, 853-858.
- Lagos-Quintana, M., Rauhut, R., Meyer, J., Borkhardt, A., and Tuschl, T. (2003). New microRNAs from mouse and human. *RNA* **9**, 175-179.
- Lagos-Quintana, M., Rauhut, R., Yalcin, A., Meyer, J., Lendeckel, W., and Tuschl, T. (2002). Identification of tissue-specific microRNAs from mouse. *Curr Biol* **12**, 735-739.
- Landgraf, P., Rusu, M., Sheridan, R., Sewer, A., Iovino, N., Aravin, A., Pfeffer, S., Rice, A., Kamphorst, A.O., Landthaler, M., *et al.* (2007). A mammalian microRNA expression atlas based on small RNA library sequencing. *Cell* **129**, 1401-1414.
- Latronico, M.V., and Condorelli, G. (2009). MicroRNAs and cardiac pathology. *Nat Rev Cardiol* **6**, 419-429.
- Lau, N.C., Lim, L.P., Weinstein, E.G., and Bartel, D.P. (2001). An abundant class of tiny RNAs with probable regulatory roles in *Caenorhabditis elegans*. *Science* **294**, 858-862.
- Leamon, J.H., Lee, W.L., Tartaro, K.R., Lanza, J.R., Sarkis, G.J., deWinter, A.D., Berka, J., Weiner, M., Rothberg, J.M., and Lohman, K.L. (2003). A massively parallel PicoTiterPlate based platform for discrete picoliter-scale polymerase chain reactions. *Electrophoresis* **24**, 3769-3777.
- Lee, R.C., and Ambros, V. (2001). An extensive class of small RNAs in *Caenorhabditis elegans*. *Science* **294**, 862-864.
- Lee, R.C., Feinbaum, R.L., and Ambros, V. (1993). The *C. elegans* heterochronic gene *lin-4* encodes

- small RNAs with antisense complementarity to lin-14. *Cell* **75**, 843-854.
- Lee, Y., Ahn, C., Han, J., Choi, H., Kim, J., Yim, J., Lee, J., Provost, P., Radmark, O., Kim, S., *et al.* (2003). The nuclear RNase III Drosha initiates microRNA processing. *Nature* **425**, 415-419.
- Lee, Y., Kim, M., Han, J., Yeom, K.H., Lee, S., Baek, S.H., and Kim, V.N. (2004). MicroRNA genes are transcribed by RNA polymerase II. *EMBO J* **23**, 4051-4060.
- Lee, Y.S., and Dutta, A. (2009). MicroRNAs in cancer. *Annu Rev Pathol* **4**, 199-227.
- Lewis, B.P., Burge, C.B., and Bartel, D.P. (2005). Conserved seed pairing, often flanked by adenosines, indicates that thousands of human genes are microRNA targets. *Cell* **120**, 15-20.
- Liu, J., Carmell, M.A., Rivas, F.V., Marsden, C.G., Thomson, J.M., Song, J.J., Hammond, S.M., Joshua-Tor, L., and Hannon, G.J. (2004). Argonaute2 is the catalytic engine of mammalian RNAi. *Science* **305**, 1437-1441.
- Liu, J., Rivas, F.V., Wohlschlegel, J., Yates, J.R., 3rd, Parker, R., and Hannon, G.J. (2005). A role for the P-body component GW182 in microRNA function. *Nat Cell Biol* **7**, 1261-1266.
- Llave, C., Kasschau, K.D., Rector, M.A., and Carrington, J.C. (2002). Endogenous and silencing-associated small RNAs in plants. *Plant Cell* **14**, 1605-1619.
- Lo, A.K., To, K.F., Lo, K.W., Lung, R.W., Hui, J.W., Liao, G., and Hayward, S.D. (2007). Modulation of LMP1 protein expression by EBV-encoded microRNAs. *Proc Natl Acad Sci U S A* **104**, 16164-16169.
- Lodish, H.F., Zhou, B., Liu, G., and Chen, C.Z. (2008). Micromanagement of the immune system by microRNAs. *Nat Rev Immunol* **8**, 120-130.
- Lund, E., Guttinger, S., Calado, A., Dahlberg, J.E., and Kutay, U. (2004). Nuclear export of microRNA precursors. *Science* **303**, 95-98.
- Margulies, M., Egholm, M., Altman, W.E., Attiya, S., Bader, J.S., Bemben, L.A., Berka, J., Braverman, M.S., Chen, Y.J., Chen, Z., *et al.* (2005). Genome sequencing in microfabricated high-density picolitre reactors. *Nature* **437**, 376-380.
- Mathonnet, G., Fabian, M.R., Svitkin, Y.V., Parsyan, A., Huck, L., Murata, T., Biffo, S., Merrick, W.C., Darzynkiewicz, E., Pillai, R.S., *et al.* (2007). MicroRNA inhibition of translation initiation in vitro by targeting the cap-binding complex eIF4F. *Science* **317**, 1764-1767.
- McGeoch, D.J. (1989). The genomes of the human herpesviruses: contents, relationships, and evolution. *Annu Rev Microbiol* **43**, 235-265.
- McPherson, J.D. (2009). Next-generation gap. *Nat Methods* **6**, S2-5.
- Meister, G., Landthaler, M., Dorsett, Y., and Tuschl, T. (2004a). Sequence-specific inhibition of microRNA- and siRNA-induced RNA silencing. *RNA* **10**, 544-550.
- Meister, G., Landthaler, M., Patkaniowska, A., Dorsett, Y., Teng, G., and Tuschl, T. (2004b). Human Argonaute2 mediates RNA cleavage targeted by miRNAs and siRNAs. *Mol Cell* **15**, 185-197.
- Meister, G., Landthaler, M., Peters, L., Chen, P.Y., Urlaub, H., Luhrmann, R., and Tuschl, T. (2005). Identification of novel argonaute-associated proteins. *Curr Biol* **15**, 2149-2155.
- Meister, G., and Tuschl, T. (2004). Mechanisms of gene silencing by double-stranded RNA. *Nature* **431**, 343-349.
- Metzker, M.L. (2005). Emerging technologies in DNA sequencing. *Genome Res* **15**, 1767-1776.
- Metzker, M.L. (2010). Sequencing technologies - the next generation. *Nat Rev Genet* **11**, 31-46.
- Morozova, O., Hirst, M., and Marra, M.A. (2009). Applications of new sequencing technologies for transcriptome analysis. *Annu Rev Genomics Hum Genet* **10**, 135-151.
- Mourelatos, Z., Dostie, J., Paushkin, S., Sharma, A., Charroux, B., Abel, L., Rappsilber, J., Mann, M., and Dreyfuss, G. (2002). miRNPs: a novel class of ribonucleoproteins containing numerous microRNAs. *Genes Dev* **16**, 720-728.
- Niller, H.H., Wolf, H., and Minarovits, J. (2008). Regulation and dysregulation of Epstein-Barr virus latency: implications for the development of autoimmune diseases. *Autoimmunity* **41**, 298-328.
- Noonan, J.P., Coop, G., Kudaravalli, S., Smith, D., Krause, J., Alessi, J., Chen, F., Platt, D., Paabo, S., Pritchard, J.K., *et al.* (2006). Sequencing and analysis of Neanderthal genomic DNA. *Science* **314**,

1113-1118.

Olsen, P.H., and Ambros, V. (1999). The lin-4 regulatory RNA controls developmental timing in *Caenorhabditis elegans* by blocking LIN-14 protein synthesis after the initiation of translation. *Dev Biol* 216, 671-680.

Ozsolak, F., Platt, A.R., Jones, D.R., Reifenger, J.G., Sass, L.E., McInerney, P., Thompson, J.F., Bowers, J., Jarosz, M., and Milos, P.M. (2009). Direct RNA sequencing. *Nature* 461, 814-818.

Pall, G.S., Codony-Servat, C., Byrne, J., Ritchie, L., and Hamilton, A. (2007). Carbodiimide-mediated cross-linking of RNA to nylon membranes improves the detection of siRNA, miRNA and piRNA by northern blot. *Nucleic Acids Res* 35, e60.

Pantano, L., Estivill, X., and Marti, E. (2010). SeqBuster, a bioinformatic tool for the processing and analysis of small RNAs datasets, reveals ubiquitous miRNA modifications in human embryonic cells. *Nucleic Acids Res* 38, e34.

Parameswaran, P., Sklan, E., Wilkins, C., Burgon, T., Samuel, M.A., Lu, R., Ansel, K.M., Heissmeyer, V., Einav, S., Jackson, W., *et al.* (2010). Six RNA viruses and forty-one hosts: viral small RNAs and modulation of small RNA repertoires in vertebrate and invertebrate systems. *PLoS Pathog* 6, e1000764.

Pasquinelli, A.E., Reinhart, B.J., Slack, F., Martindale, M.Q., Kuroda, M.I., Maller, B., Hayward, D.C., Ball, E.E., Degnan, B., Muller, P., *et al.* (2000). Conservation of the sequence and temporal expression of let-7 heterochronic regulatory RNA. *Nature* 408, 86-89.

Perry, R.P. (1976). Processing of RNA. *Annu Rev Biochem* 45, 605-629.

Peters, L., and Meister, G. (2007). Argonaute proteins: mediators of RNA silencing. *Mol Cell* 26, 611-623.

Petersen, C.P., Bordeleau, M.E., Pelletier, J., and Sharp, P.A. (2006). Short RNAs repress translation after initiation in mammalian cells. *Mol Cell* 21, 533-542.

Pfeffer, S., Sewer, A., Lagos-Quintana, M., Sheridan, R., Sander, C., Grasser, F.A., van Dyk, L.F., Ho, C.K., Shuman, S., Chien, M., *et al.* (2005). Identification of microRNAs of the herpesvirus family. *Nat Methods* 2, 269-276.

Pfeffer, S., Zavolan, M., Grasser, F.A., Chien, M., Russo, J.J., Ju, J., John, B., Enright, A.J., Marks, D., Sander, C., *et al.* (2004). Identification of virus-encoded microRNAs. *Science* 304, 734-736.

Pillai, R.S., Bhattacharyya, S.N., Artus, C.G., Zoller, T., Cougot, N., Basyuk, E., Bertrand, E., and Filipowicz, W. (2005). Inhibition of translational initiation by Let-7 MicroRNA in human cells. *Science* 309, 1573-1576.

Rahadiani, N., Takakuwa, T., Tresnasari, K., Morii, E., and Aozasa, K. (2008). Latent membrane protein-1 of Epstein-Barr virus induces the expression of B-cell integration cluster, a precursor form of microRNA-155, in B lymphoma cell lines. *Biochem Biophys Res Commun* 377, 579-583.

Rajewsky, N. (2006). microRNA target predictions in animals. *Nat Genet* 38 *Suppl*, S8-13.

Rao, V.N., Shao, N., Ahmad, M., and Reddy, E.S. (1996). Antisense RNA to the putative tumor suppressor gene BRCA1 transforms mouse fibroblasts. *Oncogene* 12, 523-528.

Reese, T.A., Xia, J., Johnson, L.S., Zhou, X., Zhang, W., and Virgin, H.W. (2010). Identification of novel microRNA-like molecules generated from herpesvirus and host tRNA transcripts. *J Virol*.

Rehwinkel, J., Behm-Ansmant, I., Gatfield, D., and Izaurralde, E. (2005). A crucial role for GW182 and the DCP1:DCP2 decapping complex in miRNA-mediated gene silencing. *RNA* 11, 1640-1647.

Reinhart, B.J., Slack, F.J., Basson, M., Pasquinelli, A.E., Bettinger, J.C., Rougvié, A.E., Horvitz, H.R., and Ruvkun, G. (2000). The 21-nucleotide let-7 RNA regulates developmental timing in *Caenorhabditis elegans*. *Nature* 403, 901-906.

Reinhart, B.J., Weinstein, E.G., Rhoades, M.W., Bartel, B., and Bartel, D.P. (2002). MicroRNAs in plants. *Genes Dev* 16, 1616-1626.

Ronaghi, M., Karamohamed, S., Pettersson, B., Uhlen, M., and Nyren, P. (1996). Real-time DNA sequencing using detection of pyrophosphate release. *Anal Biochem* 242, 84-89.

Ronaghi, M., Uhlen, M., and Nyren, P. (1998). A sequencing method based on real-time pyrophosphate. *Science* 281, 363, 365.

Sambrook, J., Fritsch, E.F., and Maniatis, T. (1989). *Molecular cloning : a laboratory manual*, 2nd edn

(Cold Spring Harbor, Cold Spring Harbor Laboratory Press).

Schratt, G. (2009). Fine-tuning neural gene expression with microRNAs. *Curr Opin Neurobiol* 19, 213-219.

Schwarz, D.S., Hutvagner, G., Du, T., Xu, Z., Aronin, N., and Zamore, P.D. (2003). Asymmetry in the assembly of the RNAi enzyme complex. *Cell* 115, 199-208.

Sen, G.L., and Blau, H.M. (2005). Argonaute 2/RISC resides in sites of mammalian mRNA decay known as cytoplasmic bodies. *Nat Cell Biol* 7, 633-636.

Sharma, C.M., and Vogel, J. (2009). Experimental approaches for the discovery and characterization of regulatory small RNA. *Curr Opin Microbiol* 12, 536-546.

Simas, J.P., and Efstathiou, S. (1998). Murine gammaherpesvirus 68: a model for the study of gammaherpesvirus pathogenesis. *Trends Microbiol* 6, 276-282.

Skalsky, R.L., and Cullen, B.R. (2010). Viruses, microRNAs, and Host Interactions. *Annu Rev Microbiol*.

Skalsky, R.L., Samols, M.A., Plaisance, K.B., Boss, I.W., Riva, A., Lopez, M.C., Baker, H.V., and Renne, R. (2007). Kaposi's sarcoma-associated herpesvirus encodes an ortholog of miR-155. *J Virol* 81, 12836-12845.

Slack, F.J., Basson, M., Liu, Z., Ambros, V., Horvitz, H.R., and Ruvkun, G. (2000). The lin-41 RBCC gene acts in the *C. elegans* heterochronic pathway between the let-7 regulatory RNA and the LIN-29 transcription factor. *Mol Cell* 5, 659-669.

Sunil-Chandra, N.P., Efstathiou, S., and Nash, A.A. (1992). Murine gammaherpesvirus 68 establishes a latent infection in mouse B lymphocytes in vivo. *J Gen Virol* 73 (Pt 12), 3275-3279.

Svobodova, J., Blaskovic, D., and Mistrikova, J. (1982). Growth characteristics of herpesviruses isolated from free living small rodents. *Acta Virol* 26, 256-263.

Szymanski, M., Erdmann, V.A., and Barciszewski, J. (2003). Noncoding regulatory RNAs database. *Nucleic Acids Res* 31, 429-431.

Tarasov, V., Jung, P., Verdoodt, B., Lodygin, D., Epanchintsev, A., Menssen, A., Meister, G., and Hermeking, H. (2007). Differential regulation of microRNAs by p53 revealed by massively parallel sequencing: miR-34a is a p53 target that induces apoptosis and G1-arrest. *Cell Cycle* 6, 1586-1593.

Tawfik, D.S., and Griffiths, A.D. (1998). Man-made cell-like compartments for molecular evolution. *Nat Biotechnol* 16, 652-656.

Thermann, R., and Hentze, M.W. (2007). Drosophila miR2 induces pseudo-polysomes and inhibits translation initiation. *Nature* 447, 875-878.

Trang, P., Weidhaas, J.B., and Slack, F.J. (2008). MicroRNAs as potential cancer therapeutics. *Oncogene* 27 Suppl 2, S52-57.

Walz, N., Christalla, T., Tessmer, U., and Grundhoff, A. (2010). A global analysis of evolutionary conservation among known and predicted gammaherpesvirus microRNAs. *J Virol* 84, 716-728.

Wang, W. (2007). Emergence of a DNA-damage response network consisting of Fanconi anaemia and BRCA proteins. *Nat Rev Genet* 8, 735-748.

Wang, W.C., Lin, F.M., Chang, W.C., Lin, K.Y., Huang, H.D., and Lin, N.S. (2009a). miRExpress: analyzing high-throughput sequencing data for profiling microRNA expression. *BMC Bioinformatics* 10, 328.

Wang, Z., Gerstein, M., and Snyder, M. (2009b). RNA-Seq: a revolutionary tool for transcriptomics. *Nat Rev Genet* 10, 57-63.

Wei, W.I., and Sham, J.S. (2005). Nasopharyngeal carcinoma. *Lancet* 365, 2041-2054.

Weinmann, L., Hock, J., Ivacevic, T., Ohrt, T., Mutze, J., Schwill, P., Kremmer, E., Benes, V., Urlaub, H., and Meister, G. (2009). Importin 8 is a gene silencing factor that targets argonaute proteins to distinct mRNAs. *Cell* 136, 496-507.

Whitehead, K.A., Langer, R., and Anderson, D.G. (2009). Knocking down barriers: advances in siRNA delivery. *Nat Rev Drug Discov* 8, 129-138.

Wightman, B., Ha, I., and Ruvkun, G. (1993). Posttranscriptional regulation of the heterochronic gene lin-14 by lin-4 mediates temporal pattern formation in *C. elegans*. *Cell* 75, 855-862.

- Willenbrock, H., Salomon, J., Sokilde, R., Barken, K.B., Hansen, T.N., Nielsen, F.C., Moller, S., and Litman, T. (2009). Quantitative miRNA expression analysis: comparing microarrays with next-generation sequencing. *RNA* 15, 2028-2034.
- Wu, L., Fan, J., and Belasco, J.G. (2006). MicroRNAs direct rapid deadenylation of mRNA. *Proc Natl Acad Sci U S A* 103, 4034-4039.
- Xia, T., O'Hara, A., Araujo, I., Barreto, J., Carvalho, E., Sapucaia, J.B., Ramos, J.C., Luz, E., Pedrosa, C., Manrique, M., *et al.* (2008). EBV microRNAs in primary lymphomas and targeting of CXCL-11 by ebv-mir-BHRF1-3. *Cancer Res* 68, 1436-1442.
- Xing, L., and Kieff, E. (2007). Epstein-Barr virus BHRF1 micro- and stable RNAs during latency III and after induction of replication. *J Virol* 81, 9967-9975.
- Xiong, Y., and Steitz, T.A. (2006). A story with a good ending: tRNA 3'-end maturation by CCA-adding enzymes. *Curr Opin Struct Biol* 16, 12-17.
- Yao, Y., Zhao, Y., Xu, H., Smith, L.P., Lawrie, C.H., Sewer, A., Zavolan, M., and Nair, V. (2007). Marek's disease virus type 2 (MDV-2)-encoded microRNAs show no sequence conservation with those encoded by MDV-1. *J Virol* 81, 7164-7170.
- Yi, R., Qin, Y., Macara, I.G., and Cullen, B.R. (2003). Exportin-5 mediates the nuclear export of pre-microRNAs and short hairpin RNAs. *Genes Dev* 17, 3011-3016.
- Young, L.S., and Murray, P.G. (2003). Epstein-Barr virus and oncogenesis: from latent genes to tumours. *Oncogene* 22, 5108-5121.
- Young, L.S., and Rickinson, A.B. (2004). Epstein-Barr virus: 40 years on. *Nat Rev Cancer* 4, 757-768.
- Zhang, B., Pan, X., Wang, Q., Cobb, G.P., and Anderson, T.A. (2006). Computational identification of microRNAs and their targets. *Comput Biol Chem* 30, 395-407.
- Zhao, Y., Yao, Y., Xu, H., Lambeth, L., Smith, L.P., Kgosana, L., Wang, X., and Nair, V. (2009). A functional MicroRNA-155 ortholog encoded by the oncogenic Marek's disease virus. *J Virol* 83, 489-492.
- Zuker, M. (2003). Mfold web server for nucleic acid folding and hybridization prediction. *Nucleic Acids Res* 31, 3406-3415.

APPENDIX

Appendix Table I

Read numbers and analysis of individual miRNA in 454 sequencing libraries of NPC and control samples.

	Read number		Percentage		Read number		Percentage	
	NPC-1	control-1	NPC-1	control-1	NPC-2	control-2	NPC-2	control-2
total miRNA	20330	1287	100.0%	100.0%	6194	1476	100.0%	100.0%
hsa-let-7a	295	13	1.5%	1.0%	48	13	0.8%	0.9%
hsa-let-7a*	1	0	0.0%	0.0%	0	0	0.0%	0.0%
hsa-let-7a/c	38	1	0.2%	0.1%	3	2	0.0%	0.1%
hsa-let-7b	287	34	1.4%	2.6%	262	74	4.2%	5.0%
hsa-let-7c	128	10	0.6%	0.8%	30	10	0.5%	0.7%
hsa-let-7d	65	1	0.3%	0.1%	11	1	0.2%	0.1%
hsa-let-7d*	14	2	0.1%	0.2%	7	1	0.1%	0.1%
hsa-let-7e	49	4	0.2%	0.3%	11	5	0.2%	0.3%
hsa-let-7f	45	1	0.2%	0.1%	8	1	0.1%	0.1%
hsa-let-7f-1*	1	0	0.0%	0.0%	2	0	0.0%	0.0%
hsa-let-7f-2*	10	0	0.0%	0.0%	1	0	0.0%	0.0%
hsa-let-7g	56	0	0.3%	0.0%	5	2	0.1%	0.1%
hsa-let-7i	9	0	0.0%	0.0%	3	0	0.0%	0.0%
hsa-let-7i*	7	0	0.0%	0.0%	4	3	0.1%	0.2%
hsa-mir-7	0	0	0.0%	0.0%	2	0	0.0%	0.0%
hsa-mir-7-1*	9	1	0.0%	0.1%	0	0	0.0%	0.0%
hsa-mir-9*	1	1	0.0%	0.1%	0	1	0.0%	0.1%
hsa-mir-10a	0	1	0.0%	0.1%	0	1	0.0%	0.1%
hsa-mir-10b*	0	1	0.0%	0.1%	0	0	0.0%	0.0%
hsa-mir-15a	552	24	2.7%	1.9%	44	4	0.7%	0.3%
hsa-mir-15b	684	34	3.4%	2.6%	43	26	0.7%	1.8%
hsa-mir-16	498	19	2.4%	1.5%	31	4	0.5%	0.3%
hsa-mir-16-2*	1	0	0.0%	0.0%	1	0	0.0%	0.0%
hsa-mir-17	328	54	1.6%	4.2%	27	58	0.4%	3.9%
hsa-mir-17*	34	7	0.2%	0.5%	39	19	0.6%	1.3%
hsa-mir-19b	0	4	0.0%	0.3%	0	1	0.0%	0.1%
hsa-mir-20a	27	2	0.1%	0.2%	6	2	0.1%	0.1%
hsa-mir-20b	1	0	0.0%	0.0%	0	0	0.0%	0.0%
hsa-mir-21	146	3	0.7%	0.2%	17	0	0.3%	0.0%

hsa-mir-21*	9	1	0.0%	0.1%	2	0	0.0%	0.0%
hsa-mir-22	70	15	0.3%	1.2%	97	30	1.6%	2.0%
hsa-mir-22*	44	1	0.2%	0.1%	14	8	0.2%	0.5%
hsa-mir-23a	3422	66	16.8%	5.1%	294	30	4.7%	2.0%
hsa-mir-23a/b	1007	31	5.0%	2.4%	82	23	1.3%	1.6%
hsa-mir-23b	819	24	4.0%	1.9%	87	15	1.4%	1.0%
hsa-mir-23b*	1	0	0.0%	0.0%	1	0	0.0%	0.0%
hsa-mir-24	65	8	0.3%	0.6%	93	25	1.5%	1.7%
hsa-mir-24-1*	1	0	0.0%	0.0%	0	0	0.0%	0.0%
hsa-mir-24-2*	1	0	0.0%	0.0%	1	1	0.0%	0.1%
hsa-mir-25	1215	87	6.0%	6.8%	285	72	4.6%	4.9%
hsa-mir-25*	0	0	0.0%	0.0%	2	0	0.0%	0.0%
hsa-mir-26a	188	4	0.9%	0.3%	15	5	0.2%	0.3%
hsa-mir-26b	316	4	1.6%	0.3%	14	8	0.2%	0.5%
hsa-mir-27a	563	7	2.8%	0.5%	57	2	0.9%	0.1%
hsa-mir-27a/b	66	5	0.3%	0.4%	5	3	0.1%	0.2%
hsa-mir-27b	839	41	4.1%	3.2%	263	25	4.2%	1.7%
hsa-mir-27b*	0	0	0.0%	0.0%	1	2	0.0%	0.1%
hsa-mir-28-3p	25	2	0.1%	0.2%	5	1	0.1%	0.1%
hsa-mir-28-5p	23	0	0.1%	0.0%	8	2	0.1%	0.1%
hsa-mir-29a	52	1	0.3%	0.1%	10	0	0.2%	0.0%
hsa-mir-29b	17	2	0.1%	0.2%	4	1	0.1%	0.1%
hsa-mir-29b-2*	0	0	0.0%	0.0%	2	1	0.0%	0.1%
hsa-mir-29c	32	0	0.2%	0.0%	9	1	0.1%	0.1%
hsa-mir-29c*	1	0	0.0%	0.0%	0	1	0.0%	0.1%
hsa-mir-30a	3	0	0.0%	0.0%	4	0	0.1%	0.0%
hsa-mir-30a*	6	1	0.0%	0.1%	11	1	0.2%	0.1%
hsa-mir-30a/e*	1	0	0.0%	0.0%	1	0	0.0%	0.0%
hsa-mir-30b	9	0	0.0%	0.0%	0	0	0.0%	0.0%
hsa-mir-30c	7	1	0.0%	0.1%	1	0	0.0%	0.0%
hsa-mir-30c-2*	0	0	0.0%	0.0%	1	0	0.0%	0.0%
hsa-mir-30d	4	1	0.0%	0.1%	0	1	0.0%	0.1%
hsa-mir-30e	5	1	0.0%	0.1%	1	1	0.0%	0.1%
hsa-mir-30e*	39	1	0.2%	0.1%	0	0	0.0%	0.0%
hsa-mir-31*	0	0	0.0%	0.0%	2	0	0.0%	0.0%
hsa-mir-32	1	0	0.0%	0.0%	0	0	0.0%	0.0%
hsa-mir-33a*	2	0	0.0%	0.0%	0	0	0.0%	0.0%
hsa-mir-34a	23	2	0.1%	0.2%	31	3	0.5%	0.2%
hsa-mir-34b	3	0	0.0%	0.0%	0	0	0.0%	0.0%
hsa-mir-34b*	0	0	0.0%	0.0%	4	0	0.1%	0.0%
hsa-mir-34c-3p	5	1	0.0%	0.1%	3	0	0.0%	0.0%
hsa-mir-34c-5p	2	0	0.0%	0.0%	0	0	0.0%	0.0%
hsa-mir-92a	52	5	0.3%	0.4%	14	4	0.2%	0.3%

hsa-mir-92a-1*	0	0	0.0%	0.0%	1	0	0.0%	0.0%
hsa-mir-92b	0	0	0.0%	0.0%	1	0	0.0%	0.0%
hsa-mir-92b*	0	0	0.0%	0.0%	1	0	0.0%	0.0%
hsa-mir-93	46	8	0.2%	0.6%	6	5	0.1%	0.3%
hsa-mir-93*	0	0	0.0%	0.0%	1	0	0.0%	0.0%
hsa-mir-96	3	0	0.0%	0.0%	1	0	0.0%	0.0%
hsa-mir-96*	1	0	0.0%	0.0%	0	0	0.0%	0.0%
hsa-mir-98	3	0	0.0%	0.0%	0	0	0.0%	0.0%
hsa-mir-99a	13	1	0.1%	0.1%	2	0	0.0%	0.0%
hsa-mir-99a*	1	0	0.0%	0.0%	0	0	0.0%	0.0%
hsa-mir-99b	8	1	0.0%	0.1%	8	2	0.1%	0.1%
hsa-mir-99b*	2	0	0.0%	0.0%	0	0	0.0%	0.0%
hsa-mir-100	4	0	0.0%	0.0%	0	0	0.0%	0.0%
hsa-mir-101	13	3	0.1%	0.2%	1	1	0.0%	0.1%
hsa-mir-103	272	17	1.3%	1.3%	53	17	0.9%	1.2%
hsa-mir-103-2*	12	1	0.1%	0.1%	15	1	0.2%	0.1%
hsa-mir-103/107	72	3	0.4%	0.2%	18	1	0.3%	0.1%
hsa-mir-106a	1	0	0.0%	0.0%	5	0	0.1%	0.0%
hsa-mir-106b	364	25	1.8%	1.9%	30	21	0.5%	1.4%
hsa-mir-106b*	7	5	0.0%	0.4%	14	5	0.2%	0.3%
hsa-mir-107	5	1	0.0%	0.1%	1	0	0.0%	0.0%
hsa-mir-122a	0	0	0.0%	0.0%	1	0	0.0%	0.0%
hsa-mir-124	0	1	0.0%	0.1%	1	0	0.0%	0.0%
hsa-mir-125a-3p	2	0	0.0%	0.0%	0	0	0.0%	0.0%
hsa-mir-125a-5p	31	1	0.2%	0.1%	16	8	0.3%	0.5%
hsa-mir-125b	74	15	0.4%	1.2%	40	16	0.6%	1.1%
hsa-mir-126	92	3	0.5%	0.2%	45	15	0.7%	1.0%
hsa-mir-126*	0	0	0.0%	0.0%	0	1	0.0%	0.1%
hsa-mir-127-3p	0	0	0.0%	0.0%	2	1	0.0%	0.1%
hsa-mir-128a	47	1	0.2%	0.1%	5	1	0.1%	0.1%
hsa-mir-130a	3	0	0.0%	0.0%	1	0	0.0%	0.0%
hsa-mir-130b	3	0	0.0%	0.0%	0	1	0.0%	0.1%
hsa-mir-132	14	2	0.1%	0.2%	8	1	0.1%	0.1%
hsa-mir-134	0	7	0.0%	0.5%	3	7	0.0%	0.5%
hsa-mir-135b	4	0	0.0%	0.0%	1	0	0.0%	0.0%
hsa-mir-135b*	2	0	0.0%	0.0%	0	0	0.0%	0.0%
hsa-mir-138	7	0	0.0%	0.0%	9	3	0.1%	0.2%
hsa-mir-138-1*	2	0	0.0%	0.0%	0	0	0.0%	0.0%
hsa-mir-139-3p	0	0	0.0%	0.0%	2	0	0.0%	0.0%
hsa-mir-139-5p	13	2	0.1%	0.2%	3	0	0.0%	0.0%
hsa-mir-140-3p	68	5	0.3%	0.4%	25	5	0.4%	0.3%
hsa-mir-140-5p	3	0	0.0%	0.0%	0	0	0.0%	0.0%
hsa-mir-141	21	0	0.1%	0.0%	0	0	0.0%	0.0%

hsa-mir-142-3p	16	1	0.1%	0.1%	7	0	0.1%	0.0%
hsa-mir-142-5p	14	1	0.1%	0.1%	2	0	0.0%	0.0%
hsa-mir-143	5	0	0.0%	0.0%	3	0	0.0%	0.0%
hsa-mir-144	0	1	0.0%	0.1%	0	0	0.0%	0.0%
hsa-mir-145	7	0	0.0%	0.0%	1	1	0.0%	0.1%
hsa-mir-146a	24	1	0.1%	0.1%	7	0	0.1%	0.0%
hsa-mir-146a/b	1	0	0.0%	0.0%	0	0	0.0%	0.0%
hsa-mir-146b-5p	7	0	0.0%	0.0%	2	0	0.0%	0.0%
hsa-mir-146b-3p	1	0	0.0%	0.0%	0	0	0.0%	0.0%
hsa-mir-148a	13	1	0.1%	0.1%	6	0	0.1%	0.0%
hsa-mir-148b	3	0	0.0%	0.0%	0	1	0.0%	0.1%
hsa-mir-149	3	0	0.0%	0.0%	7	1	0.1%	0.1%
hsa-mir-150	39	0	0.2%	0.0%	7	4	0.1%	0.3%
hsa-mir-150*	2	0	0.0%	0.0%	0	1	0.0%	0.1%
hsa-mir-151-3p	36	5	0.2%	0.4%	22	9	0.4%	0.6%
hsa-mir-151-5p	432	36	2.1%	2.8%	95	17	1.5%	1.2%
hsa-mir-152	81	5	0.4%	0.4%	8	9	0.1%	0.6%
hsa-mir-153	1	0	0.0%	0.0%	0	0	0.0%	0.0%
hsa-mir-155	120	1	0.6%	0.1%	8	0	0.1%	0.0%
hsa-mir-181a	13	1	0.1%	0.1%	1	1	0.0%	0.1%
hsa-mir-181a-2*	5	1	0.0%	0.1%	6	0	0.1%	0.0%
hsa-mir-181b	5	2	0.0%	0.2%	9	1	0.1%	0.1%
hsa-mir-181c*	3	0	0.0%	0.0%	1	0	0.0%	0.0%
hsa-mir-182	74	2	0.4%	0.2%	15	1	0.2%	0.1%
hsa-mir-182*	0	0	0.0%	0.0%	1	0	0.0%	0.0%
hsa-mir-183	26	1	0.1%	0.1%	12	0	0.2%	0.0%
hsa-mir-184	73	7	0.4%	0.5%	2	1	0.0%	0.1%
hsa-mir-185	117	10	0.6%	0.8%	30	8	0.5%	0.5%
hsa-mir-186	1	0	0.0%	0.0%	0	0	0.0%	0.0%
hsa-mir-187	1	1	0.0%	0.1%	2	7	0.0%	0.5%
hsa-mir-190	24	5	0.1%	0.4%	17	8	0.3%	0.5%
hsa-mir-191	182	5	0.9%	0.4%	35	11	0.6%	0.7%
hsa-mir-192	10	0	0.0%	0.0%	2	1	0.0%	0.1%
hsa-mir-192*	1	0	0.0%	0.0%	0	0	0.0%	0.0%
hsa-mir-193a-3p	1	0	0.0%	0.0%	0	0	0.0%	0.0%
hsa-mir-193a-5p	0	0	0.0%	0.0%	1	1	0.0%	0.1%
hsa-mir-193b	0	0	0.0%	0.0%	11	1	0.2%	0.1%
hsa-mir-194	9	0	0.0%	0.0%	1	1	0.0%	0.1%
hsa-mir-195	50	1	0.2%	0.1%	3	0	0.0%	0.0%
hsa-mir-196a	0	6	0.0%	0.5%	2	5	0.0%	0.3%
hsa-mir-196b*	0	1	0.0%	0.1%	0	0	0.0%	0.0%
hsa-mir-199a-3p	646	51	3.2%	4.0%	68	53	1.1%	3.6%
hsa-mir-199a-5p	102	9	0.5%	0.7%	33	19	0.5%	1.3%

hsa-mir-199b-5p	16	0	0.1%	0.0%	1	0	0.0%	0.0%
hsa-mir-200a	4	0	0.0%	0.0%	8	1	0.1%	0.1%
hsa-mir-200a*	3	0	0.0%	0.0%	0	0	0.0%	0.0%
hsa-mir-200b	530	31	2.6%	2.4%	137	28	2.2%	1.9%
hsa-mir-200b*	9	0	0.0%	0.0%	6	1	0.1%	0.1%
hsa-mir-200c	1498	40	7.4%	3.1%	127	6	2.1%	0.4%
hsa-mir-203	1	0	0.0%	0.0%	0	1	0.0%	0.1%
hsa-mir-205	69	6	0.3%	0.5%	58	1	0.9%	0.1%
hsa-mir-205*	15	3	0.1%	0.2%	9	5	0.1%	0.3%
hsa-mir-206	0	1	0.0%	0.1%	0	0	0.0%	0.0%
hsa-mir-210	114	12	0.6%	0.9%	309	40	5.0%	2.7%
hsa-mir-212	4	0	0.0%	0.0%	2	0	0.0%	0.0%
hsa-mir-214	27	9	0.1%	0.7%	11	7	0.2%	0.5%
hsa-mir-218	14	10	0.1%	0.8%	18	4	0.3%	0.3%
hsa-mir-221	184	39	0.9%	3.0%	193	83	3.1%	5.6%
hsa-mir-221*	7	0	0.0%	0.0%	1	1	0.0%	0.1%
hsa-mir-222	92	9	0.5%	0.7%	73	17	1.2%	1.2%
hsa-mir-223	14	0	0.1%	0.0%	4	0	0.1%	0.0%
hsa-mir-223*	4	0	0.0%	0.0%	0	0	0.0%	0.0%
hsa-mir-224	17	1	0.1%	0.1%	9	1	0.1%	0.1%
hsa-mir-224*	0	0	0.0%	0.0%	2	0	0.0%	0.0%
hsa-mir-296-3p	2	1	0.0%	0.1%	0	0	0.0%	0.0%
hsa-mir-296-5p	0	0	0.0%	0.0%	0	1	0.0%	0.1%
hsa-mir-301a/b	6	1	0.0%	0.1%	0	1	0.0%	0.1%
hsa-mir-320	353	114	1.7%	8.9%	555	272	9.0%	18.4%
hsa-mir-323-3p	0	1	0.0%	0.1%	0	1	0.0%	0.1%
hsa-mir-324-3p	9	1	0.0%	0.1%	4	3	0.1%	0.2%
hsa-mir-324-5p	7	0	0.0%	0.0%	4	3	0.1%	0.2%
hsa-mir-328	0	0	0.0%	0.0%	0	1	0.0%	0.1%
hsa-mir-330-5p	1	0	0.0%	0.0%	0	0	0.0%	0.0%
hsa-mir-331-3p	1	0	0.0%	0.0%	3	0	0.0%	0.0%
hsa-mir-331-5p	1	0	0.0%	0.0%	3	0	0.0%	0.0%
hsa-mir-338-3p	3	0	0.0%	0.0%	0	0	0.0%	0.0%
hsa-mir-339-3p	1	0	0.0%	0.0%	3	0	0.0%	0.0%
hsa-mir-339-5p	0	0	0.0%	0.0%	2	0	0.0%	0.0%
hsa-mir-340	2	0	0.0%	0.0%	0	0	0.0%	0.0%
hsa-mir-342-3p	5	2	0.0%	0.2%	3	0	0.0%	0.0%
hsa-mir-345	28	5	0.1%	0.4%	36	10	0.6%	0.7%
hsa-mir-361-3p	10	1	0.0%	0.1%	2	3	0.0%	0.2%
hsa-mir-361-5p	51	1	0.3%	0.1%	0	2	0.0%	0.1%
hsa-mir-362-5p	1	0	0.0%	0.0%	1	1	0.0%	0.1%
hsa-mir-363	1	0	0.0%	0.0%	0	0	0.0%	0.0%
hsa-mir-365	1	0	0.0%	0.0%	0	0	0.0%	0.0%

hsa-mir-365-2*	0	0	0.0%	0.0%	1	0	0.0%	0.0%
hsa-mir-370	0	0	0.0%	0.0%	2	1	0.0%	0.1%
hsa-mir-374a	37	0	0.2%	0.0%	2	0	0.0%	0.0%
hsa-mir-375	0	0	0.0%	0.0%	3	3	0.0%	0.2%
hsa-mir-376a	0	1	0.0%	0.1%	0	0	0.0%	0.0%
hsa-mir-378	43	26	0.2%	2.0%	211	86	3.4%	5.8%
hsa-mir-378*	11	0	0.1%	0.0%	27	13	0.4%	0.9%
hsa-mir-409-3p	0	0	0.0%	0.0%	0	1	0.0%	0.1%
hsa-mir-410	0	1	0.0%	0.1%	0	0	0.0%	0.0%
hsa-mir-423-3p	7	0	0.0%	0.0%	9	4	0.1%	0.3%
hsa-mir-423-5p	8	4	0.0%	0.3%	2	0	0.0%	0.0%
hsa-mir-424	34	7	0.2%	0.5%	1	1	0.0%	0.1%
hsa-mir-425	6	1	0.0%	0.1%	5	2	0.1%	0.1%
hsa-mir-429	1	0	0.0%	0.0%	0	1	0.0%	0.1%
hsa-mir-432	0	1	0.0%	0.1%	0	0	0.0%	0.0%
hsa-mir-433	0	7	0.0%	0.5%	1	8	0.0%	0.5%
hsa-mir-449a	3	0	0.0%	0.0%	1	0	0.0%	0.0%
hsa-mir-449b	1	0	0.0%	0.0%	0	0	0.0%	0.0%
hsa-mir-449b*	1	0	0.0%	0.0%	0	0	0.0%	0.0%
hsa-mir-450a	1	0	0.0%	0.0%	0	0	0.0%	0.0%
hsa-mir-451	3	5	0.0%	0.4%	16	0	0.3%	0.0%
hsa-mir-452	1	0	0.0%	0.0%	1	0	0.0%	0.0%
hsa-mir-455-3p	82	3	0.4%	0.2%	32	1	0.5%	0.1%
hsa-mir-455-5p	2	0	0.0%	0.0%	6	1	0.1%	0.1%
hsa-mir-484	12	2	0.1%	0.2%	8	4	0.1%	0.3%
hsa-mir-486-3p	1	0	0.0%	0.0%	0	0	0.0%	0.0%
hsa-mir-486-5p	26	66	0.1%	5.1%	105	11	1.7%	0.7%
hsa-mir-487b	1	0	0.0%	0.0%	0	0	0.0%	0.0%
hsa-mir-497	71	0	0.3%	0.0%	7	0	0.1%	0.0%
hsa-mir-500	4	0	0.0%	0.0%	3	1	0.0%	0.1%
hsa-mir-500*	2	0	0.0%	0.0%	0	0	0.0%	0.0%
hsa-mir-503	7	1	0.0%	0.1%	1	0	0.0%	0.0%
hsa-mir-505	1	0	0.0%	0.0%	0	0	0.0%	0.0%
hsa-mir-505*	2	0	0.0%	0.0%	1	0	0.0%	0.0%
hsa-mir-517a	0	0	0.0%	0.0%	2	0	0.0%	0.0%
hsa-mir-532-3p	30	3	0.1%	0.2%	17	3	0.3%	0.2%
hsa-mir-532-5p	17	0	0.1%	0.0%	0	3	0.0%	0.2%
hsa-mir-551b	4	0	0.0%	0.0%	0	0	0.0%	0.0%
hsa-mir-551b*	4	0	0.0%	0.0%	0	0	0.0%	0.0%
hsa-mir-574-3p	3	0	0.0%	0.0%	0	0	0.0%	0.0%
hsa-mir-574-5p	6	2	0.0%	0.2%	10	0	0.2%	0.0%
hsa-mir-584	2	0	0.0%	0.0%	2	0	0.0%	0.0%
hsa-mir-590-3p	4	0	0.0%	0.0%	0	0	0.0%	0.0%

hsa-mir-598	10	1	0.0%	0.1%	1	0	0.0%	0.0%
hsa-mir-607	0	1	0.0%	0.1%	0	0	0.0%	0.0%
hsa-mir-615-3p	8	3	0.0%	0.2%	2	5	0.0%	0.3%
hsa-mir-624	2	0	0.0%	0.0%	2	0	0.0%	0.0%
hsa-mir-628-3p	1	0	0.0%	0.0%	0	0	0.0%	0.0%
hsa-mir-629	2	0	0.0%	0.0%	0	0	0.0%	0.0%
hsa-mir-652	97	31	0.5%	2.4%	42	21	0.7%	1.4%
hsa-mir-660	0	0	0.0%	0.0%	1	0	0.0%	0.0%
hsa-mir-744	3	3	0.0%	0.2%	13	2	0.2%	0.1%
hsa-mir-758	0	0	0.0%	0.0%	1	3	0.0%	0.2%
hsa-mir-766	12	4	0.1%	0.3%	2	3	0.0%	0.2%
hsa-mir-768-3p	1	0	0.0%	0.0%	0	0	0.0%	0.0%
hsa-mir-768-5p	1	0	0.0%	0.0%	0	0	0.0%	0.0%
hsa-mir-769-3p	1	0	0.0%	0.0%	1	0	0.0%	0.0%
hsa-mir-769-5p	1	0	0.0%	0.0%	0	0	0.0%	0.0%
hsa-mir-874	15	0	0.1%	0.0%	11	8	0.2%	0.5%
hsa-mir-942	8	0	0.0%	0.0%	6	3	0.1%	0.2%
hsa-mir-1301	15	1	0.1%	0.1%	5	0	0.1%	0.0%
hsa-mir-1307	22	8	0.1%	0.6%	79	22	1.3%	1.5%
hsa-mir-2110	3	1	0.0%	0.1%	2	3	0.0%	0.2%
ebv-mir-BART1-3p	8	0	0.0%	0.0%	4	0	0.1%	0.0%
ebv-mir-BART1-5p	136	6	0.7%	0.5%	169	0	2.7%	0.0%
ebv-mir-BART2-5p	6	0	0.0%	0.0%	1	0	0.0%	0.0%
ebv-mir-BART3	6	0	0.0%	0.0%	3	0	0.0%	0.0%
ebv-mir-BART3*	2	0	0.0%	0.0%	7	0	0.1%	0.0%
ebv-mir-BART4	38	7	0.2%	0.5%	424	0	6.8%	0.0%
ebv-mir-BART4*	6	0	0.0%	0.0%	9	0	0.1%	0.0%
ebv-mir-BART5	18	0	0.1%	0.0%	4	0	0.1%	0.0%
ebv-mir-BART5*	0	0	0.0%	0.0%	1	0	0.0%	0.0%
ebv-mir-BART6-3p	27	0	0.1%	0.0%	73	0	1.2%	0.0%
ebv-mir-BART6-5p	2	0	0.0%	0.0%	0	0	0.0%	0.0%
ebv-mir-BART7	292	5	1.4%	0.4%	37	0	0.6%	0.0%
ebv-mir-BART8	1	0	0.0%	0.0%	2	0	0.0%	0.0%
ebv-mir-BART8*	18	1	0.1%	0.1%	24	0	0.4%	0.0%
ebv-mir-BART9	36	0	0.2%	0.0%	22	0	0.4%	0.0%
ebv-mir-BART10	14	0	0.1%	0.0%	2	0	0.0%	0.0%
ebv-mir-BART11-3p	9	1	0.0%	0.1%	56	0	0.9%	0.0%
ebv-mir-BART11-5p	21	1	0.1%	0.1%	13	0	0.2%	0.0%
ebv-mir-BART12	13	1	0.1%	0.1%	64	0	1.0%	0.0%
ebv-mir-BART13	10	1	0.0%	0.1%	6	0	0.1%	0.0%
ebv-mir-BART14	11	1	0.1%	0.1%	10	0	0.2%	0.0%
ebv-mir-BART14*	3	0	0.0%	0.0%	6	0	0.1%	0.0%
ebv-mir-BART15	1	0	0.0%	0.0%	0	0	0.0%	0.0%

ebv-mir-BART16	36	2	0.2%	0.2%	23	0	0.4%	0.0%
ebv-mir-BART17-3p	23	0	0.1%	0.0%	34	0	0.5%	0.0%
ebv-mir-BART17-5p	26	0	0.1%	0.0%	16	0	0.3%	0.0%
ebv-mir-BART18-5p	0	0	0.0%	0.0%	1	0	0.0%	0.0%
ebv-mir-BART19-3p	6	1	0.0%	0.1%	85	0	1.4%	0.0%
ebv-mir-BART20-3p	1	0	0.0%	0.0%	0	0	0.0%	0.0%
ebv-mir-BART20-5p	0	0	0.0%	0.0%	0	0	0.0%	0.0%
ebv-mir-BART21-3P	10	1	0.0%	0.1%	6	0	0.1%	0.0%
ebv-mir-BART21-5P	19	1	0.1%	0.1%	7	0	0.1%	0.0%
ebv-mir-BART22	201	1	1.0%	0.1%	81	0	1.3%	0.0%

The libraries were analysed in the reference of miRBase v11.0. The human and EBV miRNAs that are not present here have no reads in all four libraries.

Appendix Table II

Read numbers and analysis of individual murine miRNA in 454 sequencing libraries of MHV-68 infected cell lines.

	Read Number		Percentage		Read Number		Percentage	
	NIH 3T3-	NIH 3T3+	NIH 3T3-	NIH 3T3+	S11-	S11+	S11-	S11+
total miRNA	50069	47011	100%	100%	30055	39037	100%	100%
mmu-let-7a	74	109	0.1%	0.2%	37	138	0.1%	0.3%
mmu-let-7a*	21	8	0.0%	0.0%	4	5	0.0%	0.0%
mmu-let-7a-2*	1	1	0.0%	0.0%	1	0	0.0%	0.0%
mmu-let-7b	155	199	0.3%	0.4%	0	0	0.0%	0.0%
mmu-let-7b*	7	2	0.0%	0.0%	0	0	0.0%	0.0%
mmu-let-7c	280	382	0.6%	0.8%	58	127	0.1%	0.3%
mmu-let-7c-1*	0	1	0.0%	0.0%	0	0	0.0%	0.0%
mmu-let-7d	35	44	0.1%	0.1%	14	68	0.0%	0.1%
mmu-let-7d*	29	15	0.1%	0.0%	9	25	0.0%	0.1%
mmu-let-7e	78	138	0.2%	0.3%	0	0	0.0%	0.0%
mmu-let-7e*	7	15	0.0%	0.0%	0	0	0.0%	0.0%
mmu-let-7f	161	357	0.3%	0.8%	146	504	0.3%	1.1%
mmu-let-7f*	7	10	0.0%	0.0%	3	1	0.0%	0.0%
mmu-let-7f-2*	6	2	0.0%	0.0%	5	5	0.0%	0.0%
mmu-let-7g	117	131	0.2%	0.3%	219	711	0.4%	1.5%
mmu-let-7g*	3	1	0.0%	0.0%	5	5	0.0%	0.0%
mmu-let-7i	743	326	1.5%	0.7%	30	80	0.1%	0.2%
mmu-let-7i*	71	8	0.1%	0.0%	3	6	0.0%	0.0%
mmu-mir-7a	36	35	0.1%	0.1%	46	100	0.1%	0.2%
mmu-mir-7a*	11	12	0.0%	0.0%	10	27	0.0%	0.1%
mmu-mir-9	55	60	0.1%	0.1%	444	374	0.9%	0.8%
mmu-mir-9*	10	10	0.0%	0.0%	103	106	0.2%	0.2%
mmu-mir-10a	0	11	0.0%	0.0%	4	5	0.0%	0.0%
mmu-mir-10a*	0	0	0.0%	0.0%	1	0	0.0%	0.0%
mmu-mir-10b	73	11	0.1%	0.0%	62	119	0.1%	0.3%
mmu-mir-10b*	6	0	0.0%	0.0%	3	5	0.0%	0.0%
mmu-mir-15a	509	433	1.0%	0.9%	552	542	1.1%	1.2%
mmu-mir-15a*	26	4	0.1%	0.0%	9	9	0.0%	0.0%
mmu-mir-15b	807	1872	1.6%	4.0%	1165	1284	2.3%	2.7%
mmu-mir-15b*	16	4	0.0%	0.0%	4	12	0.0%	0.0%
mmu-mir-16	2823	5705	5.6%	12.1%	5135	5708	10.3%	12.1%
mmu-mir-16*	1	1	0.0%	0.0%	0	4	0.0%	0.0%
mmu-mir-16-2*	27	24	0.1%	0.1%	16	24	0.0%	0.1%
mmu-mir-17	1205	1060	2.4%	2.3%	278	361	0.6%	0.8%
mmu-mir-17*	138	43	0.3%	0.1%	35	66	0.1%	0.1%
mmu-mir-18a	185	88	0.4%	0.2%	13	27	0.0%	0.1%
mmu-mir-18a*	5	3	0.0%	0.0%	7	9	0.0%	0.0%

mmu-mir-18b	3	0	0.0%	0.0%	0	0	0.0%	0.0%
mmu-mir-19a	25	2	0.0%	0.0%	12	12	0.0%	0.0%
mmu-mir-19b	370	126	0.7%	0.3%	142	199	0.3%	0.4%
mmu-mir-19b-1*	2	1	0.0%	0.0%	0	0	0.0%	0.0%
mmu-mir-20a	593	625	1.2%	1.3%	177	296	0.4%	0.6%
mmu-mir-20a*	0	1	0.0%	0.0%	0	0	0.0%	0.0%
mmu-mir-20b*	0	0	0.0%	0.0%	1	1	0.0%	0.0%
mmu-mir-21	2904	1665	5.8%	3.5%	2372	3427	4.7%	7.3%
mmu-mir-21*	34	9	0.1%	0.0%	13	31	0.0%	0.1%
mmu-mir-22	1566	826	3.1%	1.8%	57	112	0.1%	0.2%
mmu-mir-22*	142	83	0.3%	0.2%	12	25	0.0%	0.1%
mmu-mir-23a	2836	3270	5.7%	7.0%	417	460	0.8%	1.0%
mmu-mir-23a*	0	0	0.0%	0.0%	3	0	0.0%	0.0%
mmu-mir-23b	385	524	0.8%	1.1%	246	231	0.5%	0.5%
mmu-mir-24	529	1100	1.1%	2.3%	129	178	0.3%	0.4%
mmu-mir-24-2*	44	23	0.1%	0.0%	4	6	0.0%	0.0%
mmu-mir-25	478	558	1.0%	1.2%	301	304	0.6%	0.6%
mmu-mir-25*	0	2	0.0%	0.0%	0	0	0.0%	0.0%
mmu-mir-26a	815	1295	1.6%	2.8%	194	222	0.4%	0.5%
mmu-mir-26a-2*	1	1	0.0%	0.0%	0	0	0.0%	0.0%
mmu-mir-26b	133	314	0.3%	0.7%	217	612	0.4%	1.3%
mmu-mir-26b*	0	0	0.0%	0.0%	1	0	0.0%	0.0%
mmu-mir-27a	1843	1617	3.7%	3.4%	310	351	0.6%	0.7%
mmu-mir-27a*	5	3	0.0%	0.0%	0	1	0.0%	0.0%
mmu-mir-27b	622	670	1.2%	1.4%	603	588	1.2%	1.3%
mmu-mir-27b*	2	2	0.0%	0.0%	0	0	0.0%	0.0%
mmu-mir-28	110	111	0.2%	0.2%	2	4	0.0%	0.0%
mmu-mir-28*	90	46	0.2%	0.1%	1	1	0.0%	0.0%
mmu-mir-29a	918	910	1.8%	1.9%	296	434	0.6%	0.9%
mmu-mir-29a*	9	7	0.0%	0.0%	2	1	0.0%	0.0%
mmu-mir-29b	116	44	0.2%	0.1%	40	50	0.1%	0.1%
mmu-mir-29b*	0	3	0.0%	0.0%	4	2	0.0%	0.0%
mmu-mir-29b-2*	0	0	0.0%	0.0%	1	0	0.0%	0.0%
mmu-mir-29c	25	26	0.0%	0.1%	35	26	0.1%	0.1%
mmu-mir-30a	146	237	0.3%	0.5%	0	0	0.0%	0.0%
mmu-mir-30a*	39	102	0.1%	0.2%	2	2	0.0%	0.0%
mmu-mir-30b	234	239	0.5%	0.5%	193	224	0.4%	0.5%
mmu-mir-30b*	2	3	0.0%	0.0%	1	1	0.0%	0.0%
mmu-mir-30c	231	416	0.5%	0.9%	87	104	0.2%	0.2%
mmu-mir-30c-1*	0	1	0.0%	0.0%	0	2	0.0%	0.0%
mmu-mir-30c-2*	0	5	0.0%	0.0%	0	1	0.0%	0.0%
mmu-mir-30d	61	112	0.1%	0.2%	39	80	0.1%	0.2%
mmu-mir-30d*	7	2	0.0%	0.0%	0	1	0.0%	0.0%
mmu-mir-30e	231	210	0.5%	0.4%	159	177	0.3%	0.4%
mmu-mir-30e*	23	23	0.0%	0.0%	17	14	0.0%	0.0%
mmu-mir-31	1294	1005	2.6%	2.1%	0	0	0.0%	0.0%
mmu-mir-31*	720	354	1.4%	0.8%	0	0	0.0%	0.0%
mmu-mir-32	23	7	0.0%	0.0%	7	16	0.0%	0.0%

mmu-mir-32*	2	0	0.0%	0.0%	0	1	0.0%	0.0%
mmu-mir-33	8	4	0.0%	0.0%	0	4	0.0%	0.0%
mmu-mir-33*	6	4	0.0%	0.0%	7	13	0.0%	0.0%
mmu-mir-34a	162	137	0.3%	0.3%	306	461	0.6%	1.0%
mmu-mir-34a*	11	2	0.0%	0.0%	22	33	0.0%	0.1%
mmu-mir-34b-3p	42	70	0.1%	0.1%	15	23	0.0%	0.0%
mmu-mir-34b-5p	77	46	0.2%	0.1%	48	63	0.1%	0.1%
mmu-mir-34c	182	137	0.4%	0.3%	73	118	0.1%	0.3%
mmu-mir-34c*	41	33	0.1%	0.1%	18	15	0.0%	0.0%
mmu-mir-92a	264	395	0.5%	0.8%	104	211	0.2%	0.4%
mmu-mir-92a-1*	1	1	0.0%	0.0%	0	0	0.0%	0.0%
mmu-mir-92b	0	0	0.0%	0.0%	0	4	0.0%	0.0%
mmu-mir-93	423	626	0.8%	1.3%	218	291	0.4%	0.6%
mmu-mir-93*	5	7	0.0%	0.0%	2	5	0.0%	0.0%
mmu-mir-96	21	6	0.0%	0.0%	45	41	0.1%	0.1%
mmu-mir-96*	1	0	0.0%	0.0%	0	0	0.0%	0.0%
mmu-mir-98	14	19	0.0%	0.0%	5	10	0.0%	0.0%
mmu-mir-98*	9	1	0.0%	0.0%	0	0	0.0%	0.0%
mmu-mir-99a	5	13	0.0%	0.0%	0	0	0.0%	0.0%
mmu-mir-99b	124	472	0.2%	1.0%	0	0	0.0%	0.0%
mmu-mir-99b*	17	4	0.0%	0.0%	0	0	0.0%	0.0%
mmu-mir-100	46	19	0.1%	0.0%	7	9	0.0%	0.0%
mmu-mir-100*	1	1	0.0%	0.0%	0	0	0.0%	0.0%
mmu-mir-101a	79	34	0.2%	0.1%	18	8	0.0%	0.0%
mmu-mir-101b	275	213	0.5%	0.5%	214	245	0.4%	0.5%
mmu-mir-103	934	673	1.9%	1.4%	268	300	0.5%	0.6%
mmu-mir-103-1*	0	5	0.0%	0.0%	0	0	0.0%	0.0%
mmu-mir-103-2*	16	7	0.0%	0.0%	3	6	0.0%	0.0%
mmu-mir-106b	587	578	1.2%	1.2%	333	357	0.7%	0.8%
mmu-mir-106b*	20	39	0.0%	0.1%	10	15	0.0%	0.0%
mmu-mir-107	51	72	0.1%	0.2%	15	20	0.0%	0.0%
mmu-mir-107*	2	2	0.0%	0.0%	0	1	0.0%	0.0%
mmu-mir-122	0	0	0.0%	0.0%	1	2	0.0%	0.0%
mmu-mir-124	1	5	0.0%	0.0%	0	0	0.0%	0.0%
mmu-mir-125a-3p	10	8	0.0%	0.0%	0	0	0.0%	0.0%
mmu-mir-125a-5p	145	483	0.3%	1.0%	1	3	0.0%	0.0%
mmu-mir-125b*	1	2	0.0%	0.0%	0	0	0.0%	0.0%
mmu-mir-125b-3p	6	9	0.0%	0.0%	1	1	0.0%	0.0%
mmu-mir-125b-5p	613	955	1.2%	2.0%	17	21	0.0%	0.0%
mmu-mir-126-3p	1	0	0.0%	0.0%	4	11	0.0%	0.0%
mmu-mir-126-5p	1	0	0.0%	0.0%	6	2	0.0%	0.0%
mmu-mir-127	38	30	0.1%	0.1%	0	0	0.0%	0.0%
mmu-mir-127*	6	1	0.0%	0.0%	0	0	0.0%	0.0%
mmu-mir-128	16	11	0.0%	0.0%	10	13	0.0%	0.0%
mmu-mir-129-3p	0	1	0.0%	0.0%	0	0	0.0%	0.0%
mmu-mir-129-5p	2	6	0.0%	0.0%	0	0	0.0%	0.0%
mmu-mir-130a	492	218	1.0%	0.5%	0	0	0.0%	0.0%
mmu-mir-130b	25	24	0.0%	0.1%	72	126	0.1%	0.3%

mmu-mir-130b*	0	1	0.0%	0.0%	5	4	0.0%	0.0%
mmu-mir-132	2	6	0.0%	0.0%	9	30	0.0%	0.1%
mmu-mir-132*	0	0	0.0%	0.0%	1	1	0.0%	0.0%
mmu-mir-134	65	7	0.1%	0.0%	0	4	0.0%	0.0%
mmu-mir-134*	2	5	0.0%	0.0%	0	0	0.0%	0.0%
mmu-mir-135a	2	0	0.0%	0.0%	0	2	0.0%	0.0%
mmu-mir-135b	1	4	0.0%	0.0%	3	1	0.0%	0.0%
mmu-mir-136	16	0	0.0%	0.0%	0	0	0.0%	0.0%
mmu-mir-136*	6	0	0.0%	0.0%	0	0	0.0%	0.0%
mmu-mir-138	6	4	0.0%	0.0%	4	3	0.0%	0.0%
mmu-mir-139-5p	1	1	0.0%	0.0%	0	1	0.0%	0.0%
mmu-mir-140	33	52	0.1%	0.1%	14	13	0.0%	0.0%
mmu-mir-140*	245	352	0.5%	0.7%	54	103	0.1%	0.2%
mmu-mir-141	0	0	0.0%	0.0%	2	4	0.0%	0.0%
mmu-mir-142-3p	1	0	0.0%	0.0%	705	1171	1.4%	2.5%
mmu-mir-142-5p	0	0	0.0%	0.0%	243	446	0.5%	0.9%
mmu-mir-143	92	35	0.2%	0.1%	0	0	0.0%	0.0%
mmu-mir-143*	7	2	0.0%	0.0%	0	0	0.0%	0.0%
mmu-mir-145	364	247	0.7%	0.5%	0	1	0.0%	0.0%
mmu-mir-145*	3	0	0.0%	0.0%	0	0	0.0%	0.0%
mmu-mir-146a	6	2	0.0%	0.0%	263	301	0.5%	0.6%
mmu-mir-146b	164	22	0.3%	0.0%	175	331	0.3%	0.7%
mmu-mir-146b*	0	0	0.0%	0.0%	1	9	0.0%	0.0%
mmu-mir-148a	6	0	0.0%	0.0%	112	108	0.2%	0.2%
mmu-mir-148b	14	7	0.0%	0.0%	3	3	0.0%	0.0%
mmu-mir-149	12	20	0.0%	0.0%	1	1	0.0%	0.0%
mmu-mir-150	0	1	0.0%	0.0%	1	0	0.0%	0.0%
mmu-mir-151-3p	44	40	0.1%	0.1%	16	23	0.0%	0.0%
mmu-mir-151-5p	165	170	0.3%	0.4%	66	118	0.1%	0.3%
mmu-mir-152	381	207	0.8%	0.4%	16	15	0.0%	0.0%
mmu-mir-152*	1	0	0.0%	0.0%	0	0	0.0%	0.0%
mmu-mir-153	0	0	0.0%	0.0%	2	9	0.0%	0.0%
mmu-mir-154	19	3	0.0%	0.0%	0	0	0.0%	0.0%
mmu-mir-154*	2	1	0.0%	0.0%	0	0	0.0%	0.0%
mmu-mir-155	1059	242	2.1%	0.5%	8672	10835	17.3%	23.0%
mmu-mir-155*	0	0	0.0%	0.0%	3	6	0.0%	0.0%
mmu-mir-181a	13	12	0.0%	0.0%	13	17	0.0%	0.0%
mmu-mir-181b	27	33	0.1%	0.1%	3	9	0.0%	0.0%
mmu-mir-181b-1*	2	0	0.0%	0.0%	0	0	0.0%	0.0%
mmu-mir-181c	18	6	0.0%	0.0%	0	0	0.0%	0.0%
mmu-mir-181c*	5	1	0.0%	0.0%	0	0	0.0%	0.0%
mmu-mir-181d	15	14	0.0%	0.0%	0	0	0.0%	0.0%
mmu-mir-182	37	82	0.1%	0.2%	164	273	0.3%	0.6%
mmu-mir-182*	0	2	0.0%	0.0%	0	0	0.0%	0.0%
mmu-mir-183	42	77	0.1%	0.2%	53	111	0.1%	0.2%
mmu-mir-183*	2	6	0.0%	0.0%	1	2	0.0%	0.0%
mmu-mir-185	181	83	0.4%	0.2%	61	78	0.1%	0.2%
mmu-mir-186	48	19	0.1%	0.0%	11	18	0.0%	0.0%

mmu-mir-186*	1	1	0.0%	0.0%	0	0	0.0%	0.0%
mmu-mir-187	6	11	0.0%	0.0%	4	18	0.0%	0.0%
mmu-mir-188-3p	1	4	0.0%	0.0%	0	0	0.0%	0.0%
mmu-mir-188-5p	9	0	0.0%	0.0%	0	0	0.0%	0.0%
mmu-mir-190	33	51	0.1%	0.1%	9	12	0.0%	0.0%
mmu-mir-190*	1	0	0.0%	0.0%	0	0	0.0%	0.0%
mmu-mir-190b	4	1	0.0%	0.0%	4	6	0.0%	0.0%
mmu-mir-191	182	237	0.4%	0.5%	1245	1522	2.5%	3.2%
mmu-mir-191*	0	0	0.0%	0.0%	3	1	0.0%	0.0%
mmu-mir-192	0	1	0.0%	0.0%	1	1	0.0%	0.0%
mmu-mir-193	43	9	0.1%	0.0%	0	2	0.0%	0.0%
mmu-mir-193*	0	3	0.0%	0.0%	1	0	0.0%	0.0%
mmu-mir-193b	12	13	0.0%	0.0%	0	0	0.0%	0.0%
mmu-mir-194	7	4	0.0%	0.0%	10	23	0.0%	0.0%
mmu-mir-195	270	201	0.5%	0.4%	38	28	0.1%	0.1%
mmu-mir-195	0	1	0.0%	0.0%	0	0	0.0%	0.0%
mmu-mir-196a	4	89	0.0%	0.2%	54	77	0.1%	0.2%
mmu-mir-196a*	0	0	0.0%	0.0%	1	0	0.0%	0.0%
mmu-mir-196a-1*	0	2	0.0%	0.0%	0	0	0.0%	0.0%
mmu-mir-196b	1	8	0.0%	0.0%	2	8	0.0%	0.0%
mmu-mir-196b*	1	0	0.0%	0.0%	0	0	0.0%	0.0%
mmu-mir-197	0	0	0.0%	0.0%	1	0	0.0%	0.0%
mmu-mir-199a-3p	4027	3621	8.0%	7.7%	2	0	0.0%	0.0%
mmu-mir-199a-5p	1555	1082	3.1%	2.3%	0	0	0.0%	0.0%
mmu-mir-199b*	326	141	0.7%	0.3%	0	0	0.0%	0.0%
mmu-mir-200b	0	1	0.0%	0.0%	3	1	0.0%	0.0%
mmu-mir-200c	0	2	0.0%	0.0%	25	27	0.0%	0.1%
mmu-mir-201	0	0	0.0%	0.0%	0	1	0.0%	0.0%
mmu-mir-203	0	0	0.0%	0.0%	1	0	0.0%	0.0%
mmu-mir-206	19	50	0.0%	0.1%	0	0	0.0%	0.0%
mmu-mir-207	0	0	0.0%	0.0%	0	1	0.0%	0.0%
mmu-mir-210	250	8	0.5%	0.0%	0	2	0.0%	0.0%
mmu-mir-210*	7	1	0.0%	0.0%	0	0	0.0%	0.0%
mmu-mir-211	1	0	0.0%	0.0%	11	12	0.0%	0.0%
mmu-mir-212	1	0	0.0%	0.0%	4	8	0.0%	0.0%
mmu-mir-214	366	266	0.7%	0.6%	0	0	0.0%	0.0%
mmu-mir-214*	12	10	0.0%	0.0%	0	0	0.0%	0.0%
mmu-mir-216a	0	2	0.0%	0.0%	0	0	0.0%	0.0%
mmu-mir-216b	1	0	0.0%	0.0%	0	0	0.0%	0.0%
mmu-mir-217*	0	1	0.0%	0.0%	0	0	0.0%	0.0%
mmu-mir-218	2476	1649	4.9%	3.5%	102	94	0.2%	0.2%
mmu-mir-218-1*	4	2	0.0%	0.0%	0	0	0.0%	0.0%
mmu-mir-219	8	10	0.0%	0.0%	8	11	0.0%	0.0%
mmu-mir-221	783	434	1.6%	0.9%	0	0	0.0%	0.0%
mmu-mir-221*	8	6	0.0%	0.0%	0	0	0.0%	0.0%
mmu-mir-222	141	73	0.3%	0.2%	0	0	0.0%	0.0%
mmu-mir-222*	1	1	0.0%	0.0%	0	0	0.0%	0.0%
mmu-mir-224	3	0	0.0%	0.0%	0	0	0.0%	0.0%

mmu-mir-291a-3p	1	0	0.0%	0.0%	0	0	0.0%	0.0%
mmu-mir-292-3p	5	0	0.0%	0.0%	3	1	0.0%	0.0%
mmu-mir-292-5p	0	0	0.0%	0.0%	1	0	0.0%	0.0%
mmu-mir-296-3p	20	2	0.0%	0.0%	3	18	0.0%	0.0%
mmu-mir-296-5p	1	1	0.0%	0.0%	2	4	0.0%	0.0%
mmu-mir-297a	90	16	0.2%	0.0%	0	2	0.0%	0.0%
mmu-mir-297b-3p	3	1	0.0%	0.0%	0	0	0.0%	0.0%
mmu-mir-297b-5p	7	0	0.0%	0.0%	0	0	0.0%	0.0%
mmu-mir-297c	33	7	0.1%	0.0%	0	1	0.0%	0.0%
mmu-mir-298	7	0	0.0%	0.0%	3	6	0.0%	0.0%
mmu-mir-299	24	1	0.0%	0.0%	0	0	0.0%	0.0%
mmu-mir-299*	3	0	0.0%	0.0%	0	0	0.0%	0.0%
mmu-mir-300	77	9	0.2%	0.0%	1	1	0.0%	0.0%
mmu-mir-300*	5	1	0.0%	0.0%	0	0	0.0%	0.0%
mmu-mir-301a	215	180	0.4%	0.4%	44	61	0.1%	0.1%
mmu-mir-301a*	1	0	0.0%	0.0%	0	0	0.0%	0.0%
mmu-mir-301b	11	6	0.0%	0.0%	11	11	0.0%	0.0%
mmu-mir-302a	1	0	0.0%	0.0%	0	0	0.0%	0.0%
mmu-mir-320	178	104	0.4%	0.2%	19	59	0.0%	0.1%
mmu-mir-322	485	376	1.0%	0.8%	6	15	0.0%	0.0%
mmu-mir-322*	23	26	0.0%	0.1%	0	1	0.0%	0.0%
mmu-mir-323-3p	1	2	0.0%	0.0%	0	0	0.0%	0.0%
mmu-mir-323-5p	1	0	0.0%	0.0%	0	0	0.0%	0.0%
mmu-mir-324-3p	31	36	0.1%	0.1%	6	5	0.0%	0.0%
mmu-mir-324-5p	20	28	0.0%	0.1%	4	3	0.0%	0.0%
mmu-mir-325	0	0	0.0%	0.0%	7	2	0.0%	0.0%
mmu-mir-325*	0	0	0.0%	0.0%	8	2	0.0%	0.0%
mmu-mir-326	2	0	0.0%	0.0%	0	2	0.0%	0.0%
mmu-mir-327	0	0	0.0%	0.0%	0	0	0.0%	0.0%
mmu-mir-328	2	6	0.0%	0.0%	12	5	0.0%	0.0%
mmu-mir-329	20	7	0.0%	0.0%	0	0	0.0%	0.0%
mmu-mir-329*	0	1	0.0%	0.0%	0	0	0.0%	0.0%
mmu-mir-330	1	0	0.0%	0.0%	0	0	0.0%	0.0%
mmu-mir-330*	0	0	0.0%	0.0%	1	1	0.0%	0.0%
mmu-mir-331-3p	0	1	0.0%	0.0%	0	0	0.0%	0.0%
mmu-mir-331-5p	1	5	0.0%	0.0%	0	0	0.0%	0.0%
mmu-mir-337-3p	21	8	0.0%	0.0%	0	0	0.0%	0.0%
mmu-mir-337-5p	11	2	0.0%	0.0%	0	0	0.0%	0.0%
mmu-mir-339-3p	1	0	0.0%	0.0%	0	0	0.0%	0.0%
mmu-mir-339-5p	6	1	0.0%	0.0%	0	3	0.0%	0.0%
mmu-mir-340-3p	3	2	0.0%	0.0%	1	0	0.0%	0.0%
mmu-mir-340-5p	8	7	0.0%	0.0%	16	13	0.0%	0.0%
mmu-mir-341	1	1	0.0%	0.0%	0	0	0.0%	0.0%
mmu-mir-342-3p	36	25	0.1%	0.1%	22	44	0.0%	0.1%
mmu-mir-342-5p	0	2	0.0%	0.0%	0	0	0.0%	0.0%
mmu-mir-344	2	0	0.0%	0.0%	0	0	0.0%	0.0%
mmu-mir-345-3p	7	1	0.0%	0.0%	0	0	0.0%	0.0%
mmu-mir-345-5p	18	13	0.0%	0.0%	1	8	0.0%	0.0%

mmu-mir-346	0	0	0.0%	0.0%	0	1	0.0%	0.0%
mmu-mir-350	140	71	0.3%	0.2%	60	68	0.1%	0.1%
mmu-mir-350*	2	0	0.0%	0.0%	0	0	0.0%	0.0%
mmu-mir-351	159	211	0.3%	0.4%	1	0	0.0%	0.0%
mmu-mir-351*	2	6	0.0%	0.0%	0	0	0.0%	0.0%
mmu-mir-361	120	148	0.2%	0.3%	112	118	0.2%	0.3%
mmu-mir-361*	1	2	0.0%	0.0%	2	2	0.0%	0.0%
mmu-mir-362-3p	36	24	0.1%	0.1%	24	24	0.0%	0.1%
mmu-mir-362-5p	30	14	0.1%	0.0%	8	16	0.0%	0.0%
mmu-mir-365	28	80	0.1%	0.2%	0	1	0.0%	0.0%
mmu-mir-369-3p	18	2	0.0%	0.0%	0	0	0.0%	0.0%
mmu-mir-370	1	0	0.0%	0.0%	2	2	0.0%	0.0%
mmu-mir-370*	0	2	0.0%	0.0%	0	0	0.0%	0.0%
mmu-mir-374	286	242	0.6%	0.5%	213	180	0.4%	0.4%
mmu-mir-374*	1	1	0.0%	0.0%	0	0	0.0%	0.0%
mmu-mir-376a	11	1	0.0%	0.0%	0	0	0.0%	0.0%
mmu-mir-376a*	1	0	0.0%	0.0%	0	0	0.0%	0.0%
mmu-mir-376b	79	20	0.2%	0.0%	0	0	0.0%	0.0%
mmu-mir-376b*	0	3	0.0%	0.0%	0	0	0.0%	0.0%
mmu-mir-376c	9	2	0.0%	0.0%	0	0	0.0%	0.0%
mmu-mir-377	10	2	0.0%	0.0%	0	0	0.0%	0.0%
mmu-mir-378	403	140	0.8%	0.3%	109	193	0.2%	0.4%
mmu-mir-378*	28	21	0.1%	0.0%	7	6	0.0%	0.0%
mmu-mir-379	22	14	0.0%	0.0%	0	1	0.0%	0.0%
mmu-mir-379*	2	1	0.0%	0.0%	0	0	0.0%	0.0%
mmu-mir-380-3p	12	3	0.0%	0.0%	0	0	0.0%	0.0%
mmu-mir-380-5p	1	0	0.0%	0.0%	0	0	0.0%	0.0%
mmu-mir-381	35	1	0.1%	0.0%	0	0	0.0%	0.0%
mmu-mir-382	3	5	0.0%	0.0%	1	0	0.0%	0.0%
mmu-mir-382*	3	1	0.0%	0.0%	0	0	0.0%	0.0%
mmu-mir-384-5p	0	0	0.0%	0.0%	7	4	0.0%	0.0%
mmu-mir-409-3p	12	1	0.0%	0.0%	0	0	0.0%	0.0%
mmu-mir-410	80	43	0.2%	0.1%	0	0	0.0%	0.0%
mmu-mir-410*	1	0	0.0%	0.0%	0	0	0.0%	0.0%
mmu-mir-411	19	9	0.0%	0.0%	0	0	0.0%	0.0%
mmu-mir-411*	30	14	0.1%	0.0%	0	0	0.0%	0.0%
mmu-mir-421	50	52	0.1%	0.1%	7	9	0.0%	0.0%
mmu-mir-423-3p	12	12	0.0%	0.0%	9	11	0.0%	0.0%
mmu-mir-423-5p	7	4	0.0%	0.0%	4	5	0.0%	0.0%
mmu-mir-425	46	34	0.1%	0.1%	134	147	0.3%	0.3%
mmu-mir-425*	1	0	0.0%	0.0%	4	0	0.0%	0.0%
mmu-mir-431	9	14	0.0%	0.0%	0	0	0.0%	0.0%
mmu-mir-431*	0	1	0.0%	0.0%	0	0	0.0%	0.0%
mmu-mir-433	17	7	0.0%	0.0%	0	0	0.0%	0.0%
mmu-mir-433*	0	0	0.0%	0.0%	2	2	0.0%	0.0%
mmu-mir-434-3p	26	11	0.1%	0.0%	0	0	0.0%	0.0%
mmu-mir-434-5p	6	2	0.0%	0.0%	0	0	0.0%	0.0%
mmu-mir-449a	0	0	0.0%	0.0%	1	1	0.0%	0.0%

mmu-mir-450a-3p	4	0	0.0%	0.0%	0	0	0.0%	0.0%
mmu-mir-450a-5p	60	29	0.1%	0.1%	0	3	0.0%	0.0%
mmu-mir-450b-3p	7	1	0.0%	0.0%	0	0	0.0%	0.0%
mmu-mir-450b-5p	5	2	0.0%	0.0%	0	0	0.0%	0.0%
mmu-mir-452	1	0	0.0%	0.0%	0	0	0.0%	0.0%
mmu-mir-455	6	13	0.0%	0.0%	0	1	0.0%	0.0%
mmu-mir-455*	8	0	0.0%	0.0%	0	0	0.0%	0.0%
mmu-mir-465b-5p	0	1	0.0%	0.0%	0	0	0.0%	0.0%
mmu-mir-466a-3p	12	2	0.0%	0.0%	0	0	0.0%	0.0%
mmu-mir-466a-5p	44	3	0.1%	0.0%	0	0	0.0%	0.0%
mmu-mir-466b-5p	47	11	0.1%	0.0%	0	0	0.0%	0.0%
mmu-mir-466c-5p	83	19	0.2%	0.0%	2	0	0.0%	0.0%
mmu-mir-466d-3p	3	1	0.0%	0.0%	0	0	0.0%	0.0%
mmu-mir-466d-5p	1	0	0.0%	0.0%	2	4	0.0%	0.0%
mmu-mir-466e-5p	1	0	0.0%	0.0%	0	0	0.0%	0.0%
mmu-mir-466f	12	3	0.0%	0.0%	0	0	0.0%	0.0%
mmu-mir-466f-3p	2	0	0.0%	0.0%	0	0	0.0%	0.0%
mmu-mir-466f-5p	8	1	0.0%	0.0%	0	2	0.0%	0.0%
mmu-mir-466g	14	4	0.0%	0.0%	0	0	0.0%	0.0%
mmu-mir-466h	9	4	0.0%	0.0%	0	0	0.0%	0.0%
mmu-mir-466h-3p	1	2	0.0%	0.0%	0	0	0.0%	0.0%
mmu-mir-466i	2	0	0.0%	0.0%	0	0	0.0%	0.0%
mmu-mir-466i-5p	0	0	0.0%	0.0%	2	3	0.0%	0.0%
mmu-mir-466j	2	0	0.0%	0.0%	0	0	0.0%	0.0%
mmu-mir-466k	69	9	0.1%	0.0%	0	1	0.0%	0.0%
mmu-mir-466l-5p	1	0	0.0%	0.0%	0	0	0.0%	0.0%
mmu-mir-467a	112	62	0.2%	0.1%	0	0	0.0%	0.0%
mmu-mir-467a*	7	1	0.0%	0.0%	0	0	0.0%	0.0%
mmu-mir-467b	2	2	0.0%	0.0%	0	0	0.0%	0.0%
mmu-mir-467b*	1	0	0.0%	0.0%	0	0	0.0%	0.0%
mmu-mir-467c	44	35	0.1%	0.1%	0	0	0.0%	0.0%
mmu-mir-467d	7	2	0.0%	0.0%	0	0	0.0%	0.0%
mmu-mir-467e	58	27	0.1%	0.1%	0	0	0.0%	0.0%
mmu-mir-467f	1	0	0.0%	0.0%	0	0	0.0%	0.0%
mmu-mir-468	0	0	0.0%	0.0%	0	2	0.0%	0.0%
mmu-mir-470	1	0	0.0%	0.0%	1	0	0.0%	0.0%
mmu-mir-483	8	2	0.0%	0.0%	0	0	0.0%	0.0%
mmu-mir-483*	1	1	0.0%	0.0%	0	0	0.0%	0.0%
mmu-mir-484	57	56	0.1%	0.1%	25	33	0.0%	0.1%
mmu-mir-485	2	1	0.0%	0.0%	0	0	0.0%	0.0%
mmu-mir-485*	2	1	0.0%	0.0%	0	0	0.0%	0.0%
mmu-mir-486	1	1	0.0%	0.0%	1	0	0.0%	0.0%
mmu-mir-487b	8	3	0.0%	0.0%	0	0	0.0%	0.0%
mmu-mir-493*	1	0	0.0%	0.0%	0	0	0.0%	0.0%
mmu-mir-494	20	3	0.0%	0.0%	0	0	0.0%	0.0%
mmu-mir-495	16	9	0.0%	0.0%	0	0	0.0%	0.0%
mmu-mir-496	9	3	0.0%	0.0%	0	0	0.0%	0.0%
mmu-mir-497	231	113	0.5%	0.2%	9	9	0.0%	0.0%

mmu-mir-497*	1	0	0.0%	0.0%	0	0	0.0%	0.0%
mmu-mir-499	2	0	0.0%	0.0%	0	3	0.0%	0.0%
mmu-mir-500	16	13	0.0%	0.0%	15	26	0.0%	0.1%
mmu-mir-500*	0	0	0.0%	0.0%	0	1	0.0%	0.0%
mmu-mir-501-3p	6	13	0.0%	0.0%	2	4	0.0%	0.0%
mmu-mir-501-5p	8	6	0.0%	0.0%	0	3	0.0%	0.0%
mmu-mir-503	37	25	0.1%	0.1%	1	6	0.0%	0.0%
mmu-mir-503*	0	2	0.0%	0.0%	0	0	0.0%	0.0%
mmu-mir-511	0	0	0.0%	0.0%	0	1	0.0%	0.0%
mmu-mir-532-3p	5	10	0.0%	0.0%	1	0	0.0%	0.0%
mmu-mir-532-5p	77	29	0.2%	0.1%	29	16	0.1%	0.0%
mmu-mir-540-3p	2	0	0.0%	0.0%	0	0	0.0%	0.0%
mmu-mir-540-5p	2	0	0.0%	0.0%	0	0	0.0%	0.0%
mmu-mir-541	117	10	0.2%	0.0%	0	9	0.0%	0.0%
mmu-mir-542-3p	1	0	0.0%	0.0%	0	0	0.0%	0.0%
mmu-mir-543	10	9	0.0%	0.0%	0	0	0.0%	0.0%
mmu-mir-543*	1	0	0.0%	0.0%	0	0	0.0%	0.0%
mmu-mir-547	1	0	0.0%	0.0%	0	0	0.0%	0.0%
mmu-mir-574-3p	4	17	0.0%	0.0%	0	3	0.0%	0.0%
mmu-mir-574-5p	48	37	0.1%	0.1%	4	10	0.0%	0.0%
mmu-mir-582-3p	0	1	0.0%	0.0%	0	0	0.0%	0.0%
mmu-mir-582-5p	2	5	0.0%	0.0%	0	0	0.0%	0.0%
mmu-mir-598	4	11	0.0%	0.0%	0	1	0.0%	0.0%
mmu-mir-615-3p	6	9	0.0%	0.0%	3	4	0.0%	0.0%
mmu-mir-615-5p	4	0	0.0%	0.0%	2	3	0.0%	0.0%
mmu-mir-652	137	271	0.3%	0.6%	32	67	0.1%	0.1%
mmu-mir-652*	3	0	0.0%	0.0%	2	0	0.0%	0.0%
mmu-mir-654-3p	1	0	0.0%	0.0%	5	9	0.0%	0.0%
mmu-mir-664	0	13	0.0%	0.0%	9	13	0.0%	0.0%
mmu-mir-664*	1	4	0.0%	0.0%	0	0	0.0%	0.0%
mmu-mir-665	13	4	0.0%	0.0%	0	0	0.0%	0.0%
mmu-mir-666-3p	3	0	0.0%	0.0%	1	3	0.0%	0.0%
mmu-mir-666-5p	5	0	0.0%	0.0%	0	0	0.0%	0.0%
mmu-mir-668	0	0	0.0%	0.0%	1	0	0.0%	0.0%
mmu-mir-669a	376	113	0.8%	0.2%	0	0	0.0%	0.0%
mmu-mir-669a-1*	22	6	0.0%	0.0%	0	0	0.0%	0.0%
mmu-mir-669b	204	44	0.4%	0.1%	0	0	0.0%	0.0%
mmu-mir-669c	29	24	0.1%	0.1%	2	0	0.0%	0.0%
mmu-mir-669d	99	12	0.2%	0.0%	0	0	0.0%	0.0%
mmu-mir-669d*	1	0	0.0%	0.0%	0	0	0.0%	0.0%
mmu-mir-669e	28	5	0.1%	0.0%	0	2	0.0%	0.0%
mmu-mir-669f	1	2	0.0%	0.0%	0	0	0.0%	0.0%
mmu-mir-669f-5p	7	1	0.0%	0.0%	0	0	0.0%	0.0%
mmu-mir-669g	0	0	0.0%	0.0%	1	0	0.0%	0.0%
mmu-mir-669h-5p	1	0	0.0%	0.0%	0	0	0.0%	0.0%
mmu-mir-669i	50	17	0.1%	0.0%	0	0	0.0%	0.0%
mmu-mir-669o	35	8	0.1%	0.0%	0	0	0.0%	0.0%
mmu-mir-670	0	7	0.0%	0.0%	0	0	0.0%	0.0%

mmu-mir-670*	0	3	0.0%	0.0%	0	0	0.0%	0.0%
mmu-mir-671-3p	0	1	0.0%	0.0%	0	1	0.0%	0.0%
mmu-mir-671-5p	54	12	0.1%	0.0%	5	7	0.0%	0.0%
mmu-mir-673-3p	0	0	0.0%	0.0%	0	1	0.0%	0.0%
mmu-mir-673-5p	5	0	0.0%	0.0%	0	0	0.0%	0.0%
mmu-mir-674	100	26	0.2%	0.1%	13	15	0.0%	0.0%
mmu-mir-674*	30	19	0.1%	0.0%	2	0	0.0%	0.0%
mmu-mir-676	1	0	0.0%	0.0%	0	0	0.0%	0.0%
mmu-mir-677	1	0	0.0%	0.0%	5	14	0.0%	0.0%
mmu-mir-677*	0	0	0.0%	0.0%	0	2	0.0%	0.0%
mmu-mir-679	2	0	0.0%	0.0%	0	0	0.0%	0.0%
mmu-mir-689	1	0	0.0%	0.0%	2	1	0.0%	0.0%
mmu-mir-690	2	0	0.0%	0.0%	1	3	0.0%	0.0%
mmu-mir-696	0	0	0.0%	0.0%	0	3	0.0%	0.0%
mmu-mir-700	2	2	0.0%	0.0%	0	0	0.0%	0.0%
mmu-mir-700*	2	1	0.0%	0.0%	0	0	0.0%	0.0%
mmu-mir-703	0	0	0.0%	0.0%	0	2	0.0%	0.0%
mmu-mir-705	0	0	0.0%	0.0%	1	0	0.0%	0.0%
mmu-mir-707	1	0	0.0%	0.0%	0	0	0.0%	0.0%
mmu-mir-708	10	11	0.0%	0.0%	0	0	0.0%	0.0%
mmu-mir-708*	0	0	0.0%	0.0%	1	0	0.0%	0.0%
mmu-mir-709	0	0	0.0%	0.0%	0	1	0.0%	0.0%
mmu-mir-710	3	0	0.0%	0.0%	0	0	0.0%	0.0%
mmu-mir-711	0	0	0.0%	0.0%	1	0	0.0%	0.0%
mmu-mir-712	0	0	0.0%	0.0%	0	0	0.0%	0.0%
mmu-mir-712*	1	0	0.0%	0.0%	1	2	0.0%	0.0%
mmu-mir-718	0	1	0.0%	0.0%	2	0	0.0%	0.0%
mmu-mir-720	9	10	0.0%	0.0%	13	15	0.0%	0.0%
mmu-mir-743a	0	0	0.0%	0.0%	0	1	0.0%	0.0%
mmu-mir-744	42	48	0.1%	0.1%	2	10	0.0%	0.0%
mmu-mir-744*	2	0	0.0%	0.0%	0	0	0.0%	0.0%
mmu-mir-758	2	0	0.0%	0.0%	0	0	0.0%	0.0%
mmu-mir-760	0	2	0.0%	0.0%	1	0	0.0%	0.0%
mmu-mir-762	3	0	0.0%	0.0%	0	3	0.0%	0.0%
mmu-mir-763	2	0	0.0%	0.0%	0	0	0.0%	0.0%
mmu-mir-764-5p	1	0	0.0%	0.0%	0	0	0.0%	0.0%
mmu-mir-770-3p	0	0	0.0%	0.0%	0	2	0.0%	0.0%
mmu-mir-770-5p	1	0	0.0%	0.0%	0	0	0.0%	0.0%
mmu-mir-804	1	0	0.0%	0.0%	0	1	0.0%	0.0%
mmu-mir-805	36	62	0.1%	0.1%	70	63	0.1%	0.1%
mmu-mir-805*	0	1	0.0%	0.0%	0	0	0.0%	0.0%
mmu-mir-872	18	24	0.0%	0.1%	4	4	0.0%	0.0%
mmu-mir-872*	21	23	0.0%	0.0%	2	5	0.0%	0.0%
mmu-mir-874	1	0	0.0%	0.0%	0	0	0.0%	0.0%
mmu-mir-877	2	2	0.0%	0.0%	0	0	0.0%	0.0%
mmu-mir-879*	0	0	0.0%	0.0%	1	0	0.0%	0.0%
mmu-mir-881	0	0	0.0%	0.0%	0	2	0.0%	0.0%
mmu-mir-883b-5p	0	0	0.0%	0.0%	0	1	0.0%	0.0%

mmu-mir-1187	1	1	0.0%	0.0%	0	0	0.0%	0.0%
mmu-mir-1188	4	1	0.0%	0.0%	3	3	0.0%	0.0%
mmu-mir-1190	1	0	0.0%	0.0%	0	0	0.0%	0.0%
mmu-mir-1191	3	0	0.0%	0.0%	0	1	0.0%	0.0%
mmu-mir-1195	0	0	0.0%	0.0%	0	1	0.0%	0.0%
mmu-mir-1196	0	0	0.0%	0.0%	2	0	0.0%	0.0%
mmu-mir-1198	19	17	0.0%	0.0%	11	15	0.0%	0.0%
mmu-mir-1224	0	0	0.0%	0.0%	0	1	0.0%	0.0%
mmu-mir-1274a	171	108	0.3%	0.2%	59	56	0.1%	0.1%
mmu-mir-1306	1	1	0.0%	0.0%	1	2	0.0%	0.0%
mmu-mir-1839-3p	3	0	0.0%	0.0%	0	0	0.0%	0.0%
mmu-mir-1839-5p	23	15	0.0%	0.0%	7	14	0.0%	0.0%
mmu-mir-1893	0	0	0.0%	0.0%	0	1	0.0%	0.0%
mmu-mir-1895	0	0	0.0%	0.0%	0	1	0.0%	0.0%
mmu-mir-1896	0	0	0.0%	0.0%	0	1	0.0%	0.0%
mmu-mir-1897-3p	0	0	0.0%	0.0%	0	4	0.0%	0.0%
mmu-mir-1904	0	0	0.0%	0.0%	0	1	0.0%	0.0%
mmu-mir-1906	0	0	0.0%	0.0%	1	1	0.0%	0.0%
mmu-mir-1927	0	0	0.0%	0.0%	0	2	0.0%	0.0%
mmu-mir-1930	0	0	0.0%	0.0%	1	3	0.0%	0.0%
mmu-mir-1933-5p	0	0	0.0%	0.0%	0	1	0.0%	0.0%
mmu-mir-1935	0	1	0.0%	0.0%	0	0	0.0%	0.0%
mmu-mir-1937a	6	21	0.0%	0.0%	5	14	0.0%	0.0%
mmu-mir-1937b	0	1	0.0%	0.0%	0	0	0.0%	0.0%
mmu-mir-1937c	0	0	0.0%	0.0%	0	1	0.0%	0.0%
mmu-mir-1939	46	255	0.1%	0.5%	60	65	0.1%	0.1%
mmu-mir-1940	0	0	0.0%	0.0%	2	3	0.0%	0.0%
mmu-mir-1941-3p	3	1	0.0%	0.0%	0	0	0.0%	0.0%
mmu-mir-1941-5p	0	1	0.0%	0.0%	0	0	0.0%	0.0%
mmu-mir-1944	83	16	0.2%	0.0%	16	18	0.0%	0.0%
mmu-mir-1944*	1	1	0.0%	0.0%	3	9	0.0%	0.0%
mmu-mir-1946a	0	0	0.0%	0.0%	1	0	0.0%	0.0%
mmu-mir-1947	0	0	0.0%	0.0%	1	2	0.0%	0.0%
mmu-mir-1948	0	0	0.0%	0.0%	1	0	0.0%	0.0%
mmu-mir-1948*	1	0	0.0%	0.0%	0	1	0.0%	0.0%
mmu-mir-1949	0	1	0.0%	0.0%	1	2	0.0%	0.0%
mmu-mir-1955	1	1	0.0%	0.0%	0	0	0.0%	0.0%
mmu-mir-1957	1	0	0.0%	0.0%	0	0	0.0%	0.0%
mmu-mir-1959	0	1	0.0%	0.0%	2	5	0.0%	0.0%
mmu-mir-1961	0	0	0.0%	0.0%	0	3	0.0%	0.0%
mmu-mir-1965	0	0	0.0%	0.0%	1	0	0.0%	0.0%
mmu-mir-1967	1	0	0.0%	0.0%	0	0	0.0%	0.0%
mmu-mir-1968	0	0	0.0%	0.0%	1	1	0.0%	0.0%
mmu-mir-1981	4	6	0.0%	0.0%	1	3	0.0%	0.0%
mmu-mir-1981*	1	2	0.0%	0.0%	0	0	0.0%	0.0%
mmu-mir-1982*	0	1	0.0%	0.0%	0	1	0.0%	0.0%
mmu-mir-1983	0	4	0.0%	0.0%	0	1	0.0%	0.0%
mmu-mir-2132	1	0	0.0%	0.0%	0	7	0.0%	0.0%

mmu-mir-2133	0	0	0.0%	0.0%	0	1	0.0%	0.0%
mmu-mir-2133-1*	6	1	0.0%	0.0%	7	12	0.0%	0.0%
mmu-mir-2133-2*	0	0	0.0%	0.0%	1	2	0.0%	0.0%
mmu-mir-2134	0	0	0.0%	0.0%	3	11	0.0%	0.0%
mmu-mir-2134-1*	0	0	0.0%	0.0%	1	1	0.0%	0.0%
mmu-mir-2134-4*	0	0	0.0%	0.0%	0	2	0.0%	0.0%
mmu-mir-2135	5	2	0.0%	0.0%	7	9	0.0%	0.0%
mmu-mir-2135-1*	2	0	0.0%	0.0%	2	10	0.0%	0.0%
mmu-mir-2137	0	0	0.0%	0.0%	1	4	0.0%	0.0%
mmu-mir-2138	0	0	0.0%	0.0%	3	3	0.0%	0.0%
mmu-mir-2138*	0	0	0.0%	0.0%	0	3	0.0%	0.0%
mmu-mir-2140	0	0	0.0%	0.0%	1	3	0.0%	0.0%
mmu-mir-2141	0	0	0.0%	0.0%	5	4	0.0%	0.0%
mmu-mir-2142	23	207	0.0%	0.4%	90	184	0.2%	0.4%
mmu-mir-2143	3	2	0.0%	0.0%	2	8	0.0%	0.0%
mmu-mir-2143-3*	0	0	0.0%	0.0%	0	1	0.0%	0.0%
mmu-mir-2144	0	0	0.0%	0.0%	4	0	0.0%	0.0%
mmu-mir-2144*	0	0	0.0%	0.0%	3	14	0.0%	0.0%
mmu-mir-2145	0	1	0.0%	0.0%	10	45	0.0%	0.1%
mmu-mir-2146	1	0	0.0%	0.0%	2	6	0.0%	0.0%
mmu-mir-2183	0	0	0.0%	0.0%	9	18	0.0%	0.0%

The libraries were analysed in the reference of miRBase v14.0. The murine miRNAs that are not present here have no reads in all four libraries.

Appendix Table III

Read numbers of individual murine miRNA in Solexa sequencing libraries of wt, *Dicer1*^{-/-} and *Dgcr8*^{-/-} mESCs.

	wt		<i>Dicer1</i> ^{-/-}		<i>Dgcr8</i> ^{-/-}	
	mismatch0	mismatch1	mismatch0	mismatch1	mismatch0	mismatch1
total miRNA	2610803	340757	18198	12351	116462	30508
mmu-let-7a	967	110	102	5	30	2
mmu-let-7a*	9	10	0	0	0	0
mmu-let-7b	73	39	11	0	11	1
mmu-let-7b*	0	1	0	0	0	0
mmu-let-7c	1802	167	24	1	2	0
mmu-let-7d	383	46	18	2	6	2
mmu-let-7d*	1	0	0	0	1	0
mmu-let-7e	635	70	9	2	6	2
mmu-let-7f	725	52	107	6	42	0
mmu-let-7f*	0	1	0	1	0	0
mmu-let-7g	455	47	7	1	10	0
mmu-let-7g*	2	0	0	0	0	0
mmu-let-7i	153	17	20	1	13	1
mmu-let-7i*	5	1	0	0	1	0
mmu-mir-1	84	10	2	0	7	0
mmu-mir-1-2-as	1	1	0	1	0	0
mmu-mir-7a	25777	2330	108	3	0	0
mmu-mir-7a*	155	21	3	1	0	0
mmu-mir-7b	202	31	1	0	0	0
mmu-mir-9	794	79	4	1	0	0
mmu-mir-9*	111	19	0	0	2	0
mmu-mir-10a	5	0	6	0	0	0
mmu-mir-10b	0	1	0	0	0	0
mmu-mir-10b*	1	0	0	0	0	0
mmu-mir-15a	4357	461	25	1	5	2
mmu-mir-15a*	70	18	0	0	0	0
mmu-mir-15b	7640	649	47	0	2	0
mmu-mir-15b*	216	26	1	0	0	0
mmu-mir-16	23030	2333	237	13	21	1
mmu-mir-16*	158	32	6	0	0	0
mmu-mir-17	39624	6214	10	1	4	1
mmu-mir-17*	242	33	5	0	0	0
mmu-mir-18a	22525	2622	10	1	3	0
mmu-mir-18a*	515	55	1	0	0	0
mmu-mir-18b	2835	271	10	0	0	0
mmu-mir-19a	6866	810	3	0	0	0
mmu-mir-19a*	118	8	0	0	0	0

mmu-mir-19b	36048	4886	8	1	7	1
mmu-mir-20a	48483	6528	68	5	5	1
mmu-mir-20a*	91	22	1	0	0	0
mmu-mir-20b	27029	3857	10	0	0	0
mmu-mir-20b*	809	74	0	0	0	0
mmu-mir-21	67968	5876	850	35	139	11
mmu-mir-21*	466	51	47	3	1	0
mmu-mir-23a	6751	788	33	3	14	2
mmu-mir-23b	5820	657	62	1	70	3
mmu-mir-24	28902	3982	150	14	111	16
mmu-mir-24-1*	72	11	0	0	0	0
mmu-mir-24-2*	522	69	13	0	2	1
mmu-mir-25	4752	510	3	1	3	1
mmu-mir-26a	13317	1440	61	7	32	5
mmu-mir-26b	6507	500	47	2	14	0
mmu-mir-26b*	40	1	0	0	0	0
mmu-mir-27a	11531	1533	22	6	23	4
mmu-mir-27a*	576	53	13	0	0	0
mmu-mir-27b	9681	1609	51	7	38	7
mmu-mir-27b*	196	24	1	0	0	0
mmu-mir-28	1425	140	1	0	0	0
mmu-mir-28*	598	86	1	1	2	0
mmu-mir-29a	1836	154	66	1	47	2
mmu-mir-29a*	34	3	6	0	1	0
mmu-mir-29b	1139	102	18	1	10	2
mmu-mir-29b*	18	8	0	0	0	0
mmu-mir-29c	390	45	1	0	0	0
mmu-mir-29c*	9	2	0	0	0	0
mmu-mir-30a	707	65	6	0	1	0
mmu-mir-30a*	63	51	0	0	0	0
mmu-mir-30b	1560	119	21	1	0	0
mmu-mir-30b*	20	5	2	1	0	0
mmu-mir-30c	3776	409	8	0	1	0
mmu-mir-30c-1*	58	6	0	0	0	0
mmu-mir-30c-2*	47	5	0	0	0	0
mmu-mir-30d	881	91	14	1	3	0
mmu-mir-30e	3769	351	19	1	0	0
mmu-mir-30e*	74	96	1	1	0	0
mmu-mir-31	223	18	1	0	0	0
mmu-mir-31*	56	10	0	0	0	0
mmu-mir-32	3582	399	4	2	0	0
mmu-mir-33	4387	431	2	0	3	0
mmu-mir-33*	36	9	0	0	0	0
mmu-mir-34a	7188	679	104	3	8	0
mmu-mir-34b-3p	48	6	1	0	0	0
mmu-mir-34b-5p	220	29	5	0	0	0
mmu-mir-34c	470	57	14	4	8	1
mmu-mir-34c*	10	2	0	0	0	0

mmu-mir-92a	24729	2985	9	1	9	1
mmu-mir-92a*	226	37	1	0	0	0
mmu-mir-92b	551	101	0	0	0	0
mmu-mir-93	20191	3159	15	3	4	1
mmu-mir-93*	193	24	1	0	0	0
mmu-mir-96	33575	2904	210	4	7	0
mmu-mir-98	54	13	3	0	2	0
mmu-mir-99a	2	0	3	1	8	1
mmu-mir-99b	360	51	0	0	1	0
mmu-mir-99b*	44	7	0	0	0	0
mmu-mir-100	0	1	2	0	2	0
mmu-mir-101a	2902	535	7	1	10	0
mmu-mir-101a*	74	6	8	0	0	0
mmu-mir-101b	5746	697	1	0	0	0
mmu-mir-103	18627	2604	18	3	18	5
mmu-mir-106a	21904	3759	5	1	0	0
mmu-mir-106b	20134	2461	106	10	6	1
mmu-mir-106b*	168	41	0	1	0	0
mmu-mir-107	631	91	0	0	0	1
mmu-mir-122	43	8	63	1	93	3
mmu-mir-124	2482	351	0	0	0	0
mmu-mir-124*	73	8	0	0	0	0
mmu-mir-125a-3p	77	13	0	0	1	0
mmu-mir-125a-5p	1503	196	8	3	5	1
mmu-mir-125b-3p	14	4	1	5	1	0
mmu-mir-125b-5p	275	33	71	6	54	7
mmu-mir-126-3p	844	104	1	0	0	0
mmu-mir-126-5p	212	21	1	0	0	0
mmu-mir-127	12994	1908	13	1	13	1
mmu-mir-127*	1336	155	5	1	0	0
mmu-mir-128	957	138	0	0	1	0
mmu-mir-129-3p	130	52	0	0	5	0
mmu-mir-129-5p	66	6	0	0	1	0
mmu-mir-130a	57203	6417	33	3	34	7
mmu-mir-130b	13134	1495	2	0	3	0
mmu-mir-130b*	1169	103	1	0	0	0
mmu-mir-132	32	4	0	0	0	0
mmu-mir-133a	11	0	2	0	5	0
mmu-mir-133a*	2	1	0	0	0	0
mmu-mir-134	1323	281	15	2	0	3
mmu-mir-135a	60	66	0	0	0	0
mmu-mir-135a*	1	0	0	0	0	0
mmu-mir-135b	13291	1672	56	4	0	0
mmu-mir-136	12177	1156	37	4	7	0
mmu-mir-136*	1123	84	2	0	4	0
mmu-mir-137	10	0	0	0	0	0
mmu-mir-138	169	30	1	0	0	0
mmu-mir-139-3p	1	0	0	0	0	0

mmu-mir-139-5p	107	23	1	0	0	0
mmu-mir-140	781	130	5	0	0	0
mmu-mir-140*	710	85	1	0	1	2
mmu-mir-141	3671	336	0	0	0	0
mmu-mir-141*	76	9	2	0	0	0
mmu-mir-142-3p	1523	255	7	0	7	0
mmu-mir-142-5p	206	17	1	0	0	0
mmu-mir-143	193	19	8	0	4	0
mmu-mir-144	12	3	6	0	13	0
mmu-mir-145	317	36	35	3	18	4
mmu-mir-145*	9	1	0	0	0	0
mmu-mir-146a	115	9	13	0	2	0
mmu-mir-146b	126	10	0	0	0	0
mmu-mir-146b*	3	0	0	0	0	0
mmu-mir-147	70	3	0	0	0	0
mmu-mir-148a	6761	679	24	0	28	1
mmu-mir-148a*	80	7	7	1	0	0
mmu-mir-148b	3287	358	9	0	9	0
mmu-mir-149	320	35	0	0	0	0
mmu-mir-150	1381	134	7	0	4	0
mmu-mir-150*	5	1	0	0	0	0
mmu-mir-151-3p	603	102	1	0	0	1
mmu-mir-151-5p	2492	236	6	0	0	0
mmu-mir-152	204	23	3	1	7	0
mmu-mir-153	35	3	0	0	0	0
mmu-mir-154	893	96	7	0	0	0
mmu-mir-154*	7185	826	1	1	0	0
mmu-mir-155	446	53	0	0	0	0
mmu-mir-181a	46	13	14	0	6	0
mmu-mir-181a-1*	0	3	0	0	0	0
mmu-mir-181b	22	11	2	0	2	0
mmu-mir-181c	1991	258	5	0	1	0
mmu-mir-181d	2654	339	0	0	0	0
mmu-mir-182	4140	612	49	3	0	0
mmu-mir-183	9716	927	60	2	0	0
mmu-mir-183*	838	113	3	1	0	0
mmu-mir-184	2	0	0	0	0	0
mmu-mir-185	643	123	0	0	0	0
mmu-mir-186	2114	215	2	0	0	0
mmu-mir-186*	60	19	1	0	0	0
mmu-mir-187	83	57	0	0	0	0
mmu-mir-188-3p	14	0	0	0	0	0
mmu-mir-188-5p	191	31	1	0	0	0
mmu-mir-190	841	85	3	0	1	0
mmu-mir-190b	19	4	0	0	0	0
mmu-mir-191	10843	1643	42	4	7	0
mmu-mir-191*	104	17	0	0	1	0
mmu-mir-192	134	17	7	0	0	0

mmu-mir-193	63	26	2	0	2	0
mmu-mir-193*	17	2	1	1	0	1
mmu-mir-194	156	13	0	0	0	0
mmu-mir-195	1272	194	7	0	1	0
mmu-mir-196a	55	8	7	0	0	1
mmu-mir-196b	8	1	1	0	0	0
mmu-mir-199a-3p	235	26	108	6	70	7
mmu-mir-199a-5p	20	4	12	4	15	1
mmu-mir-199b*	21	2	0	1	0	0
mmu-mir-200a	4915	433	0	0	0	0
mmu-mir-200a*	52	7	1	0	0	0
mmu-mir-200b	4890	479	0	0	0	0
mmu-mir-200b*	191	14	1	0	0	0
mmu-mir-200c	4089	642	2	0	0	0
mmu-mir-200c*	18	3	0	0	0	0
mmu-mir-202-3p	0	1	0	0	0	0
mmu-mir-202-5p	4	0	0	0	0	0
mmu-mir-203	123	24	4	2	7	1
mmu-mir-203*	4	0	0	0	0	0
mmu-mir-204	9	0	0	0	0	0
mmu-mir-205	1131	132	61	3	2	0
mmu-mir-206	1	0	2	0	0	0
mmu-mir-208a	9	1	0	0	0	0
mmu-mir-208b	4	1	0	0	0	0
mmu-mir-210	1722	414	1	0	0	0
mmu-mir-211	9	1	0	0	0	0
mmu-mir-212	18	3	0	0	0	0
mmu-mir-214	0	0	0	0	1	0
mmu-mir-214*	0	0	1	0	1	0
mmu-mir-215	1	0	0	0	0	0
mmu-mir-216b	3	0	0	0	0	0
mmu-mir-218	159	9	0	0	0	0
mmu-mir-218-1*	1	0	0	0	0	0
mmu-mir-218-2*	1	0	0	0	0	0
mmu-mir-219	160	8	0	0	1	0
mmu-mir-22	6975	790	43	2	54	4
mmu-mir-22*	257	19	4	0	1	0
mmu-mir-221	617	135	29	4	17	2
mmu-mir-222	789	76	15	1	21	2
mmu-mir-223	1	0	0	0	1	0
mmu-mir-224	64	5	1	0	0	0
mmu-mir-290-3p	1307	243	14	3	2	2
mmu-mir-290-5p	163878	22964	3325	223	19	1
mmu-mir-291a-3p	166770	18652	103	13	17	0
mmu-mir-291a-5p	51860	6735	110	15	8	0
mmu-mir-291b-3p	15311	1646	0	0	0	0
mmu-mir-291b-5p	7912	1530	9	0	1	0
mmu-mir-292-3p	177466	25698	86	5	5	0

mmu-mir-292-5p	138375	26865	338	29	7	0
mmu-mir-293	123699	14238	6	0	0	0
mmu-mir-293*	30099	2715	204	8	0	0
mmu-mir-294	260532	24171	7	1	90	3
mmu-mir-294*	7412	1037	287	28	3	0
mmu-mir-295	331261	39887	49	5	58	4
mmu-mir-295*	12115	1575	430	15	3	0
mmu-mir-296-3p	2122	568	16	3	2	2
mmu-mir-296-5p	1301	237	1	0	0	0
mmu-mir-297a	6510	702	1	0	0	1
mmu-mir-297b-3p	412	111	0	0	0	0
mmu-mir-297b-5p	222	35	1	0	0	0
mmu-mir-297c	2482	239	4	0	0	0
mmu-mir-298	1068	163	0	0	0	0
mmu-mir-299	802	124	0	0	2	0
mmu-mir-299*	1212	167	2	1	0	0
mmu-mir-300	4604	743	2	0	2	1
mmu-mir-300*	105	9	0	0	0	0
mmu-mir-301a	7094	704	3	0	4	0
mmu-mir-301b	3315	325	0	0	1	0
mmu-mir-302a	2726	385	0	0	0	0
mmu-mir-302a*	212	26	3	0	1	0
mmu-mir-302b	3939	412	0	0	0	0
mmu-mir-302b*	68	6	0	0	0	0
mmu-mir-302c	663	87	0	0	0	0
mmu-mir-302c*	36	1	0	0	0	0
mmu-mir-302d	7055	755	0	0	0	0
mmu-mir-320	3203	639	13	2	39629	5368
mmu-mir-322	568	66	4	4	2	11
mmu-mir-322*	4	0	0	0	0	0
mmu-mir-323-3p	2267	274	0	0	0	0
mmu-mir-323-5p	52	17	1	0	0	0
mmu-mir-324-3p	111	18	0	0	0	0
mmu-mir-324-5p	515	50	0	0	1	0
mmu-mir-325	2	0	0	0	0	0
mmu-mir-325*	1	0	0	0	0	0
mmu-mir-326	27	3	0	0	0	0
mmu-mir-328	52	8	0	0	0	0
mmu-mir-329	455	58	0	0	0	0
mmu-mir-330	173	20	5	0	0	0
mmu-mir-330*	58	9	0	0	0	0
mmu-mir-331-3p	147	39	1	0	0	0
mmu-mir-331-5p	15	3	1	0	0	0
mmu-mir-335-3p	1495	245	0	0	0	0
mmu-mir-335-5p	1745	179	13	0	3	1
mmu-mir-337-3p	845	104	3	0	1	0
mmu-mir-337-5p	16	4	0	0	1	0
mmu-mir-338-3p	45	9	0	0	0	0

mmu-mir-338-5p	4	0	0	0	0	0
mmu-mir-339-3p	88	15	0	0	0	0
mmu-mir-339-5p	571	148	38	4	36	5
mmu-mir-340-3p	13	2	0	0	0	0
mmu-mir-340-5p	989	74	9	0	0	0
mmu-mir-341	255	53	0	0	0	0
mmu-mir-342-3p	841	87	0	0	1	1
mmu-mir-342-5p	101	12	1	0	0	0
mmu-mir-344	67	8	0	0	196	11
mmu-mir-345-3p	11	16	0	0	0	0
mmu-mir-345-5p	187	45	0	0	0	0
mmu-mir-346	8	0	0	0	0	0
mmu-mir-350	458	39	0	0	0	0
mmu-mir-351	29	7	1	0	0	0
mmu-mir-361	1072	245	15	0	0	1
mmu-mir-362-3p	168	21	0	1	0	0
mmu-mir-362-5p	243	35	0	0	0	0
mmu-mir-363	3905	446	0	0	1	0
mmu-mir-365	158	17	6	1	1	0
mmu-mir-367	1467	160	1	0	0	0
mmu-mir-369-3p	5148	462	12	3	9	0
mmu-mir-369-5p	714	69	10	0	0	0
mmu-mir-370	962	223	0	0	0	0
mmu-mir-374	1086	172	2	0	0	0
mmu-mir-375	11	2	0	0	0	0
mmu-mir-376a	4984	569	0	0	1	0
mmu-mir-376a*	254	27	0	0	0	0
mmu-mir-376b	6132	628	0	0	3	1
mmu-mir-376b*	1083	100	8	0	5	0
mmu-mir-376c	2287	248	0	0	1	0
mmu-mir-376c*	21	5	0	0	0	0
mmu-mir-377	1633	154	2	0	0	0
mmu-mir-378	1980	205	5	1	6	1
mmu-mir-378*	48	6	0	0	0	0
mmu-mir-379	1625	129	1	0	1	0
mmu-mir-380-3p	1980	256	1	0	2	0
mmu-mir-380-5p	39	3	0	0	0	0
mmu-mir-381	2074	254	0	1	1	0
mmu-mir-382	1491	208	3	1	0	1
mmu-mir-382*	28	7	0	0	0	0
mmu-mir-384-3p	3	0	0	0	0	0
mmu-mir-384-5p	4	0	0	0	0	0
mmu-mir-409-3p	3809	618	1	2	1	0
mmu-mir-409-5p	806	77	14	0	0	0
mmu-mir-410	2552	253	2	0	3	2
mmu-mir-411	2658	241	20	0	1	0
mmu-mir-411*	3708	2680	0	1	0	0
mmu-mir-412	28	2	0	0	0	0

mmu-mir-421	642	122	1	0	0	0
mmu-mir-423-3p	882	134	1	0	0	0
mmu-mir-423-5p	771	159	66	7	10	1
mmu-mir-425	803	83	2	0	1	0
mmu-mir-425*	67	16	1	0	0	0
mmu-mir-429	3262	326	2	0	0	0
mmu-mir-431	2392	301	5	2	2	0
mmu-mir-431*	62	34	0	0	0	0
mmu-mir-433	1851	210	2	0	3	0
mmu-mir-433*	79	9	0	0	1	0
mmu-mir-434-3p	3936	361	4	0	1	0
mmu-mir-434-5p	1382	200	15	2	2	0
mmu-mir-449a	57	7	0	0	0	0
mmu-mir-449c	21	1	0	0	0	0
mmu-mir-450a-3p	17	1	0	0	0	0
mmu-mir-450a-5p	292	36	10	0	0	0
mmu-mir-450b-3p	70	3	0	0	0	0
mmu-mir-450b-5p	148	19	1	0	0	0
mmu-mir-451	111	11	127	4	115	21
mmu-mir-455	8	1	0	0	0	0
mmu-mir-455*	17	0	0	0	0	0
mmu-mir-463	2	0	0	0	0	0
mmu-mir-463*	6	0	1	0	0	0
mmu-mir-465a-3p	28	4	0	0	0	0
mmu-mir-465a-5p	5	0	1	0	0	0
mmu-mir-465b-5p	7	1	0	0	0	0
mmu-mir-465c-5p	18	1	1	0	0	0
mmu-mir-466a-3p	17151	2080	3	0	0	0
mmu-mir-466a-5p	2618	298	19	2	0	0
mmu-mir-466b-3-3p	157	21	0	0	0	0
mmu-mir-466b-5p	1337	143	1	0	0	0
mmu-mir-466c-5p	6991	673	51	2	0	0
mmu-mir-466d-3p	2730	364	0	0	0	0
mmu-mir-466d-5p	233	32	0	0	0	0
mmu-mir-466e-5p	544	43	0	0	0	0
mmu-mir-466f	1592	251	0	0	0	0
mmu-mir-466f-3p	79	10	0	1	0	5
mmu-mir-466f-5p	487	62	0	1	0	0
mmu-mir-466g	151	963	0	1	0	0
mmu-mir-466h	1345	661	0	0	0	0
mmu-mir-466i	110	583	0	0	0	0
mmu-mir-466j	314	144	6	4	0	0
mmu-mir-466k	1173	833	1	1	0	0
mmu-mir-466l	89	12	0	0	0	0
mmu-mir-467a	17237	1752	132	7	0	0
mmu-mir-467a-1*	4156	707	2	3	0	0
mmu-mir-467b	1075	125	0	0	0	0
mmu-mir-467b*	10	5	0	0	0	0

mmu-mir-467c	6161	690	75	3	0	0
mmu-mir-467d	3401	377	18	1	0	0
mmu-mir-467e	7995	682	28	0	0	0
mmu-mir-467e*	160	17	0	0	0	0
mmu-mir-467f	4	78	0	1	0	0
mmu-mir-467g	2	53	0	0	0	1
mmu-mir-467h	20	3549	0	0	0	0
mmu-mir-470	8	1	1	0	0	0
mmu-mir-470*	1	1	0	0	0	0
mmu-mir-471	7	1	0	0	0	0
mmu-mir-483	5	0	0	0	1	0
mmu-mir-483*	4	0	0	0	0	0
mmu-mir-484	2475	809	2	0	19480	4888
mmu-mir-485	149	43	2	0	0	0
mmu-mir-485*	1155	105	0	0	0	0
mmu-mir-486	8	1	2	1	2	0
mmu-mir-487b	1187	112	0	0	0	0
mmu-mir-488	4	1	0	0	0	0
mmu-mir-489	9	0	0	0	0	0
mmu-mir-491	3	1	0	0	0	0
mmu-mir-493	15	7	0	0	0	0
mmu-mir-494	2909	393	2	0	5	0
mmu-mir-495	4079	384	0	0	1	0
mmu-mir-496	248	28	0	0	2	0
mmu-mir-497	1493	103	0	0	1	0
mmu-mir-499	176	15	35	2	7	0
mmu-mir-500	393	65	0	0	2	0
mmu-mir-501-3p	148	30	0	0	0	0
mmu-mir-501-5p	143	21	28	2	0	0
mmu-mir-503	121	26	1	0	0	0
mmu-mir-503*	7	1	0	0	0	0
mmu-mir-504	2	1	1	0	0	0
mmu-mir-505	22	1	1	0	1	0
mmu-mir-532-3p	84	8	1	0	0	0
mmu-mir-532-5p	257	30	12	0	0	0
mmu-mir-539	457	53	0	0	0	0
mmu-mir-540-3p	994	113	0	0	0	0
mmu-mir-540-5p	234	35	0	0	0	0
mmu-mir-541	14331	1765	27	1	1	1
mmu-mir-542-3p	114	20	0	2	1	0
mmu-mir-542-5p	34	6	0	0	0	0
mmu-mir-543	5765	638	2	0	1	0
mmu-mir-544	39	77	0	0	0	0
mmu-mir-574-3p	2	0	0	0	0	0
mmu-mir-574-5p	39	25	0	32	3	49
mmu-mir-582-5p	279	25	8	0	1	0
mmu-mir-592	7	2	0	0	0	0
mmu-mir-598	5	0	0	0	0	0

mmu-mir-615-3p	0	0	2	1	0	0
mmu-mir-652	526	72	4	0	19	0
mmu-mir-664	14	0	1	0	171	21
mmu-mir-665	4997	685	0	0	0	0
mmu-mir-666-3p	61	8	0	0	0	0
mmu-mir-666-5p	270	52	0	0	2	0
mmu-mir-667	136	60	0	0	0	0
mmu-mir-668	34	12	0	0	42	11
mmu-mir-669a	12505	2781	62	3	5	0
mmu-mir-669b	4237	401	2	0	0	0
mmu-mir-669c	7817	769	5	0	0	3
mmu-mir-669d	2841	222	6	0	0	0
mmu-mir-669e	756	67	0	0	0	0
mmu-mir-669f	1165	716	1	0	0	1
mmu-mir-669g	28	5	0	0	0	0
mmu-mir-669h-3p	59	44	1	0	7	11
mmu-mir-669h-5p	501	84	13	1	140	16
mmu-mir-669i	22	93	0	0	15	6
mmu-mir-669j	28	4	0	0	3	0
mmu-mir-669k	32	13	0	0	1	1
mmu-mir-669l	3868	306	0	0	0	0
mmu-mir-669m	65	130	0	0	0	0
mmu-mir-669n	20	150	0	4	0	0
mmu-mir-669o	2169	204	3	0	0	0
mmu-mir-670	4	1	0	0	0	0
mmu-mir-671-3p	10	1	0	2	0	0
mmu-mir-671-5p	159	65	2	1	0	0
mmu-mir-672	1972	240	26	1	0	0
mmu-mir-673-3p	22	3	0	0	0	0
mmu-mir-673-5p	550	71	0	0	0	0
mmu-mir-674	883	123	2	0	0	0
mmu-mir-674*	635	98	0	0	0	0
mmu-mir-676	76	14	1	0	0	0
mmu-mir-676*	11	0	0	0	0	0
mmu-mir-677	62	6	53	0	120	6
mmu-mir-679	23	0	0	0	0	0
mmu-mir-688	0	0	0	0	2	0
mmu-mir-689	19	1	33	11	25	7
mmu-mir-690	110	11	65	11	140	12
mmu-mir-692	1	0	0	0	0	0
mmu-mir-693-3p	1	1	0	0	0	0
mmu-mir-696	2	1	1	1	4	2
mmu-mir-700	29	12	0	0	0	0
mmu-mir-701	3	1	0	0	0	0
mmu-mir-702	35	9	0	0	601	33
mmu-mir-703	2	0	2	0	5	0
mmu-mir-704	3	0	0	0	13	3
mmu-mir-705	0	0	1	1	0	0

mmu-mir-706	1	9	4	19	10	23
mmu-mir-707	0	0	0	0	0	0
mmu-mir-708	3106	304	3	0	3	1
mmu-mir-708*	247	24	1	0	1	0
mmu-mir-709	32	12	69	25	54	23
mmu-mir-710	0	1	0	0	0	0
mmu-mir-712	5	1	1	0	12	1
mmu-mir-712*	658	66	40	3	306	18
mmu-mir-713	0	0	0	1	0	0
mmu-mir-714	3	1	12	0	3	0
mmu-mir-715	4	2	2	0	2	0
mmu-mir-717	0	0	0	0	0	0
mmu-mir-718	0	0	0	0	0	0
mmu-mir-719	0	0	0	0	0	0
mmu-mir-720	861	118	1440	83	1975	196
mmu-mir-721	0	2	0	0	0	0
mmu-mir-741	13	1	0	0	0	0
mmu-mir-743a	7	2	0	0	0	0
mmu-mir-743b-3p	7	1	0	0	0	0
mmu-mir-743b-5p	1	0	0	0	0	0
mmu-mir-744	1569	236	5	0	0	0
mmu-mir-744*	33	7	0	0	0	0
mmu-mir-758	636	62	0	0	0	0
mmu-mir-760	4	2	0	0	0	0
mmu-mir-770-3p	13	6	1	0	0	0
mmu-mir-770-5p	32	7	0	0	0	0
mmu-mir-804	0	0	0	1	0	1
mmu-mir-871	6	2	2	0	0	0
mmu-mir-872	1144	102	5	0	0	0
mmu-mir-872*	446	43	0	0	1	0
mmu-mir-874	5	0	1	0	1	0
mmu-mir-876-5p	1	0	0	0	0	0
mmu-mir-877	25	4	0	0	419	35
mmu-mir-877*	63	7	0	1	459	62
mmu-mir-878-3p	8	0	0	0	0	0
mmu-mir-878-5p	2	1	4	0	0	0
mmu-mir-879	5	0	0	0	0	0
mmu-mir-880	4	0	0	0	0	0
mmu-mir-881	8	1	0	0	0	0
mmu-mir-883a-3p	3	0	0	0	0	0
mmu-mir-883b-5p	0	0	1	0	0	0
mmu-mir-1186	1213	317	1	19	3496	866
mmu-mir-1186b	1	7	2	7	2	2
mmu-mir-1187	181	270	3	16	2	10
mmu-mir-1188	28	11	0	0	0	0
mmu-mir-1190	12	3	0	0	0	0
mmu-mir-1191	27	3	0	0	0	0
mmu-mir-1192	0	0	0	0	0	1

mmu-mir-1193	318	34	0	0	0	0
mmu-mir-1194	0	4	0	2	1	15
mmu-mir-1195	95	85	15	59	116	166
mmu-mir-1196	2260	252	1	11	7928	641
mmu-mir-1197	221	16	1	0	0	0
mmu-mir-1198	143	44	3	1	0	0
mmu-mir-1199	12	1	0	0	0	0
mmu-mir-1224	0	1	0	0	0	0
mmu-mir-1274a	67	575	305	1659	196	1678
mmu-mir-1306	7	4	0	0	0	0
mmu-mir-1839-3p	44	13	0	0	239	47
mmu-mir-1839-5p	208	30	2	0	1642	149
mmu-mir-1894-5p	0	0	0	0	1	0
mmu-mir-1895	0	0	0	3	0	2
mmu-mir-1930	7	1	0	0	0	0
mmu-mir-1931	0	19	0	40	0	23
mmu-mir-1934	5	1	0	0	0	0
mmu-mir-1935	49	23	0	0	106	53
mmu-mir-1937a	273	38	872	67	877	94
mmu-mir-1937b	25	2	192	21	175	23
mmu-mir-1937c	1	2	0	1	2	4
mmu-mir-1939	0	111	0	422	0	437
mmu-mir-193b	78	15	1	0	0	0
mmu-mir-1940	0	0	0	0	3	0
mmu-mir-1941-5p	1	0	0	0	0	0
mmu-mir-1943	3	1	0	0	0	0
mmu-mir-1944	343	31	657	30	867	67
mmu-mir-1946a	6	25	19	36	8	35
mmu-mir-1946b	1	24	2	24	3	13
mmu-mir-1947	11	0	0	0	0	0
mmu-mir-1949	28	5	67	5	62	6
mmu-mir-1950	1	0	0	0	0	0
mmu-mir-1952	0	0	0	1	0	0
mmu-mir-1953	1	0	0	0	0	0
mmu-mir-1954	3	0	0	0	0	0
mmu-mir-1955	7	2	0	0	0	0
mmu-mir-1956	0	0	0	0	2	0
mmu-mir-1957	0	75	0	270	0	355
mmu-mir-1959	116	143	169	261	221	355
mmu-mir-1961	0	1	0	0	0	0
mmu-mir-1964	3	4	0	0	0	0
mmu-mir-1965	841	292	6	1	845	179
mmu-mir-1968	26	8	0	0	0	0
mmu-mir-1969	1	0	0	0	0	0
mmu-mir-1971	0	5	0	0	1	254
mmu-mir-1981	37	3	0	0	2770	110
mmu-mir-1982*	1	0	0	0	5	0
mmu-mir-1982.1	19	1	0	0	44	5

mmu-mir-1982.2	3	0	0	0	7	1
mmu-mir-1983	1827	367	6	1	25413	4555
mmu-mir-2132	90	31	256	62	536	147
mmu-mir-2133	41	11	334	46	232	47
mmu-mir-2134	27	3	12	3	40	6
mmu-mir-2135	514	110	304	37	501	79
mmu-mir-2137	6	4337	9	8038	12	8509
mmu-mir-2138	827	133	1091	95	1172	196
mmu-mir-2140	71	8	49	1	77	7
mmu-mir-2141	1257	164	1174	68	1779	152
mmu-mir-2145	206	26	591	69	821	94
mmu-mir-2146	489	65	353	22	515	45
mmu-mir-3072	73	14	0	0	0	0
mmu-mir-3072*	19	3	0	0	0	0
mmu-mir-3099	3	2	0	0	0	0
mmu-mir-3470a	5	2	18	5	17	6
mmu-mir-3470b	1	0	2	5	5	14
mmu-mir-3471	1	0	2	1	0	2
mmu-mir-3472	0	0	0	0	0	2
mmu-mir-3473	29	27	58	82	76	50
mmu-mir-3474	2	0	0	0	1	0
mmu-mir-3475	5	3	0	0	0	1

The libraries were analysed in the reference of miRBase v15.0. The murine miRNAs that are not present here have no reads in all three libraries.

Appendix Table IV

Read numbers of individual human miRNA in Solexa sequencing libraries of wt, Dicer1^{-/-} and Dgcr8^{-/-} mESCs.

	wt		Dicer1 ^{-/-}		Dgcr8 ^{-/-}	
	mismatch0	mismatch1	mismatch0	mismatch1	mismatch0	mismatch1
total miRNA	889563	353066	20511	32411	73599	41158
hsa-let-7a	967	115	102	6	30	2
hsa-let-7a*	11	5	3	2	0	0
hsa-let-7b	73	40	11	0	11	1
hsa-let-7b*	0	1	0	0	0	0
hsa-let-7c	1802	168	24	1	2	0
hsa-let-7c*	0	0	0	0	0	0
hsa-let-7d	383	43	18	1	6	2
hsa-let-7d*	1	0	0	0	1	0
hsa-let-7e	635	71	9	2	6	2
hsa-let-7e*	21	1	1	0	0	0
hsa-let-7f	725	53	107	6	42	0
hsa-let-7f-1*	0	1	0	1	0	0
hsa-let-7f-2*	3	1	0	0	0	0
hsa-let-7g	455	42	7	1	10	0
hsa-let-7g*	3	0	0	0	0	0
hsa-let-7i	153	16	20	1	13	1
hsa-let-7i*	5	1	0	0	1	0
hsa-mir-1	84	10	2	0	7	0
hsa-mir-7	25777	2534	108	4	0	0
hsa-mir-7-1*	155	21	3	1	0	0
hsa-mir-9	794	79	4	1	0	0
hsa-mir-9*	111	19	0	0	2	0
hsa-mir-10a	5	0	6	0	0	0
hsa-mir-10b	0	1	0	0	0	0
hsa-mir-10b*	1	0	0	0	0	0
hsa-mir-15a	4357	463	25	1	5	2
hsa-mir-15a*	0	71	0	0	0	0
hsa-mir-15b	7640	647	47	0	2	0
hsa-mir-15b*	216	26	1	0	0	0
hsa-mir-16	23030	2404	237	13	21	1
hsa-mir-16-1*	0	159	0	6	0	0
hsa-mir-16-2*	0	106	0	1	0	0
hsa-mir-17	39624	28380	10	6	4	1
hsa-mir-17*	0	242	0	5	0	0
hsa-mir-18a	22525	2649	10	3	3	0
hsa-mir-18a*	494	76	1	0	0	0
hsa-mir-18b	31	2801	0	8	0	0

hsa-mir-18b*	3	42	0	0	0	0
hsa-mir-19a	6866	911	3	0	0	0
hsa-mir-19a*	36	9	1	0	0	0
hsa-mir-19b	36048	4785	8	1	7	1
hsa-mir-19b-1*	355	64	12	0	0	0
hsa-mir-19b-2*	0	3	0	0	0	0
hsa-mir-20a	48483	6319	68	5	5	1
hsa-mir-20a*	0	91	0	1	0	0
hsa-mir-20b	27029	3920	10	0	0	0
hsa-mir-21	67968	5876	850	35	139	11
hsa-mir-21*	0	470	0	45	0	1
hsa-mir-22	6975	790	43	2	54	4
hsa-mir-22*	257	19	4	0	1	0
hsa-mir-23a	8307	960	84	4	70	5
hsa-mir-23a*	72	9	2	0	0	0
hsa-mir-23b	4264	485	11	0	14	0
hsa-mir-23b*	89	12	1	0	0	0
hsa-mir-24	28902	3982	150	14	111	16
hsa-mir-24-1*	44	9	0	0	0	0
hsa-mir-24-2*	3	7	2	0	0	0
hsa-mir-25	4752	533	3	1	3	1
hsa-mir-25*	14	2	0	0	0	0
hsa-mir-26a	13317	1440	61	7	32	5
hsa-mir-26a-1*	1	0	0	0	0	0
hsa-mir-26a-2*	0	28	0	0	0	0
hsa-mir-26b	6507	500	47	2	14	0
hsa-mir-26b*	40	1	0	0	0	0
hsa-mir-27a	11682	1632	29	7	33	5
hsa-mir-27a*	576	53	13	0	0	0
hsa-mir-27b	9530	1510	44	6	28	6
hsa-mir-27b*	196	24	1	0	0	0
hsa-mir-28-3p	1	598	0	2	0	2
hsa-mir-28-5p	1425	141	1	0	0	0
hsa-mir-29a	1836	155	66	1	47	2
hsa-mir-29a*	34	3	6	0	1	0
hsa-mir-29b	1139	101	18	1	10	2
hsa-mir-29b-1*	17	3	0	0	0	0
hsa-mir-29b-2*	4	2	0	0	0	0
hsa-mir-29c	390	45	1	0	0	0
hsa-mir-29c*	9	2	0	0	0	0
hsa-mir-30a	707	65	6	0	1	0
hsa-mir-30a*	63	51	0	0	0	0
hsa-mir-30b	1340	103	18	1	0	0
hsa-mir-30b*	0	1	0	0	0	0
hsa-mir-30c	3996	425	11	0	1	0
hsa-mir-30c-1*	58	6	0	0	0	0
hsa-mir-30c-2*	47	5	0	0	0	0
hsa-mir-30d	881	94	14	1	3	0

hsa-mir-30d*	25	11	1	0	0	0
hsa-mir-30e	3769	348	19	1	0	0
hsa-mir-30e*	74	96	1	1	0	0
hsa-mir-31	220	19	1	0	0	0
hsa-mir-31*	51	7	0	0	0	0
hsa-mir-32	3582	399	4	2	0	0
hsa-mir-32*	175	15	0	0	0	0
hsa-mir-33a	4387	431	2	0	3	0
hsa-mir-33a*	36	9	0	0	0	0
hsa-mir-33b	0	1	0	0	0	0
hsa-mir-34a	7188	679	104	3	8	0
hsa-mir-34a*	62	5	3	0	0	0
hsa-mir-34b	5	1	0	0	0	0
hsa-mir-34b*	0	46	0	0	0	2
hsa-mir-34c-3p	0	10	0	0	0	0
hsa-mir-34c-5p	470	57	14	4	8	1
hsa-mir-92a	19136	8304	9	2	9	1
hsa-mir-92b	551	108	0	0	0	0
hsa-mir-92b*	0	12	0	0	0	0
hsa-mir-93	20191	3159	15	3	4	1
hsa-mir-93*	193	24	1	0	0	0
hsa-mir-96	33575	2904	210	4	7	0
hsa-mir-96*	1	20	0	4	0	0
hsa-mir-98	54	13	3	0	2	0
hsa-mir-99a	2	0	3	1	8	1
hsa-mir-99a*	2	0	0	0	0	0
hsa-mir-99b	360	51	0	0	1	0
hsa-mir-99b*	44	7	0	0	0	0
hsa-mir-100	0	1	2	0	2	0
hsa-mir-101	2902	6281	7	2	10	0
hsa-mir-101*	71	7	8	0	0	0
hsa-mir-103	18627	2603	18	3	18	5
hsa-mir-103-2*	26	6	0	0	0	0
hsa-mir-105*	0	1	0	0	0	0
hsa-mir-106a	93	106	0	0	0	0
hsa-mir-106b	20134	2461	106	11	6	1
hsa-mir-106b*	168	41	0	1	0	0
hsa-mir-107	631	91	0	0	0	1
hsa-mir-122	43	8	63	1	93	3
hsa-mir-124	2482	351	0	0	0	0
hsa-mir-124*	73	8	0	0	0	0
hsa-mir-125a-3p	77	13	0	0	1	0
hsa-mir-125a-5p	1503	196	8	3	5	1
hsa-mir-125b	275	33	71	6	54	7
hsa-mir-125b-1*	14	4	1	5	1	0
hsa-mir-126	844	104	1	0	0	0
hsa-mir-126*	212	21	1	0	0	0
hsa-mir-127-3p	12994	1908	13	1	13	1

hsa-mir-127-5p	1336	155	5	1	0	0
hsa-mir-128	957	138	0	0	1	0
hsa-mir-129*	39	13	0	0	0	0
hsa-mir-129-3p	118	23	0	0	5	0
hsa-mir-129-5p	66	6	0	0	1	0
hsa-mir-130a	57203	6417	33	3	34	7
hsa-mir-130a*	1	0	0	0	0	0
hsa-mir-130b	13134	1495	2	0	3	0
hsa-mir-130b*	1155	96	1	0	0	0
hsa-mir-132	32	4	0	0	0	0
hsa-mir-132*	7	0	0	0	0	0
hsa-mir-133a	11	0	2	0	5	0
hsa-mir-134	1323	281	15	2	0	3
hsa-mir-135a	60	66	0	0	0	0
hsa-mir-135a*	1	0	0	0	0	0
hsa-mir-135b	13291	1672	56	4	0	0
hsa-mir-135b*	117	8	1	4	0	0
hsa-mir-136	12218	1281	36	5	7	0
hsa-mir-136*	1397	116	2	0	5	0
hsa-mir-137	10	0	0	0	0	0
hsa-mir-138	169	30	1	0	0	0
hsa-mir-138-2*	8	1	0	0	0	0
hsa-mir-139-3p	1	0	0	0	0	0
hsa-mir-139-5p	107	23	1	0	0	0
hsa-mir-140-3p	710	85	1	0	1	2
hsa-mir-140-5p	781	130	5	0	0	0
hsa-mir-141	3671	336	0	0	0	0
hsa-mir-141*	0	76	0	2	0	0
hsa-mir-142-3p	1523	255	7	0	7	0
hsa-mir-142-5p	206	17	1	0	0	0
hsa-mir-143	193	19	8	0	4	0
hsa-mir-143*	15	0	1	0	0	0
hsa-mir-144	12	3	6	0	13	0
hsa-mir-145	317	36	35	3	18	4
hsa-mir-145*	37	1	0	0	0	0
hsa-mir-146a	115	9	13	0	2	0
hsa-mir-146b-5p	126	10	0	0	0	0
hsa-mir-147	0	2	0	0	0	0
hsa-mir-147b	70	2	0	0	0	0
hsa-mir-148a	6761	679	24	0	28	1
hsa-mir-148a*	80	7	7	1	0	0
hsa-mir-148b	3287	358	9	0	9	0
hsa-mir-148b*	57	6	0	0	0	0
hsa-mir-149	320	35	0	0	0	0
hsa-mir-149*	0	0	0	1	0	2
hsa-mir-150	1381	134	7	0	4	0
hsa-mir-150*	0	5	0	0	0	0
hsa-mir-151-3p	1	604	0	1	1	0

hsa-mir-151-5p	2492	235	6	0	0	0
hsa-mir-152	204	23	3	1	7	0
hsa-mir-153	35	3	0	0	0	0
hsa-mir-154	893	96	7	0	0	0
hsa-mir-154*	7185	826	1	1	0	0
hsa-mir-155	0	446	0	0	0	0
hsa-mir-181a	46	13	14	0	6	0
hsa-mir-181b	22	11	2	0	2	0
hsa-mir-181c	1991	258	5	0	1	0
hsa-mir-181c*	73	12	0	1	0	0
hsa-mir-181d	2654	339	0	0	0	0
hsa-mir-182	1305	2831	21	27	0	0
hsa-mir-182*	53	7	3	2	0	0
hsa-mir-183	9716	927	60	2	0	0
hsa-mir-183*	838	113	3	1	0	0
hsa-mir-184	2	0	0	0	0	0
hsa-mir-185	643	123	0	0	0	0
hsa-mir-185*	11	3	0	0	0	0
hsa-mir-186	2114	215	2	0	0	0
hsa-mir-186*	1	59	0	1	0	0
hsa-mir-187	83	57	0	0	0	0
hsa-mir-187*	4	0	0	0	0	0
hsa-mir-188-3p	14	0	0	0	0	0
hsa-mir-188-5p	191	31	1	0	0	0
hsa-mir-190	841	85	3	0	1	0
hsa-mir-190b	19	4	0	0	0	0
hsa-mir-191	10843	1643	42	4	7	0
hsa-mir-191*	0	8	0	0	0	0
hsa-mir-192	134	17	7	0	0	0
hsa-mir-192*	2	0	0	0	0	0
hsa-mir-193a-3p	63	31	2	0	2	0
hsa-mir-193a-5p	0	17	1	1	0	0
hsa-mir-193b	0	74	0	1	0	0
hsa-mir-193b*	4	0	0	0	0	0
hsa-mir-194	156	13	0	0	0	0
hsa-mir-194*	3	0	0	0	0	0
hsa-mir-195	1272	123	7	0	1	0
hsa-mir-195*	5	3	0	0	0	0
hsa-mir-196a	55	8	7	0	0	1
hsa-mir-196b	8	1	1	0	0	0
hsa-mir-199a-3p	235	26	108	6	70	7
hsa-mir-199a-5p	20	24	12	4	15	1
hsa-mir-199b-5p	1	1	0	0	0	0
hsa-mir-200a	4915	433	0	0	0	0
hsa-mir-200a*	52	7	1	0	0	0
hsa-mir-200b	4890	519	0	0	0	0
hsa-mir-200b*	191	14	1	0	0	0
hsa-mir-200c	4089	642	2	0	0	0

hsa-mir-200c*	18	3	0	0	0	0
hsa-mir-202*	4	0	0	0	0	0
hsa-mir-203	123	24	4	2	7	1
hsa-mir-204	9	9	0	0	0	0
hsa-mir-205	1131	132	61	3	2	0
hsa-mir-205*	7	12	0	1	0	0
hsa-mir-206	1	0	2	0	0	0
hsa-mir-208a	9	1	0	0	0	0
hsa-mir-208b	4	1	0	0	0	0
hsa-mir-210	1722	414	1	0	0	0
hsa-mir-212	18	3	0	0	0	0
hsa-mir-214	0	0	0	0	1	0
hsa-mir-214*	0	0	1	0	1	0
hsa-mir-215	0	1	0	0	0	0
hsa-mir-216b	3	0	0	0	0	0
hsa-mir-218	159	9	0	0	0	0
hsa-mir-218-2*	1	0	0	0	0	0
hsa-mir-219-1-3p	0	5	0	0	0	0
hsa-mir-219-5p	160	8	0	0	1	0
hsa-mir-221	617	135	29	4	17	2
hsa-mir-221*	15	2	0	0	0	0
hsa-mir-222	789	76	15	1	21	2
hsa-mir-222*	4	0	0	0	0	0
hsa-mir-223	1	0	0	0	1	0
hsa-mir-224	0	64	0	1	0	0
hsa-mir-224*	1	0	0	0	0	0
hsa-mir-296-3p	2122	568	16	3	2	2
hsa-mir-296-5p	1301	237	1	0	0	0
hsa-mir-297	6469	3122	1	4	0	0
hsa-mir-299-3p	0	803	0	0	0	2
hsa-mir-299-5p	1212	167	2	1	0	0
hsa-mir-301a	7094	4019	3	0	4	1
hsa-mir-301b	1	9	0	0	0	0
hsa-mir-302a	2726	379	0	0	0	0
hsa-mir-302a*	0	223	0	3	0	1
hsa-mir-302b	3939	408	0	0	0	0
hsa-mir-302b*	0	0	0	0	0	1
hsa-mir-302c	351	66	0	0	0	0
hsa-mir-302c*	3	123	0	1	0	0
hsa-mir-302d	7055	746	0	0	0	0
hsa-mir-302d*	116	22	1	0	0	0
hsa-mir-302e	26	149	0	0	0	0
hsa-mir-302f	2	8	0	0	0	0
hsa-mir-320a	3203	601	13	2	39629	5131
hsa-mir-320b	25	12	0	1	93	50
hsa-mir-320c	13	36	0	0	96	270
hsa-mir-320d	3	0	1	0	40	91
hsa-mir-320e	5	125	0	0	60	1949

hsa-mir-323-3p	2267	274	0	0	0	0
hsa-mir-323-5p	52	17	1	0	0	0
hsa-mir-323b-3p	0	1	0	0	0	0
hsa-mir-324-3p	706	74	1	0	1	0
hsa-mir-324-5p	515	50	0	0	1	0
hsa-mir-326	27	3	0	0	0	0
hsa-mir-328	52	8	0	0	0	0
hsa-mir-330-3p	0	58	0	0	0	0
hsa-mir-330-5p	173	20	5	0	0	0
hsa-mir-331-3p	147	39	1	0	0	0
hsa-mir-331-5p	15	3	1	0	0	0
hsa-mir-335	1745	179	13	0	3	1
hsa-mir-335*	1495	245	0	0	0	0
hsa-mir-337-3p	19	1	0	0	0	1
hsa-mir-338-3p	45	7	0	0	0	0
hsa-mir-338-5p	4	0	0	0	0	0
hsa-mir-339-3p	0	90	0	0	0	0
hsa-mir-339-5p	571	148	38	4	36	5
hsa-mir-340	989	74	9	0	0	0
hsa-mir-340*	13	2	0	0	0	0
hsa-mir-342-3p	841	87	0	0	1	1
hsa-mir-342-5p	102	11	1	0	0	0
hsa-mir-361-3p	51	8	0	0	1	0
hsa-mir-361-5p	1072	245	15	0	0	1
hsa-mir-362-3p	1	168	0	0	0	0
hsa-mir-362-5p	60	194	0	0	0	0
hsa-mir-363	3905	446	0	0	1	0
hsa-mir-363*	0	3	0	0	0	0
hsa-mir-365	158	17	6	1	1	0
hsa-mir-367	1467	160	1	0	0	0
hsa-mir-367*	0	13	0	4	0	0
hsa-mir-369-3p	5148	462	12	3	9	0
hsa-mir-369-5p	714	69	10	0	0	0
hsa-mir-370	962	223	0	0	0	0
hsa-mir-371-3p	0	106	0	0	0	0
hsa-mir-371-5p	56	166273	0	3315	0	17
hsa-mir-373*	1	104	0	1	0	0
hsa-mir-374a	0	9	0	0	0	0
hsa-mir-374b	1086	163	2	0	0	0
hsa-mir-374b*	88	6	0	0	0	0
hsa-mir-375	11	2	0	0	0	0
hsa-mir-376a	39	5207	0	0	0	1
hsa-mir-376a*	275	25	2	0	0	0
hsa-mir-376b	0	48	0	0	0	0
hsa-mir-376c	0	2290	0	2	0	7
hsa-mir-377	1633	154	2	0	0	0
hsa-mir-377*	113	16	3	0	0	0
hsa-mir-378	1980	195	5	0	6	1

hsa-mir-378*	48	6	0	0	0	0
hsa-mir-378b	7	4	1	0	0	0
hsa-mir-378c	3	1	0	0	0	0
hsa-mir-379	1625	129	1	0	1	0
hsa-mir-379*	1032	329	1	0	0	0
hsa-mir-380	1	1982	0	3	0	2
hsa-mir-380*	1	2	0	0	0	0
hsa-mir-381	2088	652	0	1	1	1
hsa-mir-382	1491	208	3	1	0	1
hsa-mir-384	0	4	0	0	0	0
hsa-mir-409-3p	3809	618	1	2	1	0
hsa-mir-409-5p	806	77	14	0	0	0
hsa-mir-410	2552	253	2	0	3	2
hsa-mir-411	2658	241	20	0	1	0
hsa-mir-411*	3708	1582	0	0	0	0
hsa-mir-412	35	5	1	0	0	0
hsa-mir-421	642	122	1	0	0	0
hsa-mir-423-3p	882	134	1	0	0	0
hsa-mir-423-5p	771	159	66	7	10	1
hsa-mir-424	119	485	6	4	12	1
hsa-mir-425	803	83	2	0	1	0
hsa-mir-425*	70	20	1	0	0	0
hsa-mir-429	2	11	0	0	0	0
hsa-mir-431	2392	301	5	2	2	0
hsa-mir-431*	62	34	0	0	0	0
hsa-mir-432	0	0	2	1	0	0
hsa-mir-433	1851	210	2	0	3	0
hsa-mir-449a	57	7	0	0	0	0
hsa-mir-450a	292	36	10	0	0	0
hsa-mir-450b-3p	0	4	0	0	0	0
hsa-mir-450b-5p	0	149	0	1	0	0
hsa-mir-451	111	11	127	4	115	21
hsa-mir-452	11	1	0	0	0	0
hsa-mir-455-3p	0	8	0	0	0	0
hsa-mir-455-5p	17	0	0	0	0	0
hsa-mir-483-3p	0	4	0	0	0	0
hsa-mir-484	2475	809	2	0	19480	4888
hsa-mir-485-3p	1653	285	0	0	0	0
hsa-mir-485-5p	149	43	2	0	0	0
hsa-mir-486-5p	8	1	2	1	2	0
hsa-mir-487a	0	2	0	0	0	0
hsa-mir-487b	1187	111	0	0	0	0
hsa-mir-488	0	4	0	0	0	0
hsa-mir-491-3p	0	0	0	0	0	1
hsa-mir-491-5p	3	1	0	0	0	0
hsa-mir-493*	94	7	0	0	0	0
hsa-mir-494	2909	393	2	0	5	0
hsa-mir-495	4079	384	0	0	1	0

hsa-mir-496	248	28	0	0	2	0
hsa-mir-497	1213	78	0	0	1	0
hsa-mir-497*	14	0	0	0	0	0
hsa-mir-499-3p	5	0	0	0	0	1
hsa-mir-499-5p	176	15	35	2	7	0
hsa-mir-500	0	1	0	0	0	0
hsa-mir-500*	0	4	0	0	0	0
hsa-mir-501-3p	26	20	0	0	0	0
hsa-mir-501-5p	13	135	4	24	0	0
hsa-mir-502-3p	5	388	0	0	0	2
hsa-mir-502-5p	0	25	0	0	0	0
hsa-mir-503	1	120	0	1	0	0
hsa-mir-504	2	1	1	0	0	0
hsa-mir-505	12	10	1	0	1	0
hsa-mir-505*	14	3	0	0	0	0
hsa-mir-518a-3p	0	12	0	0	0	0
hsa-mir-520a-3p	2	24	0	0	0	0
hsa-mir-520d-3p	0	18	0	0	0	0
hsa-mir-520e	2	2917	0	0	0	1
hsa-mir-520g	13	337	0	1	0	0
hsa-mir-521	0	5	0	0	0	0
hsa-mir-526b*	0	1	0	0	0	0
hsa-mir-532-3p	84	8	1	0	0	0
hsa-mir-532-5p	257	30	12	0	0	0
hsa-mir-539	457	53	0	0	0	0
hsa-mir-541	0	0	0	0	0	3
hsa-mir-542-3p	114	20	0	2	1	0
hsa-mir-542-5p	2	3	0	0	0	0
hsa-mir-543	5765	638	2	0	1	0
hsa-mir-544	8	32	0	0	0	0
hsa-mir-549	0	0	0	1	0	0
hsa-mir-572	0	0	0	1	0	1
hsa-mir-574-3p	2	2	0	0	0	0
hsa-mir-574-5p	39	25	0	32	3	49
hsa-mir-578	0	1	0	0	0	0
hsa-mir-582-5p	277	110	6	1	1	0
hsa-mir-592	7	2	0	0	0	0
hsa-mir-598	0	1	0	0	0	0
hsa-mir-615-3p	0	0	2	1	0	0
hsa-mir-651	0	1	0	0	0	0
hsa-mir-652	526	72	4	0	19	0
hsa-mir-655	0	0	0	1	0	0
hsa-mir-660	0	0	0	1	0	0
hsa-mir-663b	0	0	0	1	0	0
hsa-mir-664*	0	1	0	0	0	0
hsa-mir-665	30	5073	0	0	0	0
hsa-mir-668	38	10	0	0	44	11
hsa-mir-670	0	4	0	0	0	0

hsa-mir-671-3p	10	1	0	2	0	0
hsa-mir-671-5p	159	65	2	1	0	0
hsa-mir-708	3106	304	3	0	3	1
hsa-mir-708*	247	24	1	0	1	0
hsa-mir-718	0	0	0	4	0	0
hsa-mir-720	866	119	1465	86	1996	210
hsa-mir-744	1569	236	5	0	0	0
hsa-mir-744*	33	7	0	0	0	0
hsa-mir-758	614	77	0	0	0	0
hsa-mir-760	4	2	0	0	0	0
hsa-mir-762	0	0	0	1	0	0
hsa-mir-874	5	0	1	0	1	0
hsa-mir-877	25	4	0	0	419	35
hsa-mir-877*	59	27	0	1	525	226
hsa-mir-885-5p	0	0	0	0	1	0
hsa-mir-935	24	2	0	0	0	0
hsa-mir-1197	221	16	1	0	0	0
hsa-mir-1203	0	0	0	1	0	1
hsa-mir-1225-5p	0	0	0	1	1	0
hsa-mir-1244	1	0	0	0	0	0
hsa-mir-1246	8	11	26	6	27	7
hsa-mir-1247	6	1	2	0	0	0
hsa-mir-1248	64	12	173	4	258	18
hsa-mir-1249	12	1	0	1	0	3
hsa-mir-1251	1	0	0	0	0	0
hsa-mir-1259	0	0	0	0	0	1
hsa-mir-1260	5	698	1	3314	2	3862
hsa-mir-1260b	143	11	723	29	719	56
hsa-mir-1261	0	99	0	226	0	359
hsa-mir-1265	0	0	0	1	0	0
hsa-mir-1266	0	0	0	2	0	0
hsa-mir-1268	0	137	0	417	0	374
hsa-mir-1274a	101	21	515	22	289	41
hsa-mir-1274b	660	95	1807	110	1724	191
hsa-mir-1280	12	15	27	85	94	128
hsa-mir-1285	0	0	0	0	0	1
hsa-mir-1290	0	21	0	34	0	54
hsa-mir-1297	0	7	0	0	0	0
hsa-mir-1298	2	0	0	0	0	0
hsa-mir-1306	7	5	0	0	0	0
hsa-mir-1307	0	0	0	0	0	0
hsa-mir-1308	1555	5658	10237	21398	5165	20376
hsa-mir-1322	0	0	2	0	0	0
hsa-mir-1323	0	1	0	0	0	0
hsa-mir-1469	0	60	1	422	0	377
hsa-mir-1471	0	1	0	2	0	1
hsa-mir-1826	376	313	625	176	616	194
hsa-mir-1827	0	2	0	0	0	0

hsa-mir-1915	0	0	0	0	0	1
hsa-mir-1973	6	2	3	0	16	5
hsa-mir-1979	27	301	151	1670	180	1284
hsa-mir-3065-5p	1	0	0	0	0	0
hsa-mir-3074	9	0	0	0	0	0
hsa-mir-3141	0	0	0	0	0	1
hsa-mir-3142	0	0	0	1	0	3
hsa-mir-3154	0	0	1	1	0	0
hsa-mir-3168	0	158	1	325	2	392
hsa-mir-3178	0	1	0	0	0	0
hsa-mir-3182	0	18	0	81	0	67
hsa-mir-3186-3p	0	1	0	0	0	0
hsa-mir-3195	0	8	0	1	0	6
hsa-mir-4286	250	108	482	187	554	229
hsa-mir-4289	1	14	0	0	0	0
hsa-mir-4291	1	18	0	0	0	0
hsa-mir-4298	0	0	0	1	0	0
hsa-mir-4305	0	1	0	0	0	0
hsa-mir-4306	0	11	0	0	0	0
hsa-mir-4317	0	7	0	0	0	0
hsa-mir-4318	0	22	0	0	0	0
hsa-mir-4328	0	4	0	0	0	1
hsa-mir-4330	0	1	0	2	0	1

The libraries were analysed in the reference of miRBase v15.0. The human miRNAs that are not present here have no reads in all three libraries.

PUBLICATIONS

Part of this thesis has been published in the following papers:

Identification and analysis of expression of novel microRNAs of murine gamma-herpesvirus 68.

Zhu J.Y., Strehle M., Frohn A., Kremmer E., Höfig K.P., Meister G., Adler H.

Journal of Virology, 2010, 84(19) : 10266-10275.

Identification of novel Epstein-Barr virus miRNA genes from nasopharyngeal carcinomas.

Zhu J.Y., Pfuhl T., Motsch N., Barth S., Nicholls J., Grässer F.A., Meister G.

Journal of Virology, 2009, 83(1): 3333-3341

Mis-annotation of microRNA genes in miRBase.

Zhu J.Y., Meister G.

RNA, submitted

ACKNOWLEDGEMENTS

It has been a long journey to arrive here.

It was all your great favors that helped and supported me along the way to reach here.

Thanks to Prof. Gunter Meister. Thanks for offering me this opportunity so that I could jump into the fascinating miRNA field four years ago. Thanks for all the supervisions, suggestions, discussions and corrections that have helped the progression of every project. Thanks for the free and easy atmosphere always in the lab so that I learned to establish and pursue my own ideas, and gain the experiences in the failures. Thanks for encouraging and supporting me for the attendance in the conferences, which have preciously broadened my horizon. A lot of thanks, for every memorable moment in this PhD study.

Thanks to all the members of my thesis committee. Thanks to Prof. Karl Hopfner. Thanks for the acceptance of being my official Doktorvater. Thanks for spending the time supervising my PhD study.

Thanks to all my former and present lab members, wherever you are now. Thanks for the time that we have spent together. Thanks to Lasse for your patience of teaching during the first few months I was here. Thanks to Michaela for always being there for any upcoming technical discussions. Thanks to Julia, Christine, Sabine, Alex, Anne Dück and Anne Frohn, who have ever cooperated, supported and discussed in the projects. Also thanks to the former technician Sabine for the great assistance. Thanks to everyone around, for the help and inspirations.

Thanks to Prof. Friedrich Grässer and Natalie Motsch from Homburg, and Prof. John Nicholls from Hongkong, for the cooperation in the EBV project. Thanks to Dr. Heiko Adler and Martin Strehle from Munich, for the cooperation in the MHV-68 project. Thanks to Dr. Michael Sixt, for the cooperation in the dendritic cell project. Thank you for all of your great works, the experiments, the sharing of information and the discussions of projects, which have promoted every project forward. Thanks for letting me get into the other interesting fields based on the miRNA biology.

Thanks to Min, my former supervisor in DKFZ during my master study. Thanks for your understanding and support when I decided to switch my PhD project. Thanks for keeping discussions with me for the completion of my left projects. Thanks for your help when I began to learn, how to become a student in science.

Thanks to all my dear friends, in Munich, in Heidelberg, in Shanghai, in US, in wherever of the world. Thanks for always being there. Thanks for the great time we ever spent together, or shared over the long distance. Thanks for always being helpful and encouraging. Thanks for the preciousness in our memories and the brightness in our future. Thanks, that we are always adoring each other so much.

Thanks to Jiong, my dear husband. Thanks for your never-complaining support and understanding during my long study. Thanks for your encouragement for whatever I like to do. Thanks for giving me a home in Munich, and committing me a future in the life. Thanks for your love.

Thanks to my dear parents. Thanks for giving me the life. Thanks for your understanding and great support of my pursuing dream. Thanks for your ever-lasting care, even over the long distance. Thanks for your love.

Thanks to life, for all the mysteries, wonders and miracles.

Curriculum Vitae

PERSONAL DETAILS

Name	Jiayun Zhu
Date of Birth	08. October. 1981
Place of Birth	Shanghai
Citizenship	China

EDUCATION

11/2006 – 10/2010	Ph.D. student, Max-Planck-Institute of Biochemistry, Ludwig-Maximilians-Universität, Munich, Germany
08/2005 – 09/2006	Ph.D. student, German Cancer Research Center (DKFZ), Heidelberg University, Heidelberg, Germany
10/2003 – 06/2005	Master of Science, International Master Program of Molecular Cellular Biology, Heidelberg University, Heidelberg, Germany
09/1999 – 07/2003	Bachelor of Science, School of Life Sciences, Fudan University, Shanghai, China

SCIENTIFIC WORK EXPERIENCE

11/2006 – 10/2010	Ph.D. student with Dr. Gunter Meister, Max-Planck-Institute of Biochemistry, Martinsried, Germany
10/2004 – 09/2006	Master and Ph.D. student with Prof. Dr. Peter H. Krammer German Cancer Research Center (DKFZ), Heidelberg, Germany

RESEARCH ARTICLES (PEER-REVIEWED)

Zhu J.Y., Strehle M., Frohn A., Kremmer E., Höfig K.P., Meister G., Adler H. Identification and analysis of expression of novel microRNAs of murine gammaherpesvirus 68. *Journal of Virology*, 2010, 84(19): 10266-10275

Zhu J.Y., Meister G. Mis-annotation of microRNA genes in miRBase. *RNA*, submitted

Imig, J., Motsch N., **Zhu J.Y.**, Barth S., Okoniewski, M., Reineke T., Tinguely, M., Faggioni, A., M., Trivedi, P., Meister, G., Renner, C., Grässer, F.A. microRNA profiling in EBV-associated B-cell lymphomas. *Nucleic Acid Research*, 2010, in press.

Aguilar A.L., Piskol R., Beitzinger M., **Zhu J.Y.**, Kruspe D., Aszodi A., Moser M., Englert C., Meister G. The small RNA expression profile of the developing murine urinary and reproductive systems. *FEBS Letters*, 2010, Epub ahead of print.

Zhu J.Y., Pfuhl T., Motsch N., Barth S., Nicholls J., Grässer F.A., Meister G. Identification of novel Epstein-Barr virus miRNA genes from nasopharyngeal carcinomas. *Journal of Virology*, 83(1):3333-3341

Zhu J.Y., Giaisi M., Köhler R., Müller W.W., Mühleisen A., Proksch P., Krammer P.H., Li-Weber M.

Rocaglamide sensitizes leukemic T cells to activation-induced cell death by differential regulation of CD95L and c-FLIP expression.

Cell Death & Differentiation, 16(9): 1289-1299.

Beitzinger M., Peters L., **Zhu J.Y.**, Kremmer E., Meister G.

Identification of human microRNA targets from isolated Argonaute protein complexes.

RNA Biology, 4(2): 76-84.

Zhu J.Y., Lavrik I.N., Mahlkecht U., Giaisi M., Proksch P., Krammer P.H., Li-Weber M.

The traditional Chinese herbal compound rocaglamide preferentially induces apoptosis in leukemia cells by modulation of mitogen-activated protein kinase activities.

International Journal of Cancer, 121(8): 1839-1846

Fas S.C., Baumann S., **Zhu J.Y.**, Giaisi M., Treiber M.K., Krammer P.H., Li-Weber M.

Wogonin sensitizes resistant malignant cells to TNF α - and TRAIL-induced apoptosis.

Blood, 108(12): 3700-3706.

CONFERENCES ATTENDANCE

- 2010
- Keystone Symposia, RNA Silencing: Mechanism, Biology and Application, Keystone, Colorado, USA
 - Poster of "Up-regulated miRNAs during LPS-induced dendritic cell maturation suppress SOCS1 protein".
 - RNA Quality Workshop, European Science Foundation, Strasbourg, France
 - Talk of "Identification and Expression Analysis of Novel microRNAs of MHV-68".
 - NGFN (Nationales Genomforschungsnetz) Workshop, Würzburg, Germany
 - Talk of "Biochemical identification of viral miRNA targets"

PATENT

- European Patent (No. 08155136.8 -2403) Compositions and methods for microRNA expression profiling of nasopharyngeal carcinoma.

HONORS AND AWARDS

- 2003-2005 MCB Program Scholarship Award, Heidelberg University

COMPUTATIONAL SKILLS

Handling of deep sequencing data by 454 and Solexa sequencing.

Programming by BASIC language.

Skillful in Microsoft Office, Adobe Photoshop.

LANGUAGE SKILLS

Fluent in English and Chinese. Practical knowledge of German.